# Real Time Market Based Control of Flexible Distributed Energy Resources

Subhitcha Ramkumar



## Real Time Market Based Control of Flexible Distributed Energy Resources

by

## Subhitcha Ramkumar

to obtain the degree of Master of Science at the Delft University of Technology, to be defended publicly on Monday August 31, 2020 at 9:00 AM.

Student number: 4894499

Project duration: November 2019 – August 2020

Thesis committee: Dr. Simon Tindemans, Project Supervisor

Mr. Hazem Abdelghany, Daily Supervisor

Dr. ir. M. Popov, Chair

Dr. Nils van der Blij, External Member

An electronic version of this thesis is available at http://repository.tudelft.nl/.



## Acknowledgement

I would like to take this opportunity to thank all the people who have supported me in reaching this position in my academic life. First and foremost, I express my sincere gratitude towards my project supervisor, Dr.Simon Tindemans for his theoretical guidance and support throughout the course of this thesis. His calm attitude, professional approach towards his work and attention to detail are a few things that I hope to inculcate in my career. I would also like to thank my daily supervisor, Mr.Hazem Abdelghany for being very friendly and always willing to help me with a smile. I also thank Dr. Marjan Popov and Dr.Nils van der Blij for taking their time from their packed schedules to evaluate my work and joining my thesis committee.

Next, I would like to thank my family for having faith in my abilities and enabling me to pursue my dreams. No amount of gratitude would be enough to acknowledge the sacrifices made by my mother, who has been an incredible source of support in both good and bad times.Next,I would like to thank my chithappa, chithi, maama and maami for being always a call away and making me feel at home. Special mention to Abi, who has been an absolute stress reliever. Thank you making me laugh so hard every time we have a video call.Appa and Thatha, I wish you were here to celebrate my graduation and be the incredible pillars of support as you were.

Finally, I would like to thank my friends who are my chosen family. A big shoutout to "Namma Gang" members: Nithin, Abhi, Keshav, Bharath and Athira who have been always there for me since high school. I would also like to thank all my wonderful friends from SSN for all the great memories. I would also like to thank Saro, Pragati, Raj, Madhu and Sibi for the fun times we have had and for making living in the Netherlands feasible. I would like to thank Swaathishree, Sai Gautham and Priyadarshini for proofreading my thesis.

Subhitcha Ramkumar Delft, August 2020

### **Abstract**

Advancements in the field of Information and Communication Technologies (ICT) has enabled the possibility to utilize the flexibility offered by responsive assets in a better way by employing Demand Response (DR) schemes. This thesis analyzes the performance of one such DR scheme developed at TU Delft called Forecast mediated Market Based Control (F-MBC), which aims to coordinate such flexible assets by communicating "self-fulfilling forecasts" [3].

The main aim of the project is to investigate the applicability of this method in real-world settings. To do so, several simulation scenarios were formulated to understand how well F-MBC coordinates heterogeneous populations of uninterruptible time shiftable loads over an extended time horizon, both from the system perspective and devices' perspective. The thesis also proposes an approach to test the mechanism in a rolling horizon setup.

First, the performance of F-MBC is examined under several combinations of deferrable loads having identical deadlines. Then, its ability to coordinate devices with dynamic load profiles under a complex realistic setting is investigated. Trade-offs adopted when simulating such a setup is also highlighted. Results indicate that while F-MBC achieves good overall performance when coordinating devices with uniform power consumption profiles, its performance in scheduling heterogeneous populations of devices with dynamic load profiles was quite variable. When devices that consume high power when they start was considered for coordination, F-MBC was able found to allocate the devices in such a manner that steered towards overall cost minimization. However, its performance if used to schedule devices which consume low power when it starts was found to be undesirable. Hence, several recommendations were provided to deduce better conclusions about the applicability of the mechanism in reality.

## **Contents**

Lis	st of Figures	ix
Lis	st of Tables	хi
1	Introduction  1.1 Background	2
2	Overview of Demand Response techniques  2.1 Introduction	5 6 7 7 8 8 11
3	Multi agent systems and Game theory  3.1 Introduction	13 14 15 17 17 18 18
4	System description 4.1 Introduction	22 22 24 25 26 28 28
5	Facilitator generalizations and performance indicators  5.1 Introduction	31

viii Contents

	<ul><li>5.3</li><li>5.4</li><li>5.5</li></ul>	Simulating the facilitator in realistic setting       33         5.3.1 Optimistic forecast formulation       35         5.3.2 Pessimistic forecast formulation       36         Performance Indicators       37         5.4.1 Overall objective function       37         5.4.2 Cost of starting       37         5.4.3 Regret       37         Summary       37
6	Coo	ordination of heterogeneous populations using F-MBC 39
•	6.1 6.2	Motivation
		duration
		tion
		6.3.3 Combination 3: Devices with same power consumption, but with different dura-
	6.4	tion
7	Арр	olication of F-MBC in realistic setting 61
	7.1	<del>_</del>
		Implementation
	7.3	Results and Analysis
		7.3.2 Pessimistic forecast scenario
	7.4	Performance under modified load profiles
	7.5	Summary
8		iclusions and recommendations 77
	8.1 8.2	Main conclusions
Δ	hhΔ	litional results: Realistic setting 79
- •		Demand profiles under different day ahead uncertanties
Bil	bliog	raphy 81
	_	

## **List of Figures**

2.1	Graphical representation of the modifications to the load profile that can be accomplished by employing DR.(Adapted from [21])	6
2.2	Impact of DR on the market price.(Adapted from [5]).	6
2.3	Centralized control architecture. (Adapted from [21])	9
3.1	Representation of a game in a normal form.	14
3.2	Representation of a game in extensive form. The strategies of player 1 and 2 are high-lighted in red and blue respectively.	15
3.3	Graphical representation of MDP(Adapted from [13])	16
3.4	Graphical representation of MDP used in MAS(Adapted from [13])	17
3.5	Identification of subgames in a finite horizon extensive game.	18
4.1	Pictorial representation of F-MBC approach.(Based on [3])	22
4.2	Auction curves (i.e.; the supply and demand curves) in event of a tie at clearing price $x_t$ . The portion of the bid curve highlighted using a box represents the large step in the	25
4.3	curve which results a consequence of having same threshold price.(Adapted from [3]). Graphical representation of a rolling horizon framework (Adapted from [45])	25 28
5.1	Graphical representation of load profile of a device with multiple paths during its cycle.( Adopted from [11])	33
5.2	Pictorial representation of rolling forecasts generation when performing simulations. The simulation terminates after n iterations.	33
6.1	Graphical representation of the populations of devices: Combination 1	41
6.2	Demand profile comparison : Combination 1	41
6.3	Schedule comparison : Combination 1	42
6.4	Threshold bids submitted by the last allocated agent belonging to population 1 and 2	42
6.5	Auction curve at t=1	43
6.6	Top panel: Cost of starting based on MIQP schedule.	44
6.7	Bottom panel: Cost of starting based on F-MBC schedule	44
6.8	Graphical representation of the populations of devices: Combination 2	46
6.9	Demand profile comparison: Combination 2	46
	Schedule comparison: Combination 2	47
	Threshold bids and auction curve - Combination 2	47
	Cost of starting comparison: Combination 2	48
	Distribution of regret of device agents: Combination 2	49
	Graphical representation of the populations of devices: Combination 3	50
	Demand profile comparison: Combination 3	50
	Schedule comparison: Combination 3	51
	Threshold bids submitted by the agents belonging to population 1 and 2: Combination 3	52
	Prices forecasted at t=1	52
6.19	Optimal expected costs and threshold bids calculated by devices based on the prices	
	forecasted at t=1:Combination 3	53

x List of Figures

6.20	Top panel: Cost of starting based on MIQP schedule.	
	Bottom panel: Cost of starting based on F-MBC schedule	53
6.21	Distribution of regret of device agents: Combination 3	54
6.22	Graphical representation of the populations of devices : Combination 4	55
	Demand profile comparison: Combination 4	56
	Schedule comparison: Case 4	56
	Cost of starting comparison: Combination 4	57
	Distribution of regret of device agents: Combination 4	58
7.1	Load profiles of Washing Machine and Dish Washer respectively. (Adapted from [48]).	62
7.2	Top panel: Average number of WM available in a day	
7.0	Bottom panel: Average number of DW available in a day	63
7.3	Top panel: Deadline distribution of WM	C 4
7 1	recording to the control of the cont	64 64
7.4 7.5	Inflexible load and generation data used	65
7.5 7.6		66
7.7	Demand profile under optimistic forecasts	67
7.7 7.8	Schedule comparison: Optimistic forecast scenario	07
1.0	lines bidding at t=6	67
7.9		68
	Auction curve at t=6	68
	Effects of submitting bid functions with low power consumption	69
	Demand profile under pessimistic forecast scenario.	70
	Comparison of device schedules under optimistic and pessimistic forecast scenarios	71
	Prices forecasted at t=1 under optimistic and pessimistic scenario	71
	Cost of starting comparison	72
	Modified load profiles of Washing Machine and Dish Washer respectively	73
	Demand profile when threshold bids are function of high power consumption profile	73
	Auction curves when the threshold bids are function of the highest power consumption	, ,
	of the device	74
7.19	Cost of starting comparison when modified load profiles were considered for coordination	74
	Demand profile comparison with $v^{24h}=0.001$	79
	Demand profile comparison with $v^{24h} = 0.01$	79
ΔЗ	Demand profile comparison with $v^{24h} - 0.1$	20

## **List of Tables**

6.1	Possible combinations when considering two populations of devices with uniform power					
	consumption	ŀO				
6.2	Objective function comparison: Combination 1	1				
6.3	Objective function comparison: Combination 2	16				
6.4	Objective function comparison: Combination 3	51				
6.5	Objective function comparison : Combination 4	6				
7.1	Objective function comparison : Optimistic forecast scenario	6				
7.2	Objective function comparison: Pessimistic forecast scenario	'C				

## **Chapter 1**

## Introduction

This chapter describes the motivation for pursuing the research project. Section 1.1 explains the need for employing demand response programs. The main research questions that will be addressed in this thesis is listed in Section 1.2. The chapter then concludes by describing the organization of the report into different chapters in Section 1.3.

#### 1.1 Background

Affinity towards sustainable power generation has increased due to the negative environmental impact of fossil-fuel-based energy-producing units. The entire globe is witnessing a shift from the traditional "top-down" method of electricity consumption towards a decentralized structure characterized by multiple generating entities. In the "top-down" approach, electricity is transmitted from massive power plants to the points of demand. On the other hand, decentralized architecture enables consumers to attain the status of prosumers. They satisfy a share of their energy demand by deploying small energy generating units like rooftop PV generating units closer to their point of consumption. They can also feed the excess generated electricity to the grid.

Such a change is associated with increased volatility caused by the fluctuating nature of renewable generation and potential impacts of bi-directional flow of power, such as overloading of the network. To handle these issues, the concept of smart grids is proposed. Smart Grid uses information and communication technologies to better utilize the assets available at all levels of the electricity network without compromising the reliability of the system [12].

Variable nature is associated not only with power generation, but also with power consumption due to difference in the preference of end users. Since the distributed structure makes the consumers more active in terms of having options on how to consume energy, their behavioral patterns have a significant impact on security of supply. This calls for a situation where innovative operational solutions are needed to make the demand follow the generation [18][19]. This can be achieved by employing Demand Response (DR) programs [41].

Demand Response influences the power consumption of the users by providing a financial motive to alter their demand. Employing such schemes have several benefits associated like reduced investment expenditure, reduced energy bills, to name a few. User can participate in such schemes by manually responding to the requests made by the utility. This is termed as manual demand response [15]. These schemes do not capture the full potential of DR that the user could offer. In automated demand response programs, the users invest in intelligent devices to participate in the DR schemes. These schemes have resulted in higher load reductions when compared to the manual method [2]. This thesis restricts itself in employing such DR schemes in the residential sector. The way in which the flexibility can be harnessed in the residential sector depends upon the type of loads participating in the DR scheme.

2 1. Introduction

In general, flexible residential loads can be classified into the following categories [25]:

• **Uninterruptible loads:** Devices that have flexible start times or adjustable cycles. Only devices that provide deferrable nature of flexibility are considered for coordination in this thesis. Typical examples include washing machines, dishwashers etc.

• Continuously Controllable loads: Devices such as Electric Vehicles and batteries whose power consumption can be adjusted.

This thesis explores one such demand response scheme developed at TU Delft, called the Forecast mediated Market Based Control (F-MBC) [3]. The methodology aims to coordinate responsive flexible assets over multiple time steps by communicating forecast prices determined by a facilitator. Agents utilize a Markov Decision Process (MDP) based bidding strategy in formulating its bid function, taking into account the device characteristics. The aggregated bids and supply functions are then cleared in a centralized manner by an auctioneer. The methodology was found to exhibit good system level performance when used for coordinating a single population of uninterruptible loads over a fixed time horizon. However, its performance when used to schedule several populations of deferrable loads under realistic setting needs to be investigated in detail.

#### 1.2 Problem Statement and Research Questions

This project analyzes the behavior of F-MBC when used to coordinate different populations of deferrable loads under realistic settings. Thus, this thesis aims in answering the following question:

How does F-MBC perform when coordinating heterogeneous populations of deferrable loads over an extended duration?

To answer this, the following sub-questions were formulated:

- What are the main characteristics of F-MBC mechanism and what advantages does it offer when compared to other transactive methods found in scientific literature?
- What factors influence the deviation from the cost optimal allocation of heterogeneous populations of deferrable loads under the F-MBC scheme?
- How can the mechanism be tested when used for coordination in an infinite time horizon? What trade offs were adopted when simulating such a setting?
- Is the mechanism effective in coordinating heterogeneous loads of deferrable loads with complex load profiles? What is the collective and individual cost performance of the approach?

1.3. Thesis Layout 3

#### 1.3 Thesis Layout

This section provides a general overview of the content described in this document. The methodology adopted in addressing the research question stated in Section 1.2 is described by organizing into several chapters. Every chapter consists of an introduction, the main body and the summary of the main observations made in the particular chapter. The summary also explains the link that it has to the subsequent chapters. The report is structured in the following manner:

**Chapter 2** presents an overview of several DR schemes available in scientific literature and also describes the need for the development of the F-MBC mechanism by providing a very basic introduction to the scheme.

**Chapter 3** provides the necessary theoretical background pertaining to the concepts utilized in F-MBC mechanism. The concepts discussed are used to describe the desired interaction behind the different types of participants in the F-MBC mechanism and also the way in which self interested agents determine their optimal actions.

**Chapter 4** introduces the F-MBC approach. It explains the main parts of the setup, its mathematical framework and summary of the results achieved in [3].

**Chapter 5** describes the additional capabilities added to the developed mechanism which enables the performance evaluation in realistic settings. It also explains about the parameters which will be used in assessing the performance under several simulation scenarios considered in this thesis.

**Chapter 6** focuses on determining the factors that influence the allocation of several populations of deferrable loads, in a setup where all the devices are subjected to the same deadline. The chapter explains the several combinations of populations considered in this setting and analyzes why the F-MBC arrives at the schedule that was observed and its performance on both system and device level.

**Chapter 7** analyzes the performance of the mechanism in a realistic setting, where load profiles of commonly used residential devices are considered for coordination. The chapter explains the simulation setup, the methodology used in generating the data used in simulation, the approach adopted in performing the simulation, followed by the analysis of the results obtained.

**Chapter 8** summarizes the work done in this thesis. It describes the main observations from the experimental studies carried out and also provides some recommendations for future research work.

## **Chapter 2**

## Overview of Demand Response techniques

This chapter provides an overview of demand response, its significance and various methods found in scientific literature. Section 2.2 highlights the benefits of demand response, followed by the description of various demand response schemes and control mechanisms in Section 2.3. The chapter then highlights the difficulties associated with coordination of flexible Distributed Energy Resources (DERs), which led to the development of F-MBC mechanism. The chapter then concludes by describing the general features of F-MBC scheme in Section 2.4, which addresses these potential issues.

#### 2.1 Introduction

The ongoing shift towards smart grids from the conventional centralized nature of electricity generation has led to an increased proliferation of Distributed Energy Resources, like small scale flexible generation and renewable energy resources owned by customers closer to their points of consumption. Due to the intermittent nature of renewable generation, supply demand matching becomes a complicated task. Demand Response (DR) encourage the users to make effective usage of such generation sources to match with the demand and thus is one of the drivers to switch to a smart grid paradigm [51]. The upcoming sections provide a brief overview of demand response programs.

#### 2.2 Demand Response

Federal Energy Regulatory Commission (FERC) defines DR as "Changes in the electric usage by enduse customers from their normal consumption patterns in response to changes in the prices of electricity over time, or to incentive payments designed to induce lower electricity use at times of high wholesale market prices or when system reliability is jeopardized" [7]. Thus, by presenting an attractive motive to the end users, demand response results in the efficient use of generation facilities by altering the demand curve. Typical alterations to the load profile that can be realized using DR schemes include peak shaving, valley filling, load shifting, strategic conservation, strategic load growth and flexible load shape[16], which are represented in Figure 2.1.

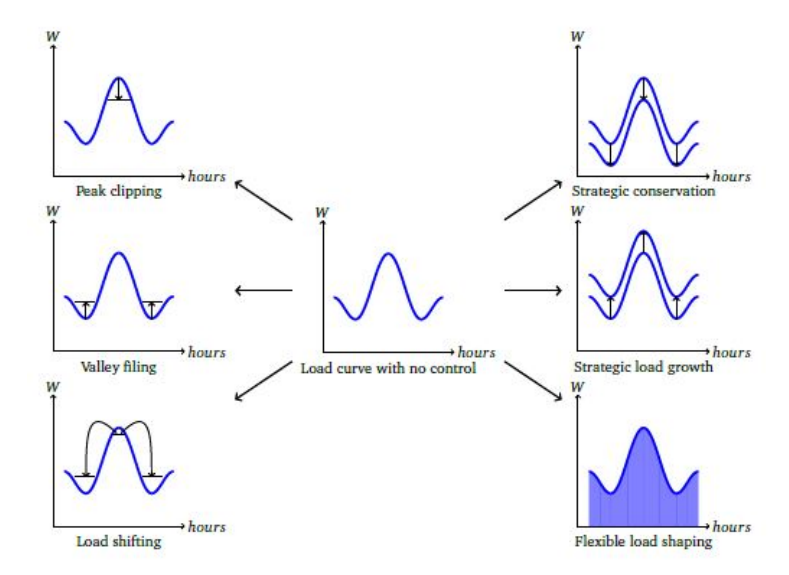


Figure 2.1: Graphical representation of the modifications to the load profile that can be accomplished by employing DR.(Adapted from [21]).

#### 2.2.1 Advantages of DR

There are several benefits associated with the implementation of DR mechanism, both from consumer and system point of view. They are:

#### **Economic benefits**

- From consumer's perspective: Implementing DR strategies lead to reduced electricity bills for the consumers without having to compromise on their consumption, which in turn encourages them to participate in such schemes.
- · From system perspective:
  - Efficient use of DERs by using DR alleviates congestion or overloading of the network, thereby prolonging huge investments to be made on upgrading the existing infrastructure.
  - DR improves the market performance in the following ways:
    - By shifting the electricity consumption to off-peak hours, cost of generation gets significantly reduced, which leads to a lower market prices [5]. This is graphically represented in Figure 2.2.

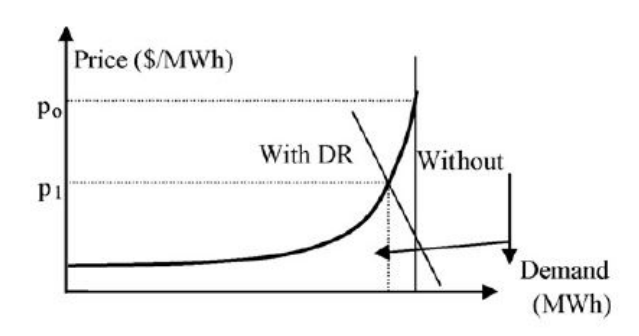


Figure 2.2: Impact of DR on the market price.(Adapted from [5]).

2.3. Classification of DR 7

 Improved responsiveness of the participants also helps in eliminating market power, a situation where generation companies can increase its marginal cost under times of high demand [4].

DR also leads to reduced price volatility.

#### Improved reliability

DR schemes enhances the reliability of smart grid as it improves the security of supply.

#### **Environmental benefits**

By employing schemes that incentivize users to consume energy at those instances when power generated by the renewable energy sources is high, DR reduces the dependency on conventional sources of power generation.

#### 2.3 Classification of DR

DR strategies are primarily classified into price based and incentive based schemes [4].

#### 2.3.1 Price Based Programs

In Price Based Programs (PBP), DR is implemented by using electricity prices as the driving force to influence the consuming pattern of consumer [54]. Based on how these price schemes are modelled, they are classified into the following categories:

#### Time of Use pricing (ToU)

In this scheme, a price schedule is communicated to the consumers usually for a day, with peak and off peak pricing defined at different blocks of the day. A typical rate structure under ToU scheme is given for both weekdays and weekends [2]. The variations in the costs presented under this scheme are subjected to average generation and delivery costs of electricity [4].

#### **Critical Peak Pricing (CPP)**

While ToU scheme can be used on a daily basis, Critical Peak Pricing schemes are used only under those circumstances where is a need to curtail huge demands for certain period(s) of the day. By generating a price schemes that reflect such huge demands by extreme prices; participants avoid consuming at those instances.

#### Real Time Pricing (RTP)

In this scheme, a dynamic price profile, reflecting the variability associated with electricity generation is presented to the users [28]. ToU represents peak and off peak periods by having constant prices under those blocks of the day, while RTP shows the actual costs at every interval of the day to the consumer [38]. This enables the users to make better decisions about usage of their resources.

#### 2.3.2 Incentive Based Programs

While in price based schemes, the users react by modifying their consumption pattern in response to the dynamic price signals received, Incentive Based Programs (IBP) focus on accomplishing the same by offering customers additional incentives/discounts for shifting their demand. Different types of IBPs include:

#### Classical schemes

**Direct Load Control (DLC):** As the name suggests, the system operator is provided the authority to control or alter the consumption time of the loads in exchange for reduced tariffs. These types of contractual agreements are made with residential loads such as air conditioners and water heaters. **Interruptible /Curtailable service (I/C):** On agreeing to provide I/C services, the user is expected to either lower the consumption or shift their cycle to another time. The difference of this scheme from DLC is that the user can be penalized if they do not adhere to the contractual terms [24].

#### Market based schemes

There are 4 typical market based schemes namely Demand Bidding, Emergency Demand Response Programs (EDRP), Capacity Market and Ancillary Service Markets.

In Demand Bidding Schemes, participants, usually large consumers, submit bids to reduce their loads in the wholesale electricity market. If the market clears at a price greater than the submitted bid, then the user has to act in accordance to the bid made. Failure to do so will subject the user to penalties. When similar bids for load curtailment are made to provide ancillary services, it is then called Ancillary Service Markets. EDRP schemes provide incentives to those customers who voluntarily reduce their consumption during a contingency. Capacity market schemes allow users to commit for a pre-planned load reduction in the event of a contingency. Under this scheme, the participants will be awarded with guaranteed payments even if load curtailment facility offered by them is not being utilized [51].

#### 2.3.3 Control strategies

Based on the control strategies , DR schemes described above can be classified into the following categories:

#### **Centralized control**

In a centralized control architecture, the central controller acquires complete knowledge about all the loads of the users taking part. Based on the available information, it decides on the consumption strategies of the devices communicates the same to the devices. The control architecture is represented pictorially in Figure 2.3.

2.3. Classification of DR

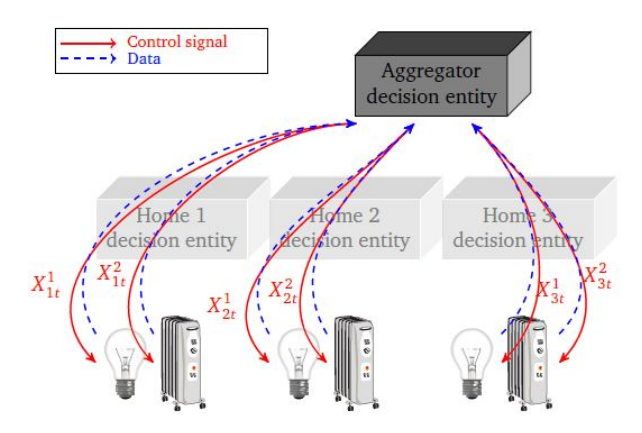


Figure 2.3: Centralized control architecture. (Adapted from [21]).

Main advantages offered by this control scheme is the better coordination that can be facilitated by the central decision maker. This is because of the visibility that the entity has that enables to make well informed decision. However the scheme suffers from various drawbacks. They are listed below:

- The scheme does not preserve the privacy of the participating agents.
- Implementation of the control scheme requires significant communication investments especially when implemented in large systems [55].
- The system has a single point of failure. That is, the decision making entity can lead to the failure of the entire system.
- Response time of the system is also slow. For instance in [32], it was found that centralized control of air-conditioning units cannot be used for frequency regulation service because of the inherent communication delays involved.

#### **Decentralized control**

In centralized schemes, there are concerns regarding the scalability and lack of privacy of the participating agents. These are addressed by utilizing distributed control schemes. In decentralized control , there is no supervisory decision making authority involved. Each user takes decisions based on the information provided, which is usually the price signals and alters its consumption pattern.

While completely decentralized control architecture provides quicker response than its counterparts, prediction of demand response under this architecture was found to be more complicated [32]. This is mainly because of the difficulty in predicting the user preferences, given the private nature of participation. For example, [53] highlights the difficulty associated in both testing and realization of a complete decentralized system. It was observed the time taken for debugging a decentralized system was significantly longer than its centralized counterpart.

#### **Transactive Control**

Increased number of resources, both generation and load, being controlled by the users with different preferences calls for a new DR approach that enables active participation of such assets . Transactive control mechanisms have found to satisfy these requirements and thus is being widely investigated [26]. According to Grid Wise Architecture Council, transactive control is defined as [30]: "A system of economic and control mechanisms that allows the dynamic balance of supply and demand across the entire electrical infrastructure using value as a key operational parameter." In transactive control mechanisms (also known as Market Based Control), autonomous decisions are made by users based on price signals received . Coordination of generation and demand is achieved based on market equilibrium price. This section explains few market based control schemes commonly found in literature.

**Iterative approaches:** One of the most commonly explored iterative approaches in transactive control is the development of P2P markets. These are characterized by establishing bilateral contracts between the agents [46]. There can be several categories of P2P market depending upon the degree of decentralization that the mechanism offers. For instance, in full P2P design, the market enables the participating agents to choose among the generating units and engage in transactions only with them with complete autonomy.

While this setup can attract the agents because of the choices that the scheme offers, implementation of such a scheme requires the establishment of several communication links between the users and generating sources, thereby affecting scalability. The system also becomes unpredictable in nature because of the complete decentralized nature of implementation.

**Negotiation schemes:** In negotiation schemes, prosumers directly negotiate or employ Virtual Power Plants (VPP) to negotiate with the aggregator to arrive at a feasible agreement which benefits all the parties involved. For instance, in [6], a negotiation framework is developed wherein negotiations between VPP and the aggregator are performed by communicating offer packages. The offer packages keep getting exchanged until the difference between the current offer package and the weighted offer package determined based on the previous negotiations is less than a convergence tolerance.

The issue with this approach is that the time taken to reach convergence scales directly with the number of prosumers participating in the scheme, thereby affecting its usability in large systems.

**Real time market based control:** This method combines the advantages of both centralized and decentralized methods of decision making. Agents representing loads submit their bid functions by making local decisions, while the equilibrium point is determined by a centralized market clearing in real time [3]. A bid function maps the demand with the price that the agent is willing to pay.

However, these mechanism perform poorly when used to coordinate uninterruptible loads. For example, in [29], oscillatory behaviour was observed when coordinating a population of Thermostatically Controlled Loads (TCL). This was found to be because of the variations in the bids submitted by the agents in response to changing prices, which led to huge variation in the overall power demands.

#### 2.4 Motivation for a new control approach

Previous sections discussed the potential issues with commonly used transactive methodologies. This section highlights how the F-MBC design approach addresses these drawbacks.

F-MBC is a real time market based control mechanism that utilizes Multi Agent Systems (MAS) to represent the flexible entities. MAS is one of the most widely used modelling approaches for capturing the complex interactions among self interested entities [52]. Game theoretical concepts such as Markov Decision Process (MDP) is used to model the decision making strategy of flexible loads, which is to minimize its payment. This also has less processing requirements. Uncertainty associated with both generation and consumer preferences are taken into account by generating probabilistic forecasts. To address the issue of bulk switching, tie breaking mechanism is formulated. The system is scalable owing to the decentralized nature of decision making and privacy preserving because the agents only submit their bid functions to the auctioneer, which does not contain any device level characteristics.

#### 2.5 Summary

This chapter provided a brief introduction to the concept and significance of DR. First, different price based and incentive based schemes were introduced, which was followed by the description of the control strategies used to realize DR. It then proceeded with the description of Transactive Control, which was found to be a convenient approach for coordination of DERs. The chapter then pointed out some of the difficulties faced by such transactive mechanisms in coordinating flexible loads of inter temporal nature, which served as the motivation behind the development of F-MBC mechanism. The chapter then concludes by providing a brief introduction about the characteristics of F-MBC, which could solve the issues found in the methods discussed. Game theoretical concepts used in the mechanism will be explained in the upcoming chapter.

### **Chapter 3**

## Multi agent systems and Game theory

The goal of this chapter is to provide a brief insight into the some of the fundamental concepts in game theory. It aims to provide some theoretical support for concepts being used to devise the decision making model used by the participants in the F-MBC mechanism. Section 3.2 introduces the concept of a game and its constituents. Section 3.3 describes the Markov Decision Process (MDP), one of the decision making strategies used by the agents. Section 3.4 deals with equilibrium points of a game and explains in brief about backward induction, which is a method used in determining such equilibrium points. The way in which the above-mentioned concepts are utilized in the F-MBC is briefly discussed in Section 3.5.

#### 3.1 Introduction

As explained in [23], Multi Agent System (MAS) based modeling techniques are gaining popularity in the field of demand response because of their ability to capture the intermittent nature of Distributed Generation and the uncertainty associated with the user consumption. In a MAS, each flexible entity is represented by its agent, which is capable of making a decision by considering several factors into account. Applications of MAS include electricity market modeling, load restoration and power system protection [37]. An Agent can be defined as a computer system that has the ability to make decisions based on the information it perceives from the environment. The main characteristics of any agent is [22][23]:

- · Ability to communicate and react to any changes in their environment.
- Ability to make necessary transitions to satisfy their design objective.

#### 3.2 Game theory

Game theory, developed from the contributions of von Neumann and Morgenstern [39], is a mathematical tool that analyzes the interaction among such self interested agents [42]. Game theory has been extensively used in several disciplines such as economics, politics, philosophy and engineering science [14] [10]. It is an effective tool that helps in developing suitable strategies such that all the participants are assured of a certain degree of payoff [9]. A game is a situation that involves a group of autonomous decision makers, whose actions affect the overall outcome and also the rewards of all the involved agents.

#### 3.2.1 Important components of a game

To define a game for the purpose of analyzing the interaction among the players, it must contain the following components [10]:

- A finite set of players  $P = \{1, 2, ....n\}$
- Strategy set for each player,  $S = \{S_1, S_2 ... S_n\}$ . Strategy set refers to the all possible actions that a player can perform in a game setup. By adopting a strategy, a player performs an action which will affect its outcome. Given the current state of the game that the player finds himself in, the players adopt those strategies that maximize their payoff.
- Information sets available to each player. Based on the information available, a player decides on a particular strategy and performs an action.
- Utility function,  $U = \{U_1, U_2, .... U_n\}$ , which is a set of rewards that each player attains for adopting a strategy. In a setting of self interested agents, players prefer those strategies that maximize their utility.

#### 3.2.2 Categories of games

Depending upon their characteristics, games can be classified into the following categories [10]:

#### Cooperative and Non cooperative games:

A game is considered to be cooperative, when the agents interact with each other and jointly work towards achieving a common reward. Non-cooperative games are those in which agents focus only on maximizing its payoff, rather than working in an alliance with other agents.

#### Normal form and Extensive form games:

Normal form games are typically represented in a matrix format. It represents all possible actions and the associated payoff for all the players in the game. It is also referred to as static or one-shot games where the players make simultaneous and autonomous decisions [49]. An example of a normal form game is presented in Figure 3.1. Here , 1a and 1b indicates the action set of player 1, while player 2's action set consists of 2a and 2b. The cells in the matrix denotes the payoff that each player gets for performing an action simultaneously. For example :  $(U_{1a}, U_{1b})$  refers to the utility that players 1 and 2 receive for performing actions 1a and 2a simultaneously.

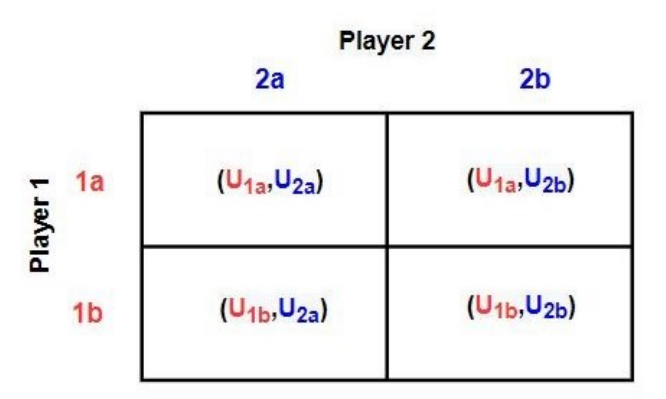


Figure 3.1: Representation of a game in a normal form.

On the other hand, extensive form games, is a strategic situation where every each players move over time in a sequential manner as in chess. An example of a sequential game is presented in Figure 3.2 . Here each player is represented as a node of the tree and the branches indicate the possible actions that a player can make. The branches terminate with the payoff that the players receive as a consequence of the action branch trail that they follow. It is worthwhile to highlight that in an extensive form game the payoff that the player receives depends on the order of actions performed. In such games, each player uses a strategy to decide on the suitable action at every

point of time based on its current state [8]. Dynamic repeated games are analyzed using extensive form representation[33].

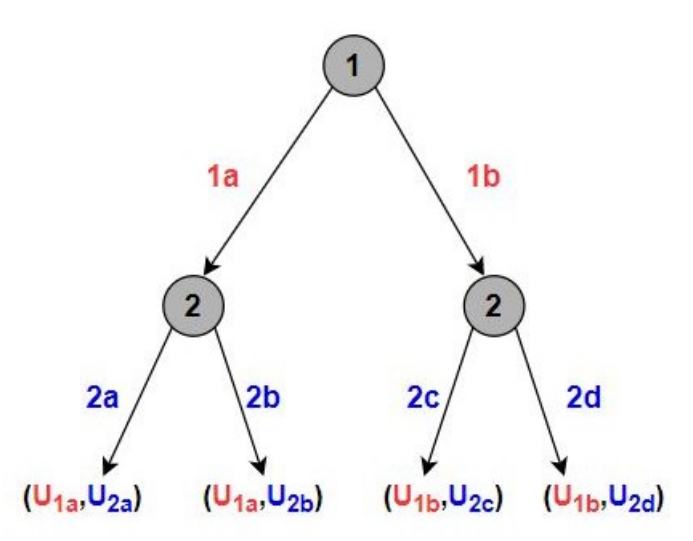


Figure 3.2: Representation of a game in extensive form. The strategies of player 1 and 2 are highlighted in red and blue respectively.

#### · Zero sum and non-zero sum games:

In games when the aggregated reward obtained by the players in a game is zero, they fall under the category of zero sum games. This gets translated to the notion that in such games, one player's gain gets compensated with other player(s)' loss, such as in basketball or poker. On the other hand, non-zero sum games are those where the sum of the rewards of the players involved are not zero, indicating that the players do have a possibility to win (or even lose) together. Such games involve players who are not perfectly competitive as in zero sum games, but are often found to have opposing interests[10]. Some famous examples of non-zero sum games include battle of the sexes, prisoner's dilemma etc. Both of these games fall under the category of static games since decisions are made by the players without the knowledge of the actions of the other players [34].

• Pure and Mixed strategy games: Pure strategy games refer to a situation where the players have a deterministic action at each state of the game. If at least one state of the game can be associated with more than one strategy set, then it becomes a mixed strategy game.

#### 3.3 Markov Decision Process

Markov Decision Process (MDP) describes in detail how an agent makes its decision in the current state to maximize its utility function in a stochastic environment [13]. It possesses the Markov (or) memoryless property, implying that the future actions predicted by the agent is dependent only on the current state. MDPs capture how the agent reacts to the information that it obtains from the external environment and makes a suitable decision. The main components of a MDP are:

- · State space
- · Action space
- · Transition Functions

#### · Reward function

**State space:** State space, represented by  $S = \{s^1, s^2, ....s^N\}$ , is a collection of all possible states that an agent can be. At any given time step, the agent finds itself in one of the states in S.

**Action space:** Action space, represented by  $A = \{a^1, a^2, ....a^p\}$ , is a collection of all possible actions that can be undertaken by an agent. Depending upon the current state of the agent, the choice of actions that an agent can make varies. This implies that the actions that can be agent is dependent on its state s, i.e;  $A(s) \subseteq A$  [50].

**Transition Functions:** When an agent in a state  $s \in S$ , applies an available action  $a \in A(s)$ , it makes a *transition* to a new state  $s' \in S$ . Transition function, T describes the probability distribution of all possible successive states that an agent can transition into, based on its current state and the possible actions that it can perform. It is mathematically expressed as  $T: S*A*S \rightarrow [0,1]$  [50].

**Reward or utility function:** Reward can be considered as the most important component of MDP. Maximizing the utility drives an agent to take an action and undergo a transition. R(s, a, s') represents the expected reward that the agent receives for reaching the state s' by doing action a, when its current state s [13].

Now that all the components of MDP are introduced , we can define MDP as a tuple (S,A,T,R); which represents the sequence of optimal actions that an agent will undertake given the local or global information, to maximize its utility function. The goal of any MDP is to establish a policy  $\pi(s)$  that results in the maximization of long term reward [35]. Policy is a function that associates an action for a given state. The whole process is summarized in Figure 3.3, where the MDP is pictorially represented as a state transition graph.

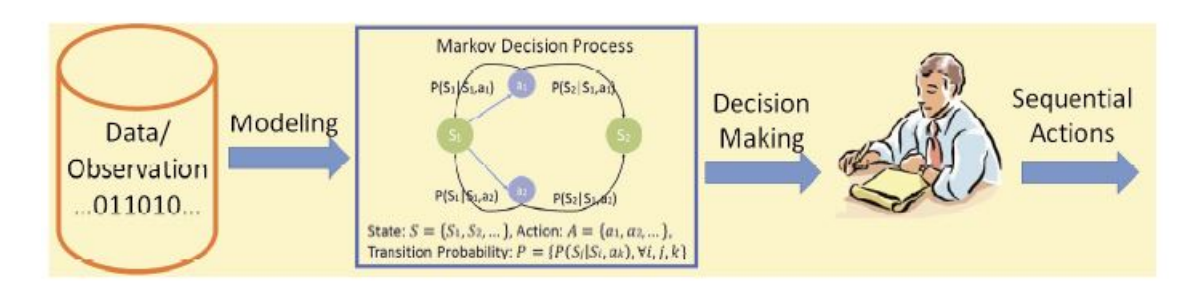


Figure 3.3: Graphical representation of MDP(Adapted from [13])

One can view MDP as a stochastic game that involves only agent, represented by a single decision maker in Figure 3.3, where the actions taken by the player does not influence the transition probabilities to another state, when played again. On the other hand , in a MAS , each player is subjected to same information which is used in developing a MDP model by all the agents to make a decision. The main difference here is that the actions taken by each agent influences both the reward of all the agents and the probabilistic transition into a certain game in the next iteration. This is represented in Figure 3.4, where the actions of the agents made at the previous instant impacts the data being utilized for MDP models at the current instant.

3.4. Solution concepts

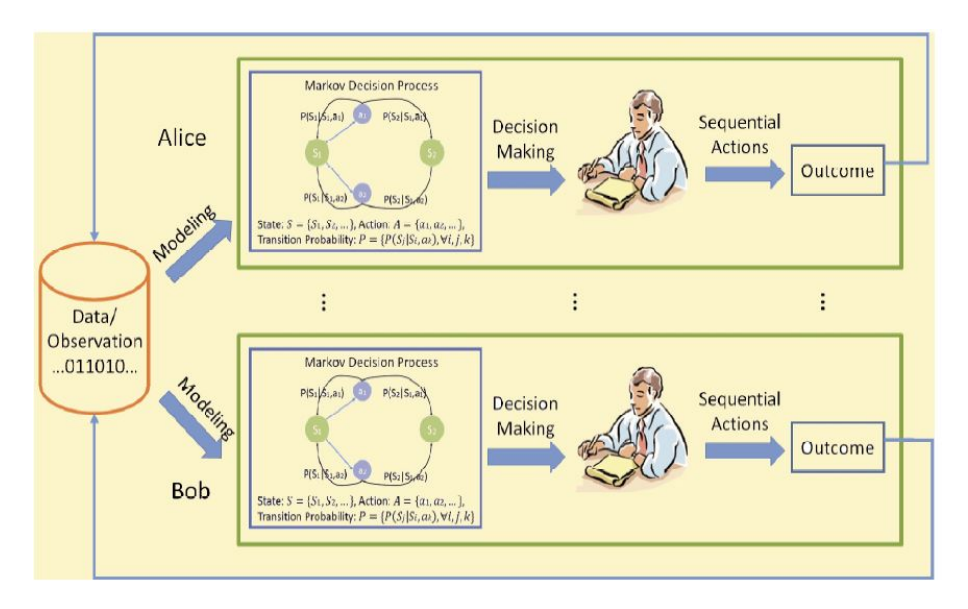


Figure 3.4: Graphical representation of MDP used in MAS(Adapted from [13])

#### 3.4 Solution concepts

In this section, a brief introduction into solution methodologies for the games is provided, in particular Nash Equilibrium and Backward induction, which is a method to determine subgame perfect equilibrium.

#### 3.4.1 Nash Equilibrium

The concept of equilibrium points was first introduced in the work of John Nash [27]. Nash equilibrium can be defined as that action profile or strategy profile which provides the best response of each agent to all the participating agents. That action is considered to provide a best response of an agent i if the payoff associated with performing it is atleast as high as any other possible strategy, given the strategies of other players.

The reason that the Nash Equilibrium has garnered significant attention from the researchers is because that it is inherently stable [42]. It implies that in a game setting where the player has a certain expectation of the action to be performed by all the other players, if the players choose the action profile that leads to a Nash Equilibrium, they are better off than adopting a different action/strategy. This also indicates that the players would not have any benefit from deviating from this equilibrium point.

It is important to understand that not all Nash Equilibrium can lead to a global optimum, which maximizes the player's utility. An example of such a situation is the infamous game of Prisoner's dilemma [10], in which the optimal action of both isolated prisoners is to confess about the crime committed by the other. Here, the utility maximizing action of the players involved is to turn the other player in. To quantify the effect of selfish actions taken by the agents, the term price of anarchy is usually used [40]. It is defined as the ratio between the worst possible utility and the utility that offers maximum social welfare.

#### 3.4.2 Determining subgame perfect equilibria

Every finite extensive game with perfect information has a subgame perfect nash equilibrium, which can be determined by employing backward induction, according to Zermelo's theorem [44]. To understand how backward induction works, the terms 'subgame' and 'perfect information' are first discussed.

• **Subgame** is that part of the game which has one starting node and all the other successive nodes. For the extensive game shown in Figure 3.2, there are 3 subgames: The entire game, and the two possible nodes that player 2. This is represented in Figure 3.5.

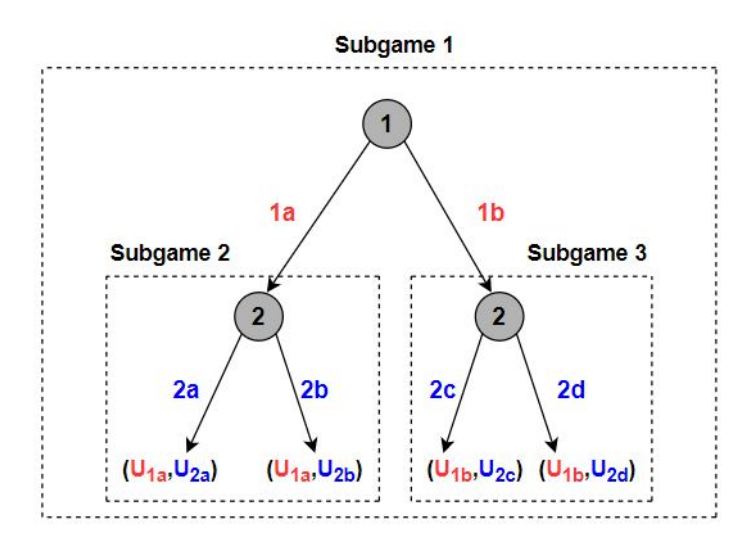


Figure 3.5: Identification of subgames in a finite horizon extensive game.

• **Perfect information** denotes that each player knows the "history" of all the actions taken in the previous plays, that has led to the current stage of the game [17].

It is a bottom up analysis, usually performed at the last possible node of the game (usually at the leaf node or final payoff node) and reasoning backward all the way up to the top node of the game tree to decide on a sequence of actions that result in the maximum payoff of the agent at each of the nodes. By determining the equilibrium of each subgame, this method helps in eliminating those branches of the subgame tree which will not be chosen by rational player, in order to arrive at the Nash Equilibrium of the original game.

#### 3.5 Application of described concepts in F-MBC scheme

This section describes how the concepts discussed in the previous sections are applied to the F-MBC scheme.

As introduced in Chapter 1, the agents representing the loads receive forecast prices from the facilitator. Based on the device level constraints such as deadlines, duration and power consumption profile, agents submit a bid function to a double auction market. The bid function is modelled using a MDP based bidding policy. Based on the current state of the load and the forecast prices, agents determine the optimal action that it has to perform by performing backward induction from the last possible timestep (the timestep at which it has to be scheduled to meet the deadline) to the current timestep, by applying the MDP model. These aspects are dealt in better detail in the upcoming chapter.

3.6. Summary 19

#### 3.6 Summary

In this chapter, the concept of agents and games was introduced. Post the description of important characteristics of agents and the constituents of games, different types of games were introduced. Markov Decision Process, which is the decision making paradigm for agents in a stochastic setting was described post which the concepts of the equilibrium was introduced. The chapter then provided a very brief explanation of backward induction, which is a method used to determine the equilibrium of extensive games with perfect information. The chapter then concluded in relating the above discussed concepts to the F-MBC mechanism, which will be discussed in the upcoming chapter.

## **Chapter 4**

## **System description**

This chapter aims to explain the underlying principles involved in establishing the F-MBC mechanism, as introduced in [3]. The chapter begins with describing the main constituents of the co-ordination mechanism and their functions in Section 4.2 . Section 4.3 explains how the forecasts generated by the facilitator is simulated. Finally, Section 4.4 provides a brief description of experimental verification of the developed method in [3]. It also highlights some of the unexplored experimental aspects to analyze the application of F-MBC mechanism in practical settings.

#### 4.1 Introduction

It was seen in Chapter 2 that scheduling privacy preferring self interested agents representing uninterruptible loads over multiple time steps resulted in undesirable performance both at the system and the device perspective, when same information was communicated to all the agents. Forecast Mediated Real Time Market Based Control (F-MBC) mechanism aims to solve this problem by developing a framework for bid formulation for decentralized decision making by individual agents and centralized clearing by using an auctioneer. This method does not require the agents to communicate its device's characteristics, thereby maintaining its privacy and is also scalable [3]. The aim of the F-MBC mechanism is to co-ordinate or schedule a set of deferrable loads over a scheduling horizon such that the overall generating cost is minimized. This problem is described as "optimal coordination problem" in [3].

In order to understand the working principle, let us consider a coordination problem with the aim to schedule a set of deferrable loads, subjected to device level constraints. These constraints include the deadlines set by the device owner, the power consumption profile of the device and the nature of the device (deferrable loads imply that the flexibility is offered only by shifting their start times. Once the device is scheduled, i.e; it starts, it cannot be interrupted). Each of these devices are represented by a device agent in a double auction market. The market is cleared successively for each time-step. It is assumed that each of the device agents acts on its self-interest. The main complexity of the problem is to schedule the devices in such a way that the optimality is achieved both at the system level (minimization of the generation cost over the scheduling horizon) and also at the device level, where the devices are scheduled at those time-steps which ensures that their economic interest is addressed, which would be to reduce their electricity consumption costs. The F-MBC mechanism aims to address this issue by the generation of "self-fulfilling forecasts" [3].

#### 4.2 Main components of F-MBC mechanism

The main overview of F-MBC mechanism, highlighting the flow of information from one component to another is illustrated in Figure 4.1.

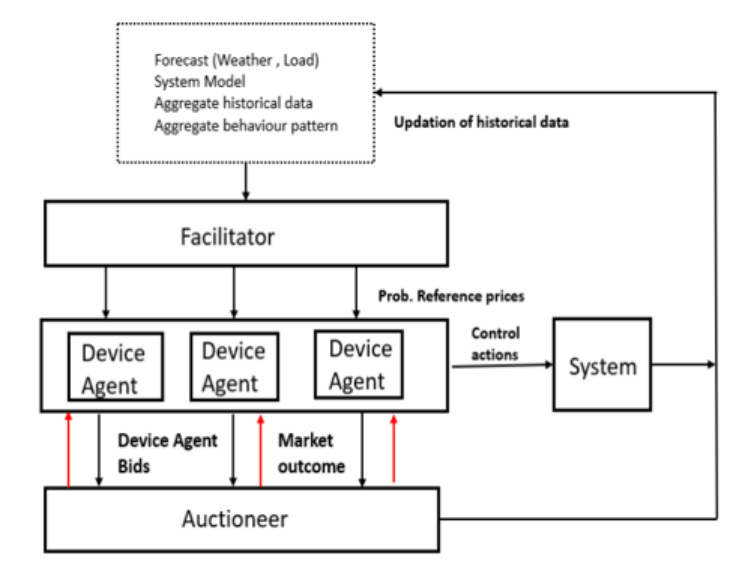


Figure 4.1: Pictorial representation of F-MBC approach.(Based on [3])

As seen in Figure 4.1, the approach involves the interaction between three types of agents:

- Facilitator
- · Device Agent
- Auctioneer

#### 4.2.1 Facilitator

The facilitator is the unit that generates reference prices that are communicated to the device agents. These prices are generated by taking into account several factors such as inflexible load and weather forecast, system model and so on. The resulting outcome is probabilistic in nature, therefore accounting for the presence of uncertainty. These prices are then communicated to the device agents. Based on these prices, the device agents submit their bids to the auctioneer. The facilitator generates an updated price forecast at each time step based on the allocation at the previous timestep.

#### 4.2.2 Device Agents

Device agents refer to the agents representing flexible loads in the market. The main aim of these agents is to ensure that the devices get scheduled at those instances which guarantee the completion of their cycle before the deadlines set by the respective owners and also lead to reduced costs. The agents must also represent the nature of flexibility offered by these devices. It does so by submitting a bid function  $b_t^a(x)$ , based on the prices received from the facilitator at time t. The forecast prices  $_{t}X_t$  are assumed to have independent probabilities for each instant with bounded expectation i.e;  $\mathbb{E}(X_t) = \bar{x_t}$ . The bid function formed by the agent at time t depends on a value which is termed as threshold price,  $\hat{x_t}$ . The threshold prices are determined by making use of a Markov Decision Process (MDP) based bidding strategy, based on the price forecast obtained at time t and also the device level constraints.

#### **Bidding strategy**

As mentioned earlier, the device agents bid in the spot market representing its economic best interest. It is assumed that the agent truthfully notifies the device' demand at time t via its bid function. The agent tries to reduce the total running cost of the device. Since deferrable loads are the participating agents, the action space consists only two possible alternatives, namely: **on** or **off**. The state space is represented by the status of the device represented by agent a in time t, denoted as  $s_t^a$ . Duration of one cycle of operation of the device is denoted as  $D^a$ . The possible alternatives for the state space at time instant t are [3]:

- $s_t^a = 0$ , when the device has not started its cycle yet.
- $s_t^a = \{1...D^{a-1}\}$ , when the device is running.
- $s_t^a = D^a$ , when the device has completed its cycle.

The reward that drives the agent to make a transition from the *off* to *on* state, is based on the optimal expected cost at time t. Let us consider a device represented by its agent  $\mathbf{a}$ , with duration  $D^a$  and deadline  $d^a$ . When switched on, the devices consumes power as per its power consumption profile, indicated as  $\{P_0^a,...,P_{D^a-1}^a\}$ . If the device starts at time t with a corresponding market clearing price  $x_t$ , the total running cost incurred by the device is given by Equation 4.1.

$$C_t^{s,a}(x_t) = x_t \cdot P_0^a \cdot \Delta t + \sum_{i=1}^{D^{a-1}} \bar{x}_{t+i} \cdot P_i^a \cdot \Delta t$$
 (4.1)

The first term in Equation 4.1 is cost of starting at time t. The second term is the cost paid by the device for the reminder of its cycle, calculated using the expected costs at the respective timesteps. The definition of threshold bids determined under each possible states is given by Theorem 1 of [3]. A brief explanation of the same is provided here.

#### Threshold bid determination

Case 1: When the device has to start in order to complete the deadline set by its owner.

This situation occurs for unscheduled devices at timesteps.  $t \ge d^a - D^a$ . In this case, the device needs to start irrespective of the market outcome. Thus, their agent bids inf. The corresponding expected costs is also considered optimal, since it is the only optimal action to take by the device.

Case 2: When the device has completed its cycle.

In this case, the devices bid with a threshold price of  $-\inf$ , implying that it will not turn on irrespective of how low the clearing price is.

#### Case 3: When the device is in the waiting state

When the device has not yet been scheduled at time t, it means that the devices have the option to evaluate the benefit or drawback of starting at t. It does so by calculating the optimal expected cost from  $t = d^a - D^a$  recursively upto t, via backward induction. The optimal expected cost is given by Equation 4.2 [3].

$$C_t^{*a} = Pr(X_t > \hat{x_t^a}) \cdot C_{t+1}^{*a} + Pr(X_t \le \hat{x_t^a}) \cdot \mathbb{E}[C_t^{s,a}(X_t) | X_t \le \hat{x_t^a}]$$
(4.2)

where

 $\hat{x_t^a}$ : Threshold bid determined by agent a at time t.

If the cost of starting at t is less than the cost of waiting and starting at a later time step, the optimal action is **on**. Conversely, if starting at a later time step is seems to be beneficial than starting at t, then the optimal action is **off** for time t. However, if the cost of starting at time t is equal to the optimal expected cost at t+1, i.e; when  $C_t^{s,a}(x_t) = C_{t+1}^{*a}$ , then the agent is indifferent from starting and waiting. In that case, the threshold bid is determined by equating Equations 4.1 and 4.2. This is given in Equation 4.3.

$$x_t^a = \frac{C_{t+1}^{*a} - \sum_{i=1}^{D^a - 1} \bar{x}_{t+i} \cdot P_i^a \cdot \Delta t}{P_0^a \cdot \Delta t}$$
(4.3)

This simply means that at time t , a device in the waiting state will start only if the market clears at a price that ensures that it pays lesser than or equal to the optimal clearing price at the subsequent time instant, else it will wait and start later. In this way, the bidding strategy adopted reflects the economic self-interest of the device.

The bid function  $b_t^a(x)$  submitted by an agent a under different cases mentioned above, is given by Theorem 1 of [3]. It can be summarized as follows:

$$b_t^a(x) = \begin{cases} P^a & x \le \hat{x}_t^a \\ 0 & x > \hat{x}_t^a \end{cases} \tag{4.4}$$

$$P^{a} = \begin{cases} P_{s_{t}^{a}}^{a} & \text{if } s_{t}^{a} < D^{a} \\ 0 & \text{otherwise} \end{cases}$$
 (4.5)

$$\hat{x}_{t}^{a} = \begin{cases} -\infty & \text{if } s_{t}^{a} = D^{a} \\ \infty & \text{if } s_{t}^{a} = 1, \dots, D^{a} - 1 \\ z_{t}^{a} & \text{if } s_{t}^{a} = 0 \end{cases}$$
(4.6)

$$z_{t}^{a} = \begin{cases} \infty & t \ge d^{a} - D^{a} \\ \frac{C_{t+1}^{a} - \sum_{t=1}^{D^{a-1}} \bar{x}_{t+i} \cdot P_{t}^{a} \cdot \Delta t}{P_{0}^{a} \cdot \Delta t} & t < d^{a} - D^{a} \end{cases}$$
(4.7)

## 4.2.3 Auctioneer

The auctioneer is responsible for market clearing at each time step. The bid curve representing the demand of the system, is the aggregation of the bid functions submitted by all the participating agents and the inflexible load that needs to be satisfied at that instant. The offer/supply curve is the aggregation of both flexible and inflexible generation. The market clears at the intersection of these two curves, or at the point where the supply matches with the demand. The clearing price,  $x_t$  is then communicated to all the device agents, as depicted in Figure 4.1.

Apart from market clearing, the auctioneer in the F-MBC mechanism also has an additional feature called tie- breaking [3]. A tie is defined as a situation when several device agents submit equal threshold bids. This situation can arise when the deadlines of the devices are equal. Since the bid function of each agent is a function of the threshold price, having the same threshold price leads to a situation in which aggregation of bids submitted by these agents happens at the same price, leading to a big step in the overall bid curve as seen in Figure 4.2. This might lead to bulk-switching, i.e; a considerable number of devices being scheduled at a particular time step, when provided the same information (price forecasts).

In order to prevent this bottleneck, each agent submits a random number  $\rho^a$  to the auctioneer along with its bid function. In case of a tie, the auctioneer determines a cut-off random number  $\rho^*$ , such that the devices with random number less than or equal to the cut-off number is only allocated. The cut-off random number  $\rho^*$ , is determined in such a way that the supply almost meets the demand at

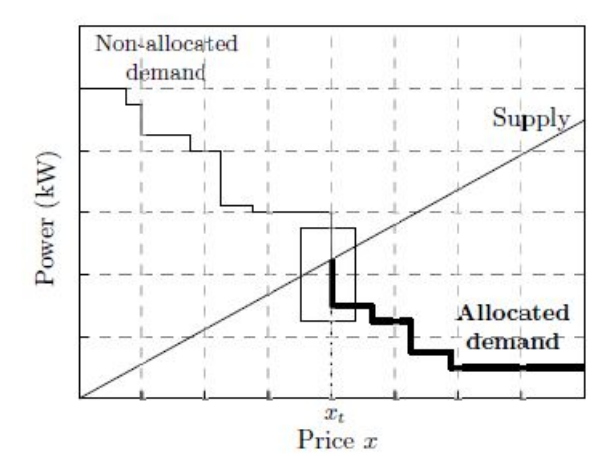


Figure 4.2: Auction curves (i.e; the supply and demand curves) in event of a tie at clearing price  $x_t$ . The portion of the bid curve highlighted using a box represents the large step in the curve which results a consequence of having same threshold price.(Adapted from [3]).

the threshold bid  $x_t$ . This cut off random number is communicated along the market clearing price.

Since ties are bound to happen only among the devices that do not have the obligation to start at that instant, the unscheduled devices that bid with the same threshold will eventually expect to pay the same price as that of the devices that were allocated. This is because at  $t < d^a - D^a$ , the agents are indifferent between starting and waiting and thus have threshold bids as described in Equation 4.3. This means that the device agents do not have any motive to game the tie breaking functionality.

Post market clearing, the information used in generating the forecasts gets updated based on the control actions taken by the devices and this process continues until T.

# 4.3 Simulation of the facilitator

This section explains how reference prices were generated in [3]. In reality, such prices would be generated employing a forecaster. However, to illustrate the importance of generating optimal prices by the facilitator, a facilitator with complete information was modelled. It was proved in Theorem 4 of [3] that the allocation realized by using a facilitator with perfect foresight using linear marginal cost function corresponds to a Nash Equilibrium. This means that, in order to achieve an optimal coordination by using the F-MBC, the facilitator should aim to realize these optimal prices.

When simulating facilitator with complete information about both generation and loads, the reference prices correspond to the outcome of Mixed Integer Quadratic Program (MIQP) that determines the optimal number of starts at each time step over the scheduling horizon such that the objective function ,i.e; the overall generation cost is minimized. Since identical devices with same power consumption pattern are being considered, the demand presented by these flexible devices can be determined by knowing the number of devices running at time t. The mathematical formulation is described in the upcoming section.

# 4.3.1 MIQP formulation

Consider a scheduling horizon T, with fixed time intervals  $\Delta$  t , where t={1,2,...T}. The optimal coordination problem involves scheduling N uninterruptible deferrable loads, each of which is represented individually by its device agent a. It is assumed that the deadlines are assigned by the user at a time step t  $\leq$ T. The duration of the devices is denoted as D. The inflexible load and the renewable generation over the above mentioned period is given by  $P_l^t$  and  $P_r^t$  respectively. The flexible generation is represented by a marginal cost function, denoted as  $m_t(P)$ . The MIQP problem is formulated in the following manner [3]:

minimize 
$$\sum_{P_t^g, \sigma_t, o_t} \frac{1}{2} \cdot \frac{(P_t^g)^2}{k} \cdot \Delta t$$
 (4.8)

subject to  $\forall t \in T$ 

$$P_t^g \ge 0 \tag{4.9}$$

$$P_t^g + P_t^r \ge o_t . P^a + P_t^l \tag{4.10}$$

$$\sum_{i=1}^{t} \sigma_i \ge \phi_d(t+D), \ t \le \mathsf{T} - D \tag{4.11}$$

$$\sum_{i=1}^{t} \sigma_i = \phi_d(\mathsf{T}), \ \mathsf{T} - D + 1 \le t \le \mathsf{T}$$
 (4.12)

$$\sigma_t \ge 0 \tag{4.13}$$

$$o_{t} = \begin{cases} \sum_{j=1}^{t} \sigma_{j} & t \leq D\\ \sigma_{t} + (o_{t-1} - \sigma_{t-D}) & t > D \end{cases}$$
 (4.14)

where

 $o_t$ : Number of devices running at time t.

 $\sigma_t$ :Number of device starts at time t.

 $\phi_t$ : Number of devices whose deadline is at or before the time instant t.

# Description of the problem formulation

#### **Objective function**

From Equation 4.8, it can be seen that the marginal cost function is modelled as a linear function with a constant slope as indicated in Equation 4.15 [3].

$$m(P^g) = \frac{P^g}{k}, P^g \ge 0 \tag{4.15}$$

## Power balance constraint

Equation 4.10 ensures that the power generated by the flexible and renewable generation can satisfy the demand of the flexible and inflexible loads.

#### **Deadlines satisfaction constraints**

Equations 4.11 and 4.12 belong to this category. Equation 4.11 implies that the sum of device starts upto time t is atleast equal to the number of devices that have their deadlines fixed at t+D, thereby ensuring that the deadlines of the devices are met. Equation 4.12 implies that the total number of device starts in the last time steps should be equal to the total number of devices that needs to be coordinated.*N*.

#### **Uninterruptibility constraints**

Since the system consists of uninterruptible loads, it is imperative to include constraints in the optimization problem that describes the nature of these loads. Equation 4.14 describes the same in the formulation. It simply implies that in the initial time steps, from t=1..D, the number of devices running is equal to the sum of device starts upto t. At instances greater than D, the number of devices that have completed their cycle is subtracted from the total number of running devices at the previous time step. This ensures that we do not take into account those devices that turn off. The resultant is then added to the number of starts at time t, in order to determine the total number of devices running at that instant.

At each time step, the optimal prices were generated by taking into account system information until T, in order to take into account the outcome at the preceding instant. This results in generating an "updated" forecast. However, in situations where devices keep becoming available at each instant, the scheduling problem becomes a continuous one and the forecasts will be generated on a "rolling" basis. To explain the rolling forecast setting, the following terms are introduced:

- **Prediction Horizon (PH):** The length of system information considered for the optimization problem.
- Control Horizon (CH) The interval at which the decision is taken by the agents.

Optimal prices are generated by taking into account the system information of length PH . Using these prices, the agents submit their bid functions in the double auction market. Based on the market outcome at the first CH, agents take their decisions to either start or wait. The updated information, based on the actions taken by the agents at the previous CH is used for solving the optimization problem in the next PH. In this way, the scheduling problem keeps moving forward in time. This is pictorially represented in Figure 4.3.

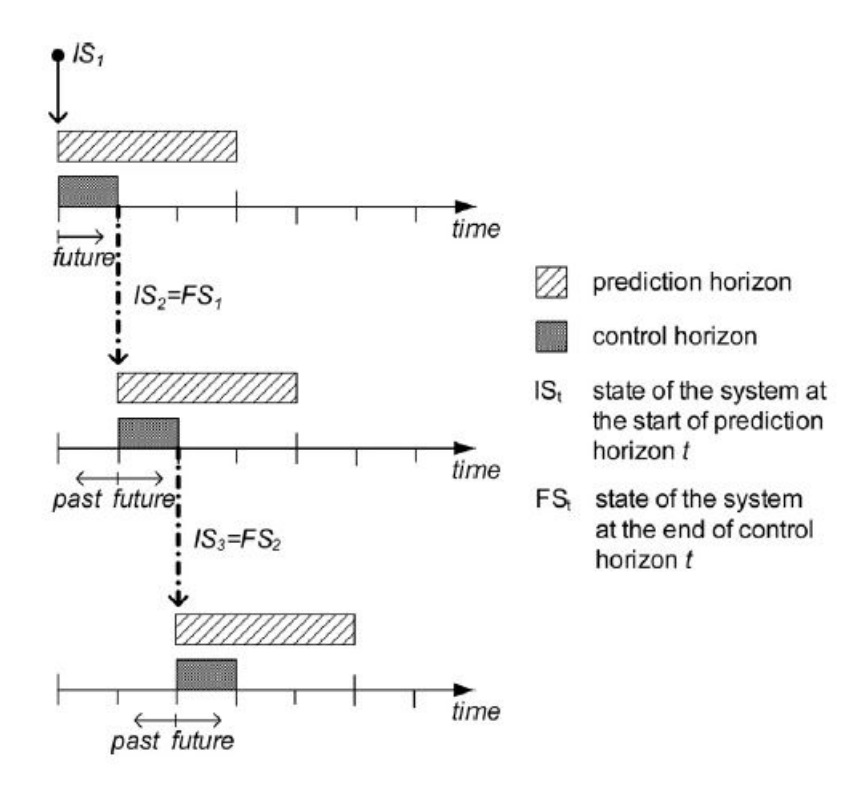


Figure 4.3: Graphical representation of a rolling horizon framework (Adapted from [45])

# 4.3.2 Generation of probabilistic reference prices

As seen in Figure 4.1, the probabilistic reference prices are communicated to the device agents. This section explains how they are developed from the optimal reference prices.

Such forecasts are generated by adding noise to the optimal reference prices. Let the optimal reference prices be represented by  $x_t^*$ . It was assumed that the price forecasts at time t,  $X_t$  are lognormally distributed with a standard deviation  $SD_t$ , which is a function of the day ahead uncertainty  $v^{24h}$  as illustrated in Equation 4.16 [3].

$$SD_t = x_t^* \cdot v^{24h} \cdot \frac{t - t'}{24h}$$
 (4.16)

The values  $SD_t$  was communicated along with the expected costs  $\bar{x_t}$  to each of the device agents, based on which the bid functions are formulated. The expected prices are sampled from the log-normal distribution with mean  $x_t^*$  and standard deviation  $SD_t$ .

# 4.4 Main results achieved

In order to validate the developed mechanism, F-MBC scheme was used to coordinate a single population of deferrable loads with different deadlines set by the owners. The simulation had a span of one day, with 5 min market clearing intervals. The optimal reference prices were distorted with negligible day ahead uncertainty and then was communicated to the agents.

F-MBC was able to follow the initial optimal schedule predicted by the facilitator thereby realizing the cost-optimal load profile with minor deviations. This points towards attaining good system level performance. It was also observed that the total cost of starting using F-MBC coincide with the costs

4.5. Summary 29

determined using MIQP prices, indicating that the coordination realizes good device performance as well. The robustness of the approach with different noise levels was also demonstrated.

However, the following aspects are yet to be investigated:

- The simulation was performed for a predetermined number of iterations. In practice, the scheduling problem is continuous in nature. Therefore, the performance of the scheme in an infinite time horizon is yet to be evaluated.
- The ability of the mechanism to coordinate multiple populations of deferrable loads has to be studied.

These topics will be dealt in the remaining chapters of this document.

# 4.5 Summary

This chapter introduces the F-MBC scheme for coordinating uninterruptible time-shiftable loads over multiple time steps. By simulating a particular case study where optimal prices with negligible uncertainty was communicated to the device agents, the mechanism was found to be able to schedule devices in such a manner that led to good overall performance, both at the system level and device level. This indicates that by communicating optimal prices to the devices, the agents are incentivized to attain these prices. The tie breaking phenomena of the scheme helps in scheduling devices who are indifferent between starting and waiting. The concepts introduced in this chapter acts as a base to understand the behaviour of the F-MBC mechanism in generalized applications and also the simulation scenarios analyzed in this thesis.

# **Chapter 5**

# Facilitator generalizations and performance indicators

This chapter explains in detail the extensions made to the facilitator that allows it to generate prices that can be used to coordinate different populations of deferrable loads. Section 5.2 explains the functionalities added to the optimal prices generation by the facilitator. Post this, Section 5.3 explains in detail how realistic settings can be investigated by performing simulations and what are the additional constraints added to the facilitator to test the robustness of the approach. Then, the metrics that will be used to assess the performance of the mechanism under different simulation scenarios are described in Section 5.4.

# 5.1 Introduction

The previous chapter provided the simulation results of the F-MBC mechanism, where it was able to achieve good overall performance both at the system and device level, when coordinating single population of uninterruptible loads. However, the performance of the scheme when used to schedule several populations of deferrable loads is still to be analyzed. Therefore, in order to do that, the formulation of the MIQP problem was extended to accommodate several populations of such loads, having different power consumption profiles (refer Figure 5.1), duration and deadlines set by their respective owners, therefore serving as a generalization of the facilitator. Here ,a single population refers to a collection of identical devices having the same duration and same demand at every timestep throughout their cycle, but can differ in their deadlines.

# 5.2 MIQP formulation for several populations of deferrable loads

The following equations describe the Mixed Integer Quadratic Program (MIQP) that provides the optimal number of device starts at each time step for n populations of identical, uninterruptible, time-shiftable devices  $(\sigma_t^1...\sigma_t^n)$ , such that the total generation cost is reduced. As mentioned before, the devices in each population vary in their duration ( $D^1....D^n$ ) and power consumption patterns.

The extended formulation is given below:

$$\underset{P_t^g, \sigma_t^1 \dots \sigma_t^n}{\text{minimize}} \quad \sum_{t \in T} \frac{1}{2} \cdot \frac{(P_t^g)^2}{k} \cdot \Delta t \tag{5.1}$$

subject to,  $\forall t \in T$ 

$$P_t^g \ge 0 \tag{5.2}$$

$$P_t^g + P_t^r \ge P_t^{flex} + P_t^l \tag{5.3}$$

$$P_t^{flex} = \sum_{i=1}^n P_t^{flex,j} \tag{5.4}$$

$$P_t^{flex,j} = \sum_{b=1}^{\min(t,D_j)} \sigma_{t-b+1}^j . P_b^j$$
 (5.5)

$$\sigma_t^j \ge 0 \tag{5.6}$$

$$\sum_{i=1}^{t} \sigma_i^j \ge \phi_d^j(t + D^j), \quad t \le T - D_j 
\sum_{i=1}^{t} \sigma_i^j = \phi_d^j(T), \quad T - D^j + 1 \le t \le T$$

$$\forall j \in [1, n]$$
(5.7)

where:

n: number of populations of flexible devices

 $P_t^{flex}$ : Power consumed by all flexible devices at time t

 $P_t^{flex,j}$ : Power consumed by the flexible devices of population j in time t

 $P_b^j$ : Power consumption of flexible devices in population j in  $b^{th}$  stage of their power consumption profile

 $D^{j}$ : Duration of flexible devices of population j

 $\sigma_i^j$ : Number of device starts in population j in time i

 $\phi_d^j(t)$ : Number of devices in population j that has a deadline at or before t

# 5.2.1 Description of the formulation

#### Power balance constraints

Equation 5.4 indicates that the total power demand of the flexible devices is the sum of the power demands of the individual populations. Equation 5.5 expresses the demand of each population at time t. Power consumption of the scheduled devices at a particular time step is the total demand presented by the devices running at t. Demand of the devices that gets scheduled at any instant is the product of the number of starts at that instant and the power consumed by the device at that instant. The power demand of population j at time t, when  $t > D_j$  is given by the sum of the power consumed by the devices scheduled from  $t - D_j + 1$  to t. Similarly, when  $t < D_j$ , the total demand of the population j is the demand associated with devices starts in that population from t to t. This equation ensures uninterruptibility and avoids scheduling devices that have completed their cycle. It is important to note that this equation enables us to schedule not only loads with equal power consumption throughout its cycle, but also devices that undergo multiple paths/states as indicated in [11]. An example of one such load profile is given in Figure 5.1.

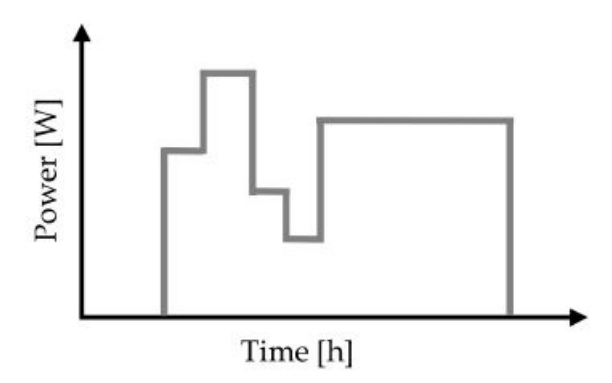


Figure 5.1: Graphical representation of load profile of a device with multiple paths during its cycle.( Adopted from [11])

Equations 5.4 and 5.5 together account for the term  $P_t^{flex}$  in Equation 5.3.

#### **Deadline satisfaction constraints**

Equation 5.7 ensures that the devices of all populations satisfies the deadlines assigned to them. These are simply the extensions of Equations 4.11 and 4.12 explained in Section 4.3.1.

# 5.3 Simulating the facilitator in realistic setting

As mentioned in Chapter 1, the main aim of the project is to simulate the coordination in a more complex setting. This involves treating it as an infinite horizon problem wherein forecasts are generated on a rolling basis. However, when simulation needs to be terminated at some point to investigate the performance. This is pictorially represented in Figure 5.2.To avoid the end of horizon effects due to this termination, the length of the scheduling horizon must be long enough [43]. The total number of iterations considered is termed as Scheduling Horizon (SH).

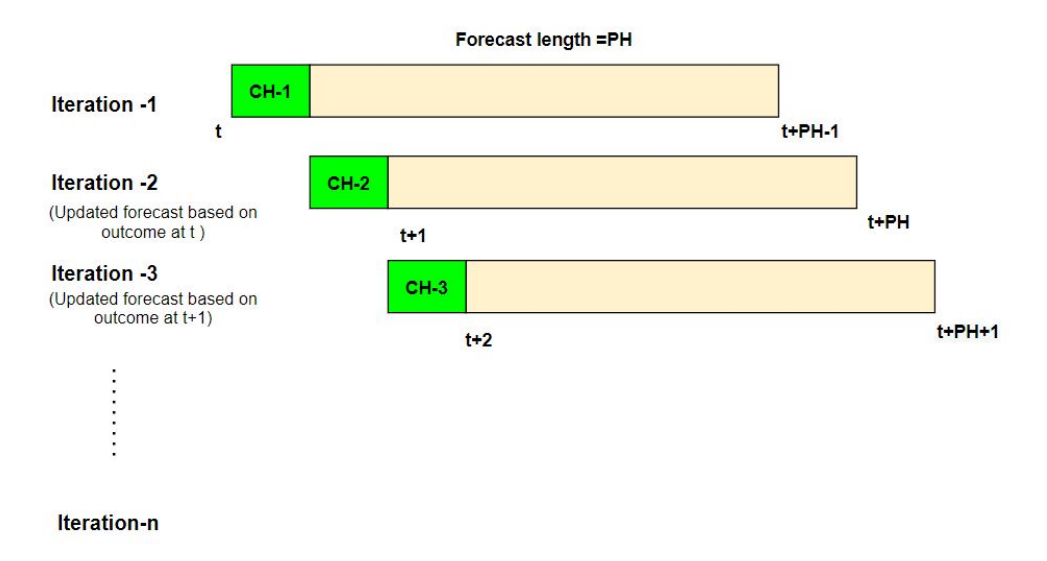


Figure 5.2: Pictorial representation of rolling forecasts generation when performing simulations. The simulation terminates after n iterations.

To test the robustness of the mechanism with the considered scheduling horizon, optimistic and pessimistic forecasts are generated by the facilitator. This analysis is important to validate the performance of the mechanism in situations when the actual environment in which the F-MBC might be put into practice is different from what is being simulated [43]. Since the forecast prices play an important role in influencing what decision the agent will make at any given time, optimistic and pessimistic scenarios are formulated with respect to how the forecasts are generated by the facilitator.

A facilitator with complete information can be considered to generate an "optimistic" forecast when it provides the prices corresponding to the optimal allocation of only those devices that has to be scheduled. Prices corresponding to this allocation are expected to be lower and hence the term optimistic. On the other hand, the "pessimistic" forecast aims to allocate all the devices that becomes available. This means that the prices are expected to be higher than the optimistic forecast. In a realistic setting in which devices become available at each instant and forecasts are communicated on a rolling basis, this means that a pessimistic forecast might not fully utilize the flexibility offered by the devices, especially of those which become available at the end of the forecast horizon.

To understand the formulations behind generating such forecasts, consider a prediction horizon of length T. Based on the availability and the deadlines, the devices can be grouped into four categories, namely:

- Category 1: Devices that become available at t <=T and have their deadlines at or before T.</li>
- Category 2: Devices that become available at t<= T, their deadlines are after T; but they must be scheduled to start to satisfy their deadlines.
- Category 3: Devices that become available at t<=T and have their deadlines after T, but can be scheduled after T to satisfy their deadlines.
- Category 4: Devices that become available after T.

# 5.3.1 Optimistic forecast formulation

The MIQP formulation to generate optimistic forecasts is given below.

$$\underset{P_t^g, \sigma_t^1...\sigma_t^n}{\text{minimize}} \quad \sum_{t \in T} \frac{1}{2} \cdot \frac{(P_t^g)^2}{k} \cdot \Delta t \tag{5.8}$$

subject to,  $\forall t \in T$ 

$$P_t^g \ge 0 \tag{5.9}$$

$$P_t^g + P_t^r \ge P_t^{flex} + P_t^l \tag{5.10}$$

$$P_t^{flex} = \sum_{j=1}^n P_t^{flex,j} \tag{5.11}$$

$$P_t^{flex,j} = \sum_{k=1}^{\min(t,D_j)} \sigma_{t-k+1}^j . P_k^j$$
 (5.12)

$$\sigma_t^j \ge 0 \tag{5.13}$$

$$\left.\begin{array}{l}
\sum_{i=1}^{t} \sigma_i^j \leq \sum_{i=1}^{t} \gamma_i^j \\
\sum_{i=1}^{t} \sigma_i^j \geq \phi_d^j(t+D_j)
\end{array}\right\} \qquad \forall j \in [1, n]$$
(5.14)

where:

 $\sigma_i^j$  Number of device starts in population j in time i  $\gamma_i^j$  Number of devices of population j available at time i  $\phi_d^j(t+D_j)$  Number of devices in population j that has a deadline at or before  $t+D_j$ 

# **Explanation of the constraints**

The optimistic forecast aims to provide the optimal allocation pertaining to the devices that must be scheduled at or before T in order to satisfy their deadlines. This means that this formulation considers the devices belonging to category 1 and category 2, as devices belonging to category 3 can be scheduled after T and still meet their deadline. This is mathematically expressed in Equation 5.14. The formulation also ensures that the total number of devices scheduled at any instant does not exceed the number of devices available.

# 5.3.2 Pessimistic forecast formulation

The optimization problem to generate pessimistic forecasts is given below.

$$\underset{P_t^g, \sigma_t^1 \dots \sigma_t^n}{\text{minimize}} \quad \sum_{t \in T} \frac{1}{2} \cdot \frac{(P_t^g)^2}{k} \cdot \Delta t \tag{5.15}$$

subject to,  $\forall t \in T$ 

$$P_t^g \ge 0 \tag{5.16}$$

$$P_t^g + P_t^r \ge P_t^{flex} + P_t^l \tag{5.17}$$

$$P_t^{flex} = \sum_{i=1}^n P_t^{flex,i}$$
 (5.18)

$$P_t^{flex,j} = \sum_{k=1}^{\min(t,D_j)} \sigma_{t-k+1}^j . P_k^j$$
 (5.19)

$$\sigma_t^j \ge 0 \tag{5.20}$$

$$\Sigma_{i=1}^{t} \sigma_{i}^{j} \leq \Sigma_{i=1}^{t} \gamma_{i}^{j} 
\Sigma_{i=1}^{t} \sigma_{i}^{j} \geq \phi_{d}^{j} (t + D_{j}) 
\Sigma_{i=1}^{t} \sigma_{i}^{j} = \Sigma_{i=1}^{t} \gamma_{i}^{j}, \quad T - D_{j} + 1 \leq t \leq T$$
(5.21)

where

T Prediction horizon  $\gamma_i^j \qquad \text{Number of devices of population } j \text{ available at time } i \\ \sigma_i^j \qquad \text{Number of device starts in population } j \text{ in time i} \\ \phi_d^j(t+D_j) \qquad \text{Number of devices in population } j \text{ that has a deadline at or before } t+D_j$ 

## **Explanation of the constraints**

The difference between 5.3.1 and 5.3.2 is the last sub-equation in 5.21. It states that the total number of devices scheduled must equal the total number of devices available. This means that all devices that become available, i.e; devices belonging to categories 1 to 3 are scheduled in this formulation.

# 5.4 Performance Indicators

This section introduces the quantities that will be used in the upcoming chapters to evaluate the performance of F-MBC mechanism as a coordination scheme.

# 5.4.1 Overall objective function

The allocation predicted by the facilitator with complete function which minimizes the overall generation costs characterized by affine marginal cost function with a constant slope, corresponds to a Nash Equilibrium, according to Theorem 4 of [3]. Therefore, comparing the value of the objective functions achieved using the demand predicted by the facilitator with complete information about the system and the demand resulting as a consequence of using F-MBC, it can be determined whether the approach attains good system level performance or not.

# 5.4.2 Cost of starting

Cost of starting refers to the total price paid by the agent when it gets scheduled at time t. By computing the cost of starting using the prices determined by the optimizer in the initial run and market clearing prices , it can be determined whether the agents pay close to the optimal costs or not. Cost of starting can also highlight the monetary advantage accompanied with taking part in the F-MBC scheme, when compared to a situation when the loads are not subjected to the coordination mechanism. Therefore, this metric can be used to answer the question :

What is the benefit of participating in F-MBC mechanism?

# 5.4.3 Regret

While the cost of starting compares the actual costs the participating agents pay with the optimal costs that the agents could have paid, regret compares among the costs paid by the agents when coordinated using the F-MBC scheme. Regret is defined as the difference between actual cost paid by the device and the lowest possible cost that it could have achieved by using the mechanism. It is evaluated for each device participating in the scheme. With 5.4.2 and 5.4.3, the following question can be answered:

Does F-MBC mechanism achieve good device level performance?

# 5.5 Summary

This chapter introduces and explains the extensions made to the MIQP formulation used by the facilitator. These help in determining the optimal outcome when scheduling heterogeneous populations of uninterruptible loads that can differ in their duration and/or power consumption, thereby enabling to test the ability of F-MBC in scheduling them. The chapter concludes by laying out the metrics which helps in assessing the performance when tested under different operation conditions, which will be discussed in the upcoming chapters.

# **Chapter 6**

# Coordination of heterogeneous populations using F-MBC

This chapter aims to investigate the attributes that affect the coordination of heterogeneous populations of deferrable loads with different device characteristics under a weakly deadline ordered case. Section 6.2 introduces the different cases considered, followed by detailed analysis of the considered test cases is presented in Section 6.3.

# 6.1 Motivation

This chapter aims in answering the research question, "What factors influence the allocation of populations with different characteristics?" This question is important to address when different populations of flexible devices are considered, because the information used by the agents when applying the bidding policy by the agents differ according to the device's characteristics, which eventually affects the schedule and performance of the mechanism when its application is extended to accommodate loads with different attributes.

In order to determine that, a system in which agents have identical deadlines is modelled in this chapter. Since the results presented in [3] consisted of a system with single population of devices with uniform power consumption, two populations of devices with uniform power consumption are considered for analysis in this chapter. The simulations are performed in MATLAB. The MIQP problem formulation is modelled using YALMIP optimization toolbox [31] and solved using Gurobi optimizer.

# 6.2 Simulation setup

The aim of this chapter is to analyze the performance of the performance of the scheme when coordinating two populations of devices with simple load profiles. Load profiles characterized by more dynamic power consumption pattern is analyzed in Chapter 7.

In general, the three main attributes of any load profile is :

- Duration
- Power Consumption at each time step
- · Overall energy consumption

Since the analysis presented in this chapter restricts itself to scheduling two populations of uniform power consuming loads, overall energy consumption is dependent on the duration and power consumption.

Therefore, by using these attributes,  $2^2 = 4$  combinations of populations of devices can be formulated. These are illustrated in Table 6.1.

Table 6.1: Possible combinations when considering two populations of devices with uniform power consumption

Duration	Power consumption at each step	Overall Energy Consumption
Different	Different	Same
Same	Different	Different
Different	Same	Different
Different	Different	Different

The upcoming sections will deal with the analysis of each of these highlighted combinations. The parameters introduced in Section 5.4 will be used to assess the performance of the mechanism.

Since this is a first attempt to extend the mechanism to heterogeneous loads, a simple experimental setting is considered. For analysis, 2 populations of 500 devices each are simulated under the following conditions.

- The scheduling horizon for the simulation, i.e; T=96.
- All devices are available from t=1.
- The deadlines of all the devices are at t=96.
- Inflexible load and renewable generation values are set to zero.
- Forecasts are assumed to have almost zero day ahead uncertainty.

# 6.3 Simulation test cases

# 6.3.1 Combination 1: Devices with same overall energy consumption , but with different duration

Under this combination, we consider two populations of devices with the following characteristics:

• Population 1: 8 kW \* 3 timesteps

• Population 2: 3 kW \* 8 timesteps

They are graphically represented in Figure 6.1.

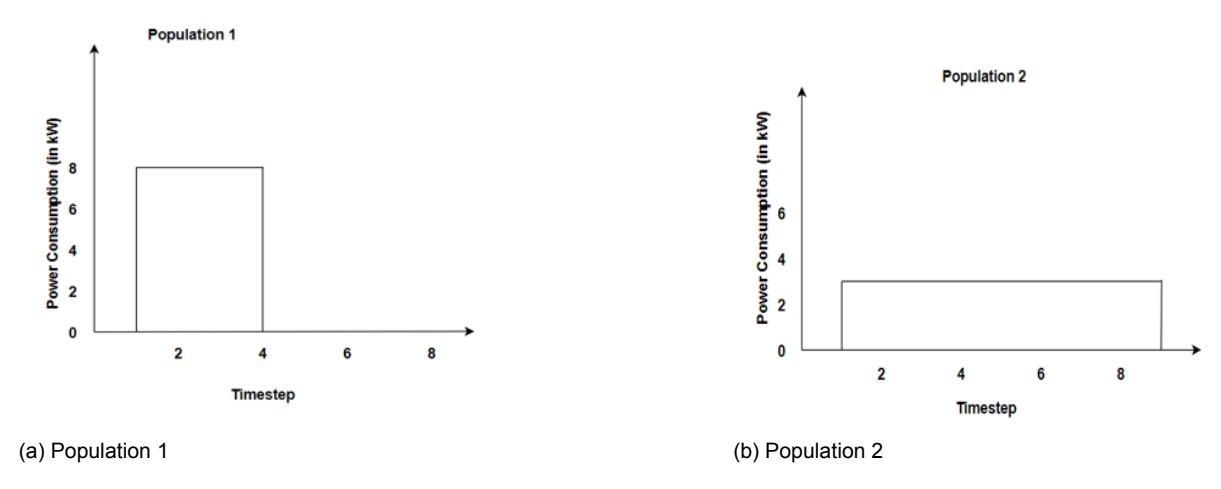


Figure 6.1: Graphical representation of the populations of devices: Combination 1

## Results and analysis

The demand profile obtained by using F-MBC and the optimal demand profile predicted by the facilitator is given in Figure 6.2.

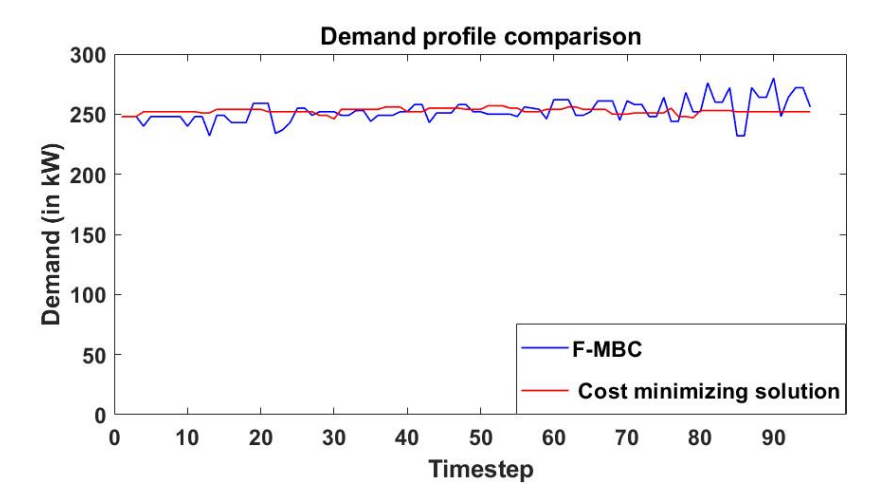


Figure 6.2: Demand profile comparison: Combination 1

To begin the analysis, the objective function is compared because the main motive behind utilizing optimal prices is to ensure that the overall generation costs are reduced. The values of the overall objective function obtained is listed in Table 6.2.

Objective function value : Optimal	Objective function value : F-MBC
3.031811 e+05	3.035572 e+05

Table 6.2: Objective function comparison: Combination 1

From Table 6.2, it can be observed that the deviation from the optimal coordination is only about 0.124 %. However, from Figure 6.2, it can be observed that there are some instances where the demand realized using F-MBC is lower than the demand from the MIQP, especially at the initial timesteps. This gets compensated by achieving demand higher than the optimal at the end of the horizon.

In order to understand the reason behind this, the schedule achieved by the F-MBC mechanism for population 1 and 2, and the scheduled predicted by the optimizer is presented in Figure 6.3.

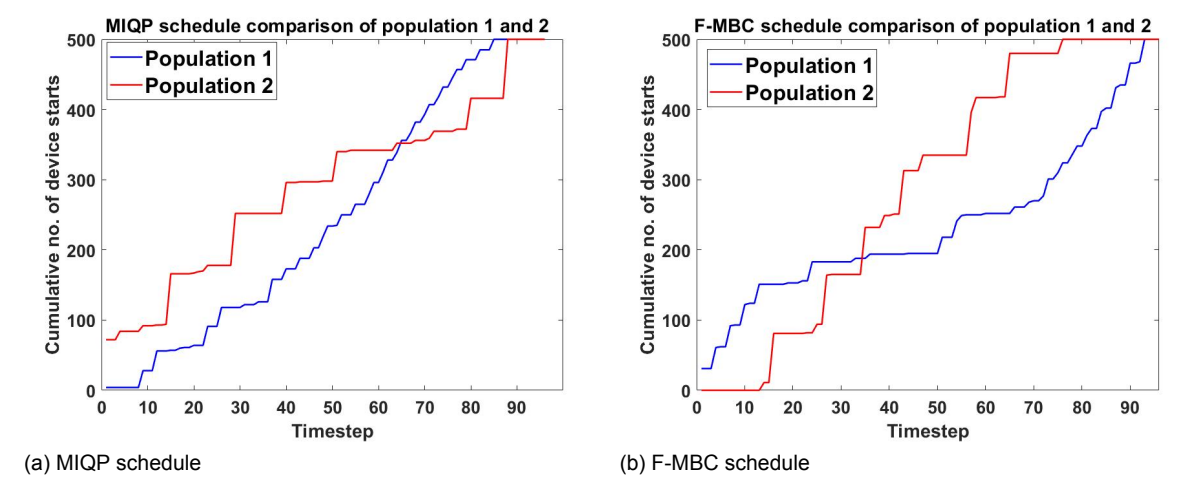


Figure 6.3: Schedule comparison: Combination 1

From Figure 6.3a, it can be seen that the optimizer determines the demand at each timestep by scheduling a certain number of devices belonging to both populations, for instance 4 and 72 devices of population 1 and 2 respectively at t=1. From the bidding perspective, this means that these devices must have the submit corresponding threshold bids in order to realize that demand. However, the characteristics of the devices and the fact that the devices are deadline ordered, lead to schedule presented in Figure 6.3b.For instance, on upon looking into the threshold bids submitted by the devices belonging to both populations in Figure 6.4, we can observe that the threshold bids submitted by the agents in these populations at the first timestep are 24.7 and 24.6 a.u respectively. Since the agents are weakly deadline ordered, the bids of all the agents in a population is the same. Moreover since all devices are available from the first timestep, each device will submit their bids to the auctioneer and even minor differences in their threshold bids (0.1 a.u for t=1) can lead to a possibility of them not getting allocated, especially at the initial timesteps, thereby leading to a lesser demand obtained than what was predicted by the optimizer. This is seen in Figure 6.5, where only the devices in population 1 get allocated.

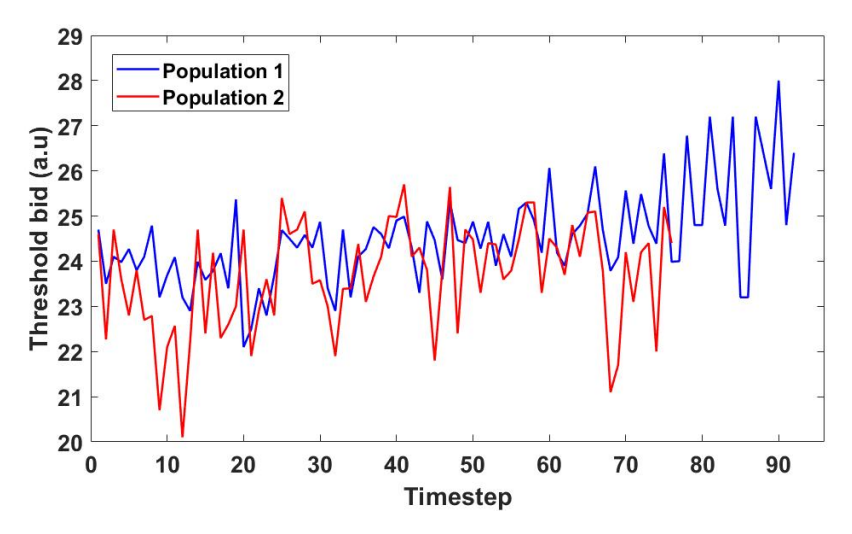


Figure 6.4: Threshold bids submitted by the last allocated agent belonging to population 1 and 2

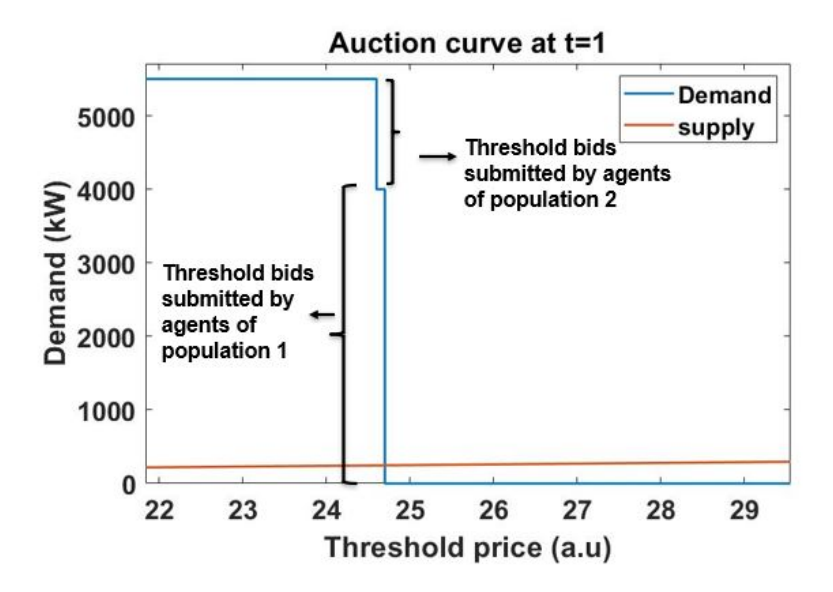


Figure 6.5: Auction curve at t=1

There are many factors that lead to a population having a higher threshold bid. To understand that, the equation for threshold bid for a population belonging to population j at time t is given in Equation 6.1. The main attribute affecting the threshold price calculation are the prices that are taken into account for calculation of the optimal expected cost, abbreviated in Equation 6.1. Since the deadlines of all the devices are all at the last timestep, the duration determines from which timestep the calculation of optimal expected costs commence via backward induction (from  $t \le d^j - D^j$ ) and also the prices that are taken into consideration for calculation of each of the terms in Equation 6.1. From Figure 6.4, it can be seen that the unallocated agents of population 1 bid higher as they approach their deadline, at the end of the scheduling horizon.

$$z_t^j = \frac{C_{t+1}^{*j} - \sum_{i=1}^{D^{j-1}} \bar{x}_{t+i} \cdot P_i^j \cdot \Delta t}{P_0^j \cdot \Delta t}$$
(6.1)

where:

 $C_{t+1}^{*j}$ : Optimal expected cost at t+1

 $\sum_{i=1}^{D^{j}-1} \bar{x}_{t+i} \cdot P_i^j \cdot \Delta t$ : Expected cost for the reminder of the device's cycle, when scheduled at time t.

 $d^{j}$ : Deadline of the device  $D^{j}$ : Duration of the device

In order to determine the effect of such deviations from the optimal schedule from the device's point of view, the total cost paid by the device as a result of starting at a particular timestep, (referred to as the cost of starting), for the devices in population 1 and 2 determined based on the MIQP and F-MBC schedule are presented in Figure 6.6. The cost of starting here is represented in terms of unit energy, since in the upcoming cases, populations with different energy consumption will be considered.

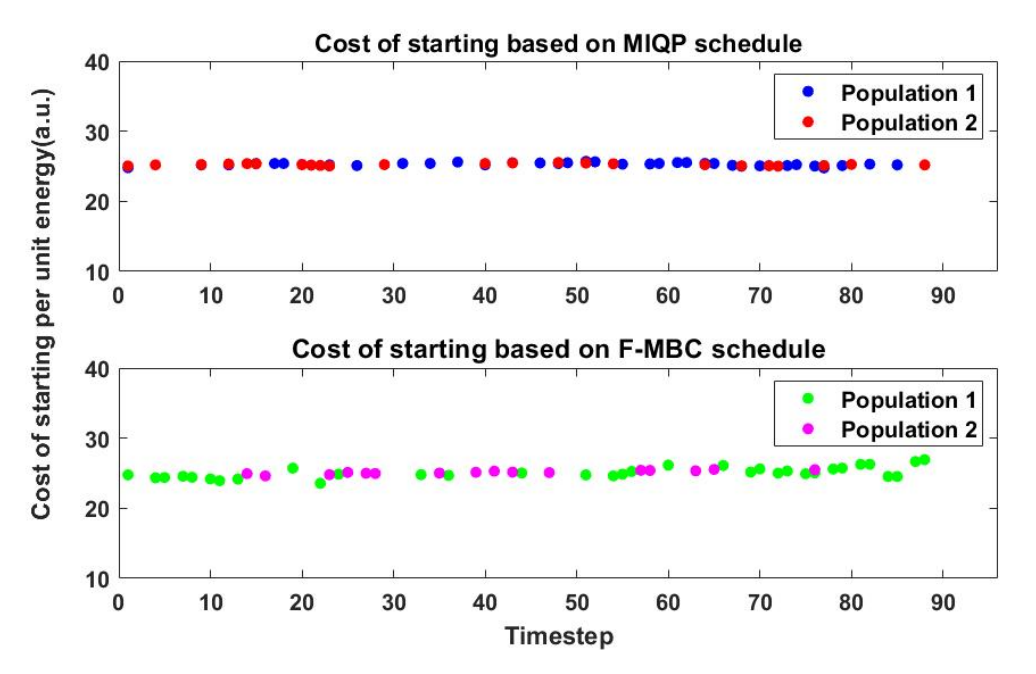


Figure 6.6: Top panel: Cost of starting based on MIQP schedule. Bottom panel: Cost of starting based on F-MBC schedule.

Upon comparison , it was observed that the optimizer has scheduled the devices of population 1 and 2 with an average of 25.28 a.u and 25.24 a.u respectively, while F-MBC was able to achieve an average cost of starting of 25.21 a.u and 25.14 a.u for the respective populations. Slightly lesser average values using F-MBC indicates that a significant number of devices in both the populations get scheduled at those instances when the demand realized is less than the optimal demand.

Now, the regret of the device agents is computed. Regret is defined as the difference between the actual price paid by the agent and the lowest possible price that could have been achieved in hindsight. Figure 6.7 represents the distribution of regret for both populations as a consequence of participating in the F-MBC scheme, expressed in percentage of the actual cost paid by the agent.

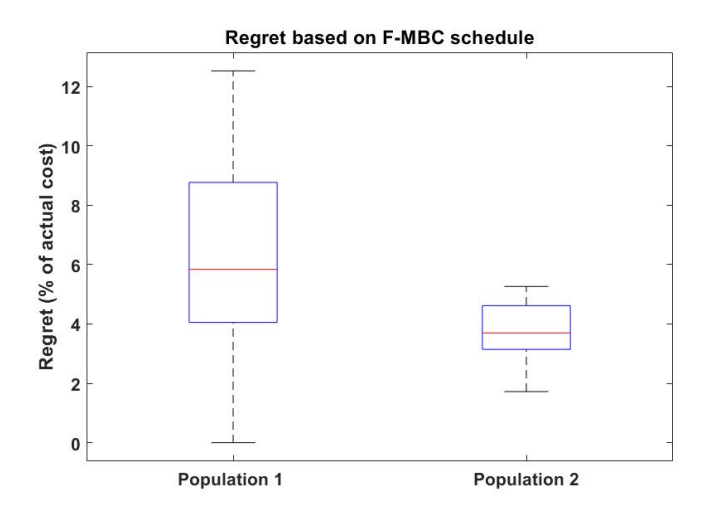


Figure 6.7: Distribution of regret of device agents: Combination 1

It can be observed from Figure 6.7 that the range of regret is larger for population 1. This is mainly because the devices belonging to population 1 get scheduled both at the initial timesteps and also at the last few timesteps closer to its deadline, thereby leading to those agents paying a higher cost than the agents scheduled at the beginning, despite having the same availability and deadline. On the other hand, the devices belonging to population 2 have a smaller regret with an average of 3.76 %, because most of the devices get scheduled at those instances (t=14 to t=75) when the total cost realized by the agents are not that significantly different from each other.

# 6.3.2 Combination 2: Devices with different power consumption , but with same duration

Since duration of the devices was identified as an important factor influencing the deviation from the optimal allocation, two populations having the same duration are considered in this section. The characteristics of the devices are as follows:

• Population 1: 3 kW \* 7 timesteps

• Population 2: 5 kW \* 7 timesteps

These are represented in Figure 6.8.

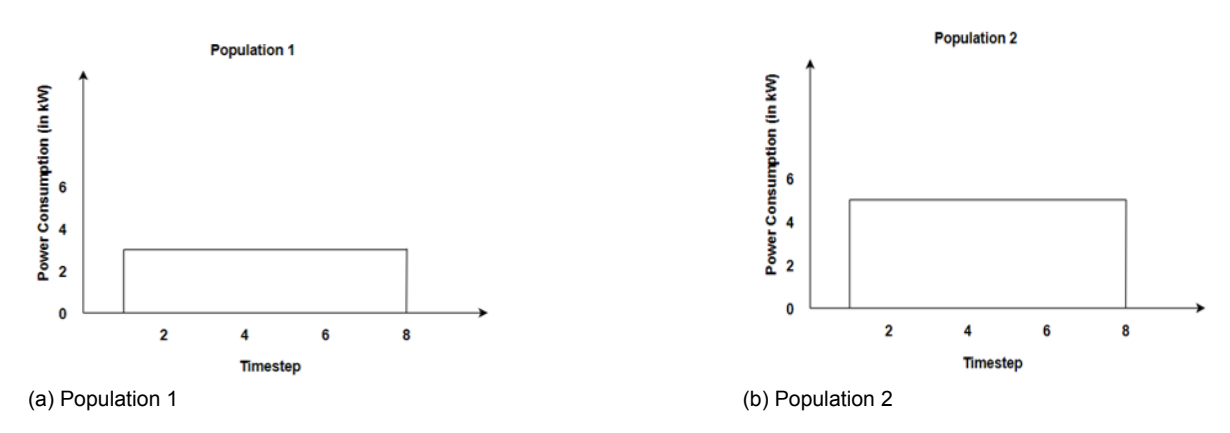


Figure 6.8: Graphical representation of the populations of devices: Combination 2

# **Results and Analysis**

Similar to the previous case, the demand profiles obtained based on the MIQP schedule and the F-MBC outcome is compared in Figure 6.9 .

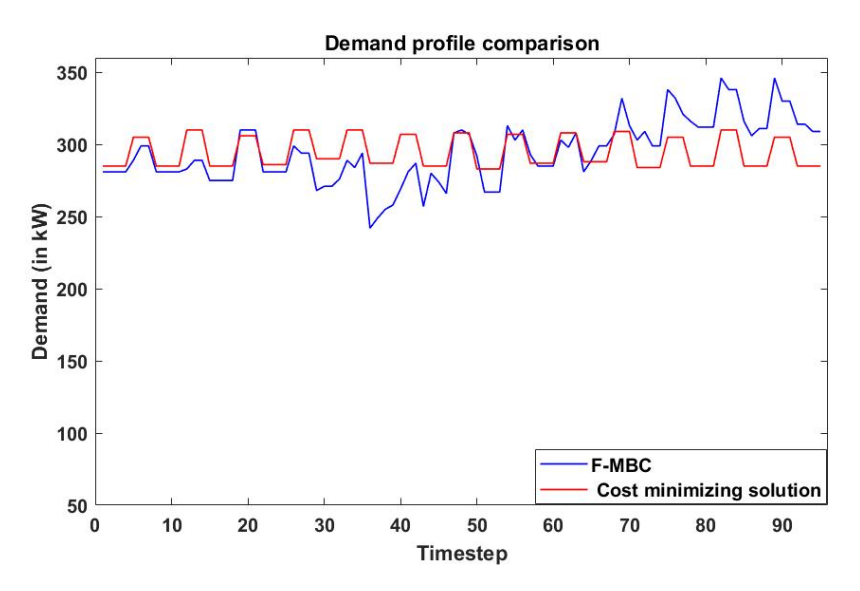


Figure 6.9: Demand profile comparison: Combination 2

The corresponding total generation cost values are listed in Table 6.3.

Objective function value : Optimal	Objective function value : F-MBC
4.13202 e+05	4.14846 e+05

Table 6.3: Objective function comparison: Combination 2

The relative error when compared to optimal generation cost is only about 0.397 %, which indicates towards system level performance. Similar to the previous testcase, when compared with the optimal profile, higher demand is observed at the end of the scheduling horizon due to lower demand realized at earlier time intervals.

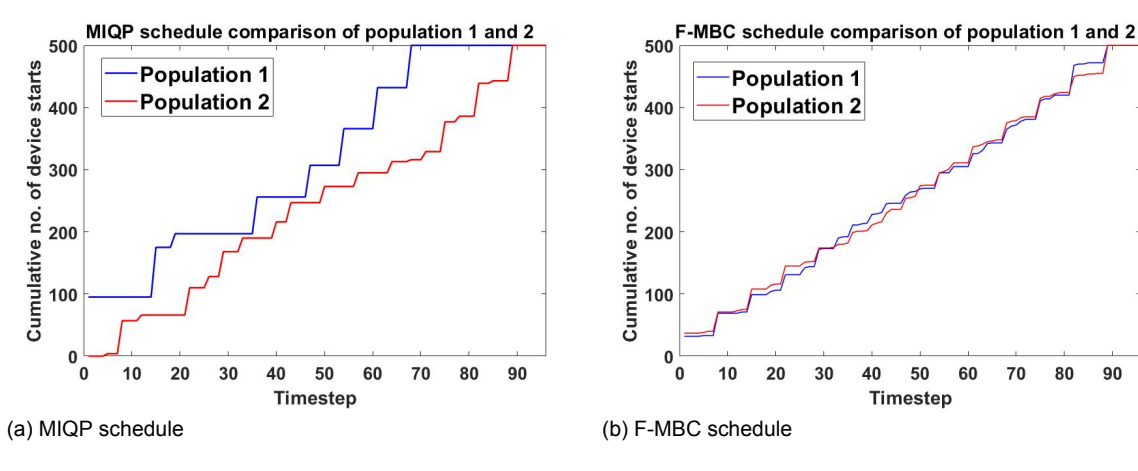


Figure 6.10: Schedule comparison: Combination 2

As anticipated from the conclusion in Section 6.3.1, devices from both the populations get allocated as seen in the F-MBC schedule from Figure 6.10b. This is because the prices used for calculating the optimal expected cost and the cost for the reminder of the cycle are essentially the same, as a consequence of having the same duration. Since populations of devices with constant power consumption are considered, the power consumption of the populations do not affect the threshold bid, as it simply acts as a scaling term. This means that all the devices bid with the same thresholds throughout the course of simulation as seen in Figure 6.11a. This means that the tie breaking mechanism resolves ties between bids of both populations, unlike in the previous combination, where ties are cleared among bids belonging to one population. This is seen in the auction curve shown in Figure 6.11b, where the demand curve is simply one large step.

90

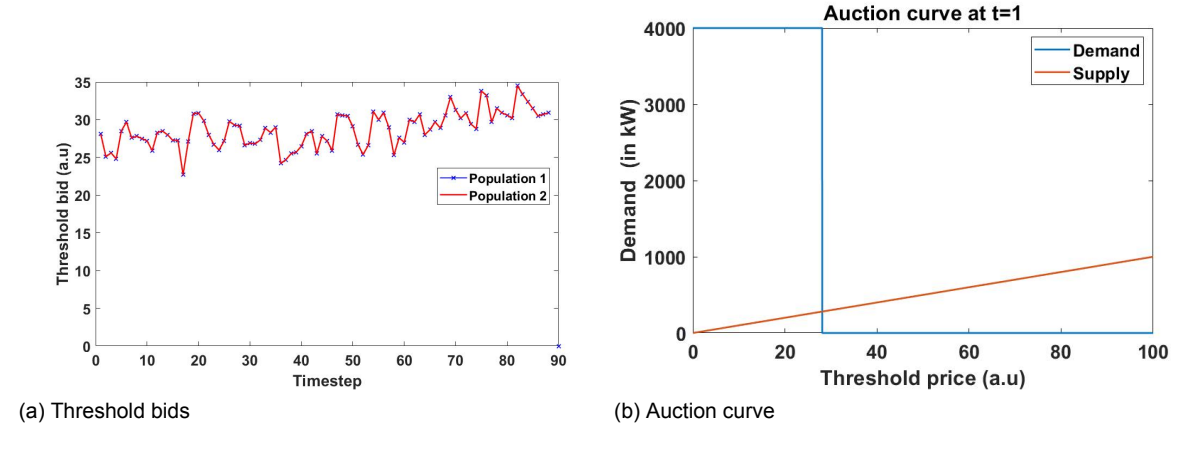


Figure 6.11: Threshold bids and auction curve - Combination 2

Though this testcase presents the possibility to schedule agents from both populations, it can be observed from the demand profile that the demand predicted by the optimizer is not being met at some instances. Moreover, the scheduled achieved by F-MBC is different from the optimizer. Also from the F-MBC schedule, it can be observed that despite having the same threshold bids, the number of devices that get allocated in each population is different. This can be linked to the working of tie breaking mechanism. As mentioned earlier in Section 4.2, when a tie situation occurs, the auctioneer selects the cut-off random number is such a way that supply matches the demand. Graphically, this indicates the point of intersection of supply and demand curves. Depending upon the demand of the system, that power consumption of the devices play a role in the number of devices that get should allocated at a particular timestep, even if the device agents have the same threshold bid.

Similar to the previous testcase, the optimality from the agents' perspective can be investigated by evaluating the cost of starting based on MIQP and F-MBC schedules, as seen in Figure 6.12. The optimizer was able to achieve an average cost of starting of 29.5 and 29.53 for population 1 and 2 respectively. The F-MBC allocation led to an average cost of starting of 29.3 a.u and 29.4 a.u for population 1 and 2.

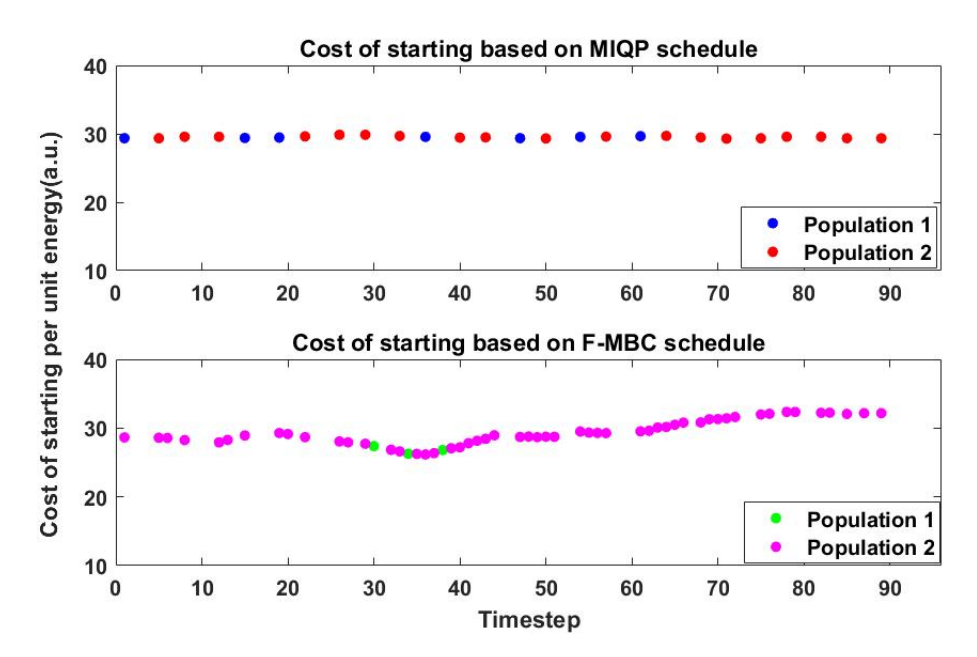


Figure 6.12: Cost of starting comparison: Combination 2

Lastly the regret distribution of the participating agents is presented in Figure 6.13. The agents belonging to both populations have similar range of regret, with average values of 10.36 and 10.63 respectively. This is primarily because the devices have same duration. Agents with the highest regret will be the ones that get scheduled at the end of the horizon and the agents with the lowest regret will be the ones that were scheduled at those instances when the cost of starting is low (from t=30 to 40, from Figure 6.12).

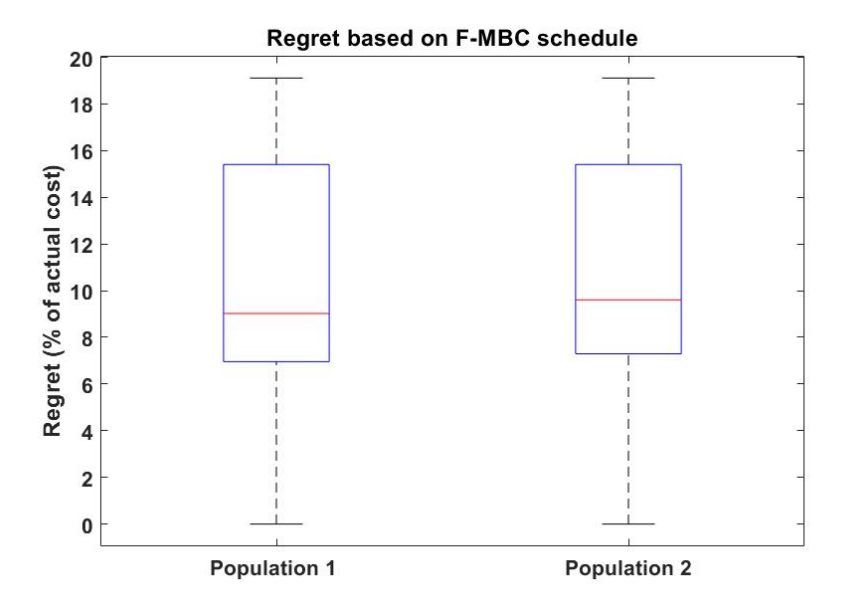


Figure 6.13: Distribution of regret of device agents: Combination 2

# 6.3.3 Combination 3: Devices with same power consumption , but with different duration

To investigate further the role of power consumption in allocation of device agents, devices with same power consumption are studied in this section. The characteristics of devices considered are as follows:

• Population 1: 6 kW \* 4 timesteps

• Population 2: 6 kW \* 7 timesteps

These are represented pictorially in Figure 6.14.

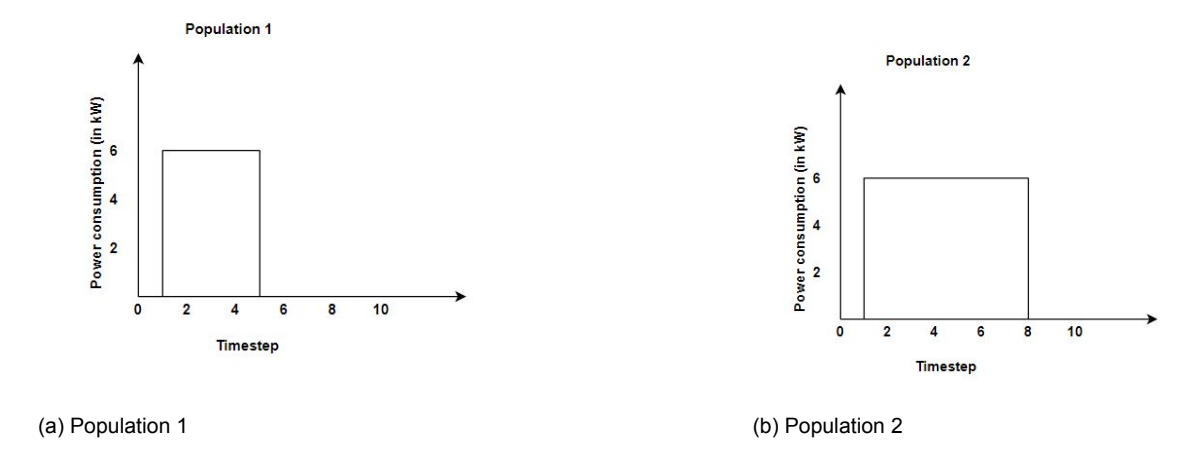


Figure 6.14: Graphical representation of the populations of devices: Combination 3

# **Results and Analysis**

Similar to the previous case, the demand profiles realized based on the MIQP and F-MBC schedule is compared, as represented in Figure 6.15 .

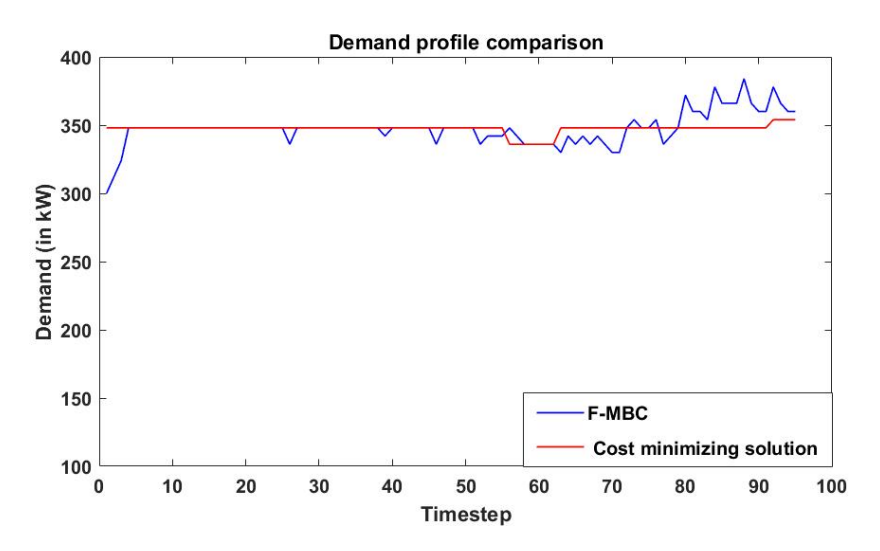


Figure 6.15: Demand profile comparison: Combination 3

The corresponding objective function values are listed in Table 6.4.

Objective function value : Optimal	Objective function value : F-MBC
5.73213 e+05	5.73829 e+05

Table 6.4: Objective function comparison: Combination 3

From Table 6.4, it can be seen that the F-MBC was able to coordinate these devices with an overall deviation of 0.1074 % from the optimal solution, thus indicating good overall performance.

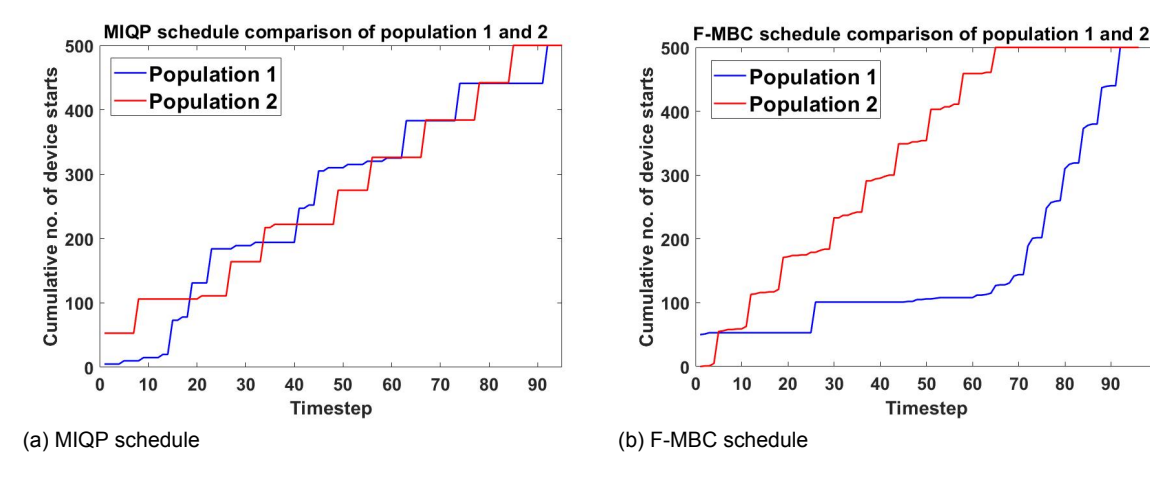


Figure 6.16: Schedule comparison: Combination 3

To understand the reason behind the deviation from the optimal allocation, the schedules of MIQP and F-MBC are studied. From Figure 6.16a, it can be seen that the facilitator predicted the optimal demand profile by scheduling certain number of devices in both the populations similar to the previous testcases. However, from Figure 6.16b, it can be seen that the devices that get of population 2 get more rapidly allocated when compared to population 1, especially from t=25 to t=61. All the devices in population 2 get scheduled at t=65, while only 127 devices in population 1 were scheduled upto that timestep. However, in spite of the mentioned difference in allocation, the F-MBC was able to attain the demand predicted by the facilitator at most instances. This is because the power demand of these populations are same, which implies the predicted demand can be realized by scheduling a certain number of devices in either populations.

Now,in order to understand the reason for this allocation, the threshold bids of the last allocated agent in both populations are given in Figure 6.17. It can be seen that both populations bid very closely, with a maximum difference between the populations being as low as 0.001 from t=3 to t=25. However since all unscheduled devices of population 2 bid with the same price, even minor differences in the bids can lead to the devices from population 1 not being allocated.

To understand the reason behind high threshold bid and the consequent allocation of population 2 in the initial timesteps, the optimal expected costs and the corresponding threshold prices are calculated by backward induction based on the prices forecasted at t=1 is given in Figure 6.19a and Figure 6.19b respectively. From the Figure 6.19a, we can see that the optimal expected costs calculated for both the populations undergo a similar trend with a drop in the prices between the timesteps t=63 to t=56, due to the dip in the forecasts in the same instances. From figure 6.19b, we can see that at t=52,

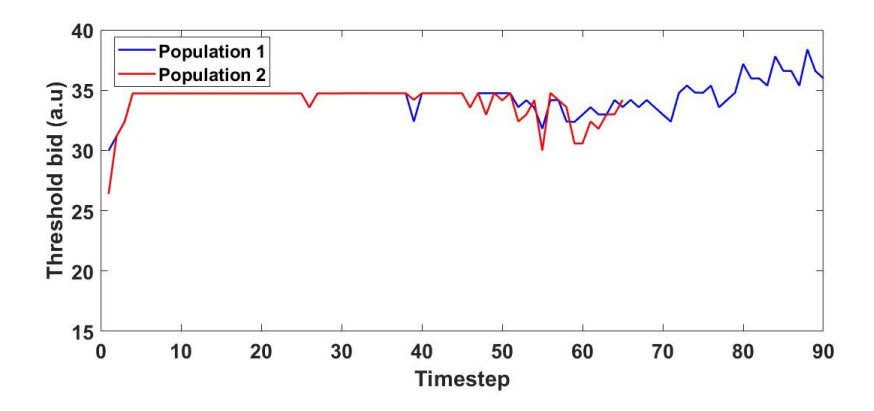


Figure 6.17: Threshold bids submitted by the agents belonging to population 1 and 2: Combination 3

both populations have the same threshold bids calculated. However, from the next iteration backward upto t=1, the bids change to 29.975 and 26.4 for population 1 and 2 respectively. To analyze the reason for this, the formula for determining the threshold prices given in Equation 6.1 is considered again .Though the optimal expected costs at t=52 are equivalent to their energy difference (1411.2/806.25= 1.75=42/24), the duration of reminder of the cycle is twice for population 2 (6 timesteps) when compared to population 1 (3 timesteps). Since the forecast prices were the same from t=1 to t=52 as seen in Figure 6.18, this led to the case where the difference between the optimal expected cost calculated and the cost of the reminder of the cycle if started at t=1 to be higher for population 2 than for population 1. Since the threshold bid was about 29.975, the auction cleared with the same price, leading to 50 devices being allocated post the tie breaking mechanism.

Therefore, we can see here that the duration has an impact on the threshold bids and the number of devices allocated in the population that bids higher depends on the difference between the demand at the equilibrium point of auction curves and the devices scheduled at previous instances. In other instances when the threshold bids were higher for population 2, means that the difference between the optimal expected cost and the cost for the reminder of the cycle was higher than that of population 1.

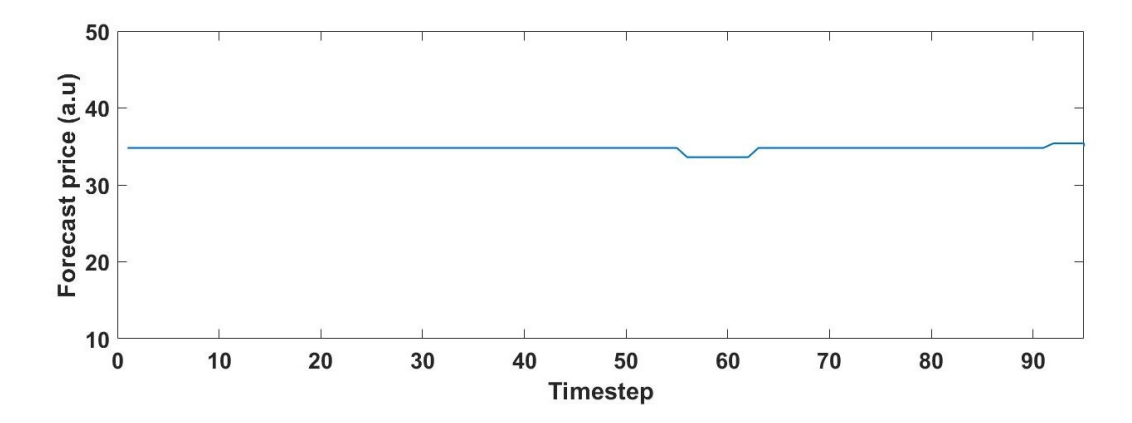
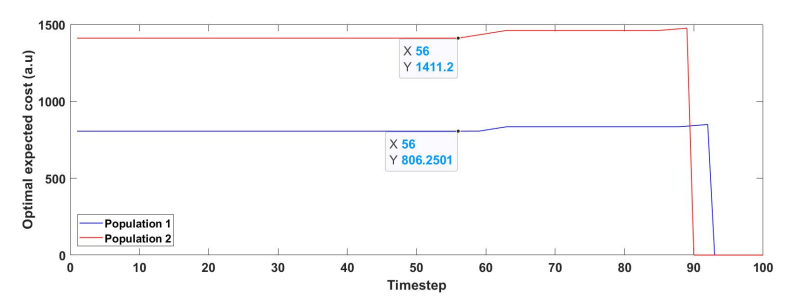
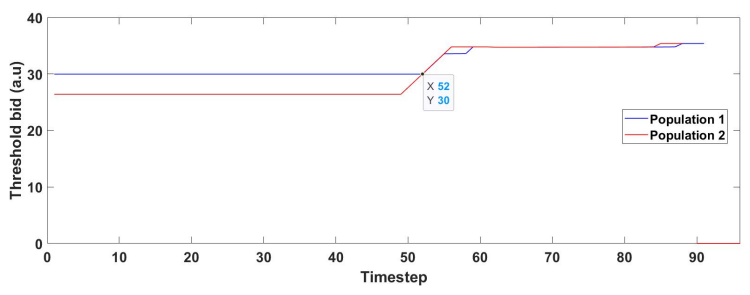


Figure 6.18: Prices forecasted at t=1



(a) Optimal expected cost calculated by backward induction at t=1



(b) Threshold bids calculated by backward induction at t=1

Figure 6.19: Optimal expected costs and threshold bids calculated by devices based on the prices forecasted at t=1:Combination 3

Now, the impact of this allocation on device level can be assessed by determining the total cost of starting based on MIQP schedule and F-MBC schedule as shown in Figure 6.20. It was found that based on the MIQP schedule , the average total cost of starting for population 1 and 2 are 34.72 a.u and 34.69 a.u respectively, while F-MBC was able to achieve an average starting cost of 34.93 a.u and 34.52 a.u for the respective populations. Average cost of starting is higher for population 1 because more than 70 % of the devices were scheduled at the end of the horizon, thereby being subjected to higher market prices.

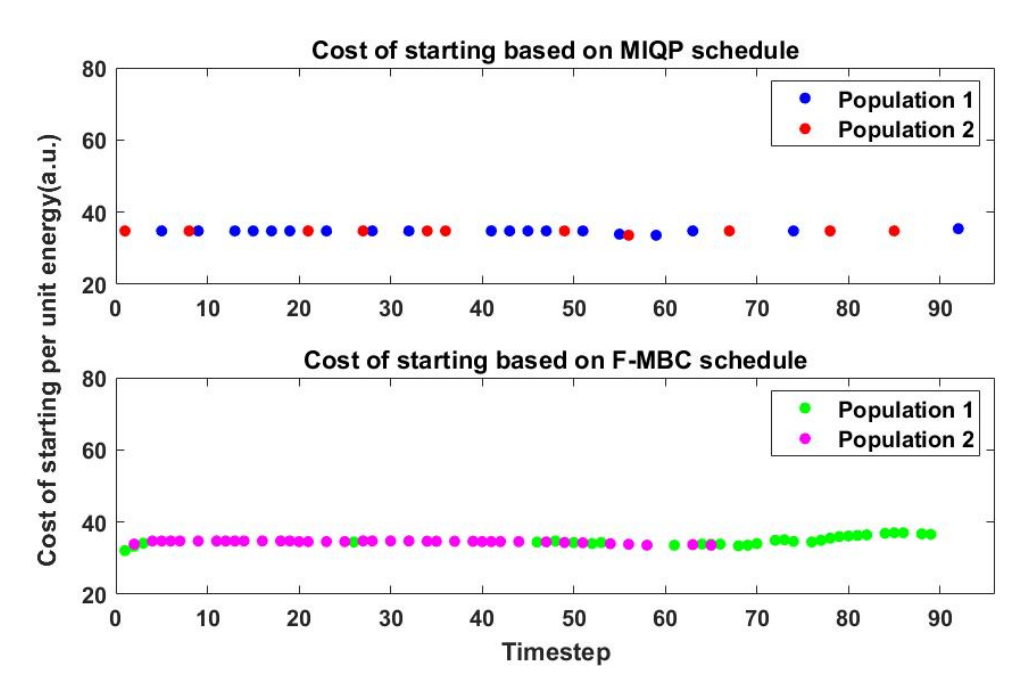


Figure 6.20: Top panel: Cost of starting based on MIQP schedule. Bottom panel: Cost of starting based on F-MBC schedule.

Similar to previous testcases, the regret distribution of the agents is compared. Based on Figure 6.21, it can be seen that the range of regret of the agents belonging to population 1 is higher than of population 2. Again, the possible reason could be due to the fact that the devices in population 1 get scheduled at the very beginning when the demand is the lowest and also the end of the horizon, during which the demand is the highest. The lower regret associated with population 2, with an average of 3.78 %, can be explained with the almost flat cost of starting in Figure 6.20 between t=2 and t=51,during which about 80 % of the devices in the population were scheduled.

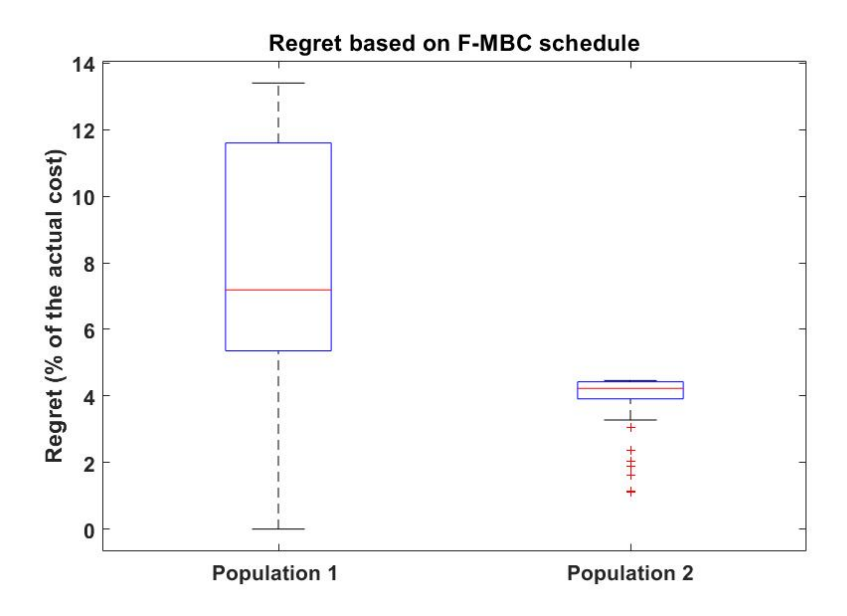


Figure 6.21: Distribution of regret of device agents: Combination 3

# 6.3.4 Combination 4: Devices with different power consumption and different duration

This testcase can be used to validate the conclusions drawn in the previous combinations. The only difference of this testcase when compared to the simulation setup in Section 6.3.1 is that the optimal expected costs will be different here, while it was almost the same in the latter as the energy consumption of the devices are the same.

• Population 1: 4 kW \* 6 timesteps

• Population 2: 7 kW \* 5 timesteps

These are represented in Figure 6.22.

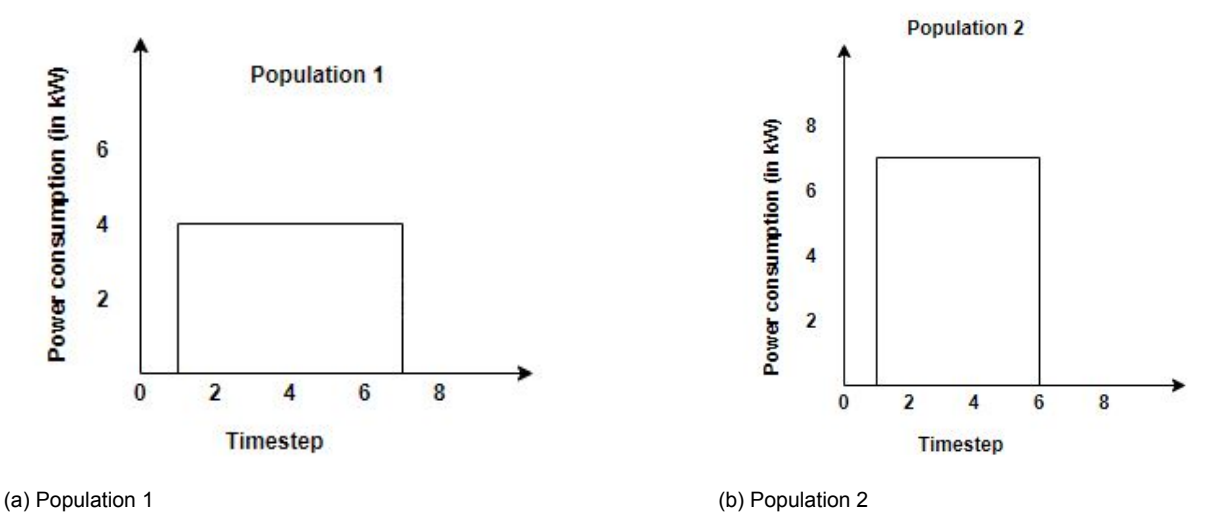


Figure 6.22: Graphical representation of the populations of devices: Combination 4

### **Results and Analysis**

The analysis is carried out in the same sequence as in the previous testcase. First, the demand profiles obtained based on the MIQP schedule and the F-MBC outcome is compared, as represented in Figure 6.23.

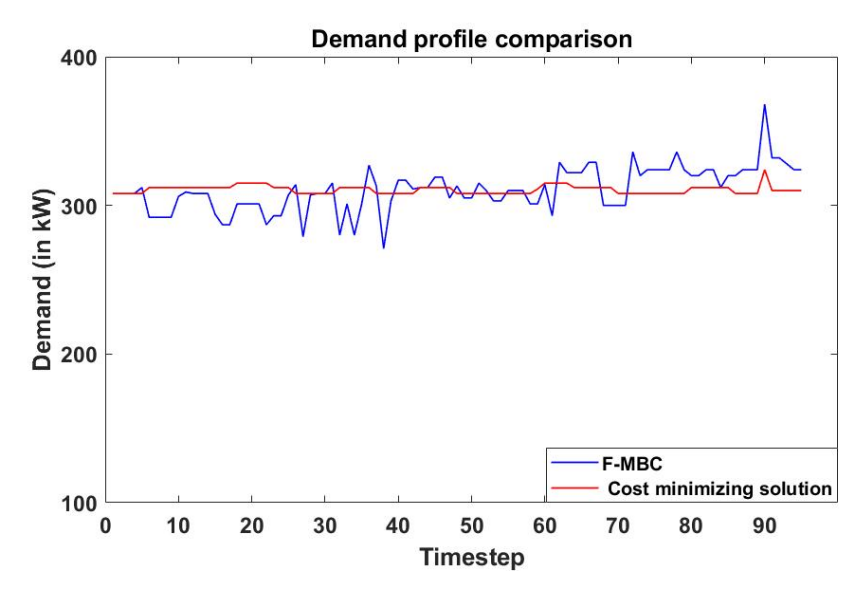


Figure 6.23: Demand profile comparison: Combination 4

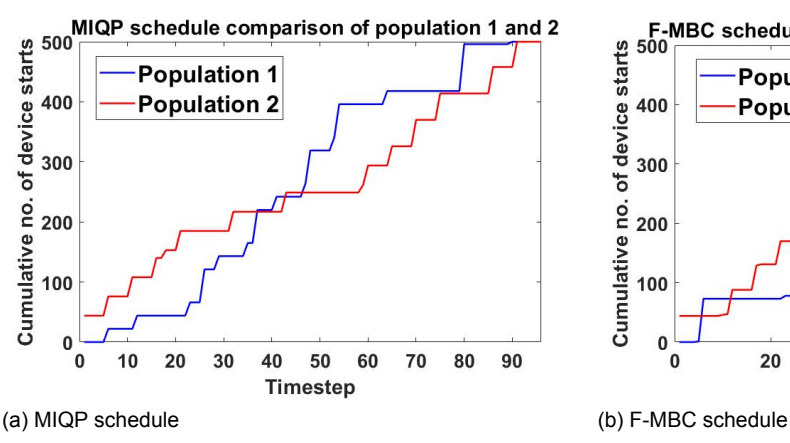
The corresponding total generation cost values are listed in Table 6.5.

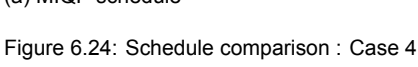
Objective function value : Optimal	Objective function value : F-MBC
4.58062 e+05	4.59058 e+05

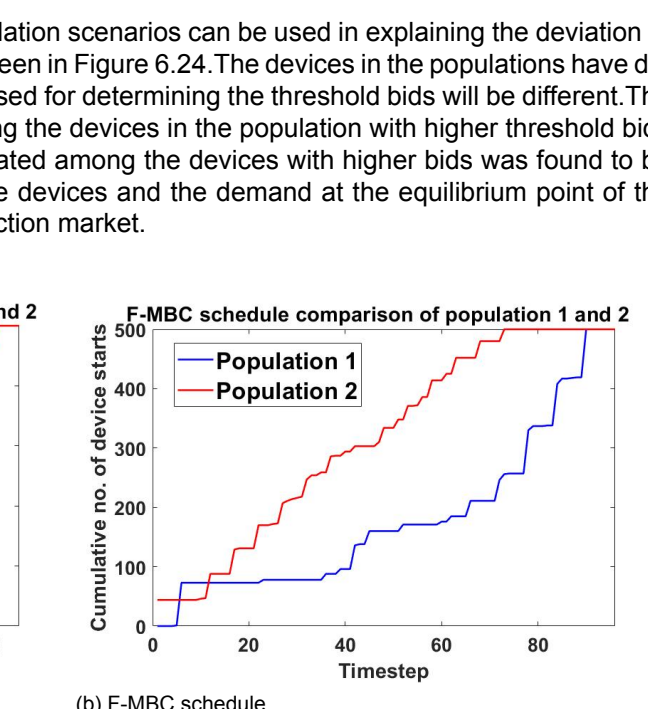
Table 6.5: Objective function comparison: Combination 4

From Table 6.5, it can be seen that the overall generation cost obtained by using F-MBC deviates as little as 0.217 % from the optimal solution, thereby indicating its ability to achieve good system level performance, when used for scheduling the above mentioned populations of devices.

The observations made in the previous simulation scenarios can be used in explaining the deviation of the allocation from the optimal allocation as seen in Figure 6.24. The devices in the populations have different duration, which imply that the prices used for determining the threshold bids will be different. The facilitator was observed to resolve ties among the devices in the population with higher threshold bids .Again, the number of devices that get allocated among the devices with higher bids was found to be dependent on the power consumption of the devices and the demand at the equilibrium point of the supply and demand curves in the double auction market.







Now to investigate the optimality from the device perspective, the cost of starting based on the MIQP and F-MBC schedule is shown in Figure 6.25. It can be observed that the optimizer schedules the devices belonging to population 1 and 2 with an average of 31 and 31.17 respectively. F-MBC allocates the same with an average of 31.68 and 30.42 respectively. Lower average cost for devices belonging to population 2 indicate that they were scheduled at those timesteps when the realized demand was less than the optimal.

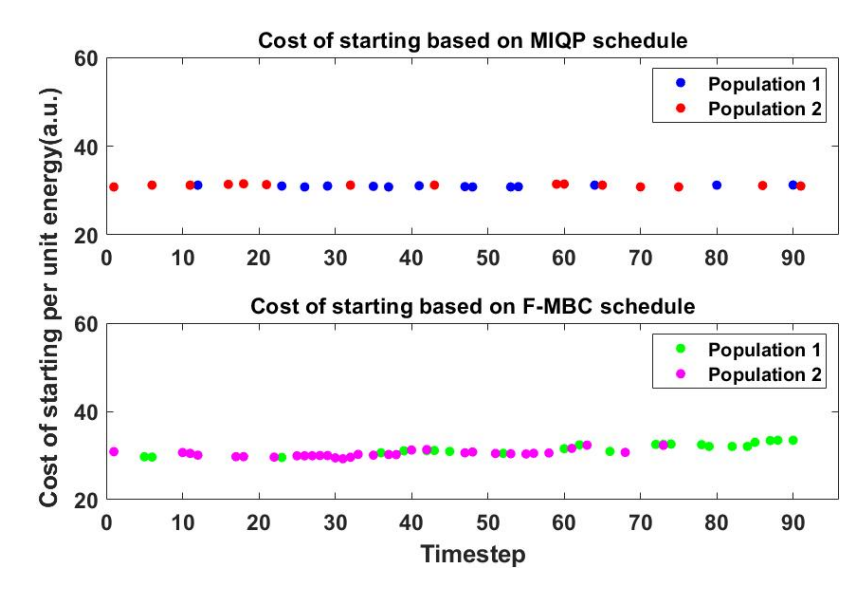


Figure 6.25: Cost of starting comparison: Combination 4

Finally, the regret of the device agents are presented in Figure 6.26. Here, the devices of population 1 have a slightly higher range of regret , with an average of. Again this can be reasoned with the timesteps at which the agents get scheduled and the realized cost of starting. The higher regret can be also be due to the availability of all the unscheduled device agents of the considered population being available , and thus consequently submitting the same bid function. The reason for them not getting allocated is again because of the demand determined during market clearing. The regret of agents belonging to population 2 , with an average of 3.73% ( almost half of the average regret of population 1 , 7.4 %) is less because significant percentage of the agents start at those timesteps when the cost of starting is almost flat.

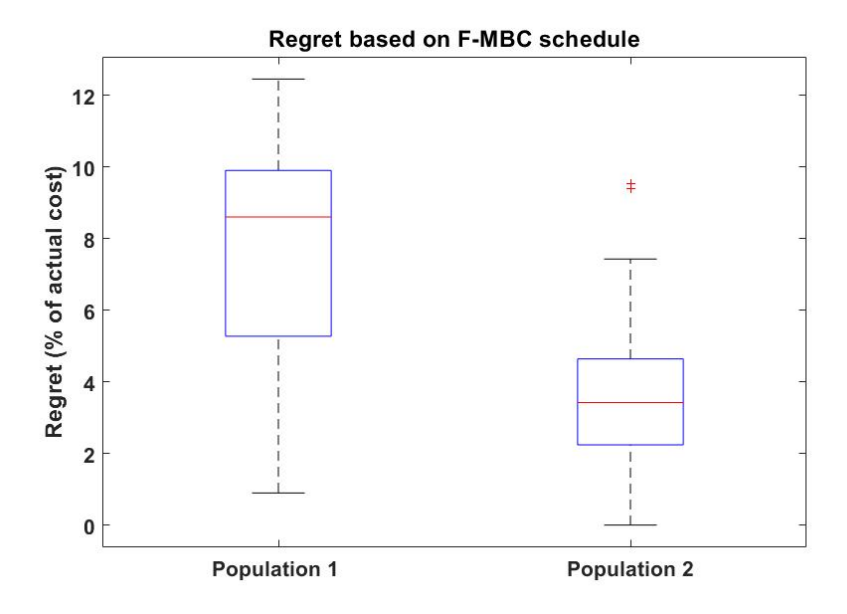


Figure 6.26: Distribution of regret of device agents: Combination 4

# 6.4 Summary

This chapter investigates the ability of the F-MBC mechanism to coordinate heterogeneous populations of deferrable loads with uniform power consumption throughout their cycles. It focuses on highlighting the factors that lead to the deviation from the initial optimal schedule and the corresponding demand profile predicted by the facilitator with complete information. A simulation setup with all the participating agents having the same deadline is considered. While the considered testcases involved only two populations of devices, the conclusions hold good for *n* populations of devices that fall under the category of the testcases considered, because the prices predicted by the facilitator and thus the threshold bids will also change according to the devices considered for coordination. The key takeaways from the analysis can be summarized as follows:

- The facilitator allocates a particular number of devices from both populations to realize the optimal demand and each timestep. To attain the same, devices must respond with corresponding threshold bids.
- Given that the same prices are communicated to the devices having identical deadlines, it was observed that the duration of the device influences the information taken into account for threshold bid formulation (deadline-duration).
- The number of devices that get allocated depends on the power consumption of the populations. Section 6.3.2 highlighted that despite having the same threshold bids, there can be instances when the devices from a certain population might not get scheduled, depending upon the demand determined at the equilibrium point of the aggregated supply and demand functions.

In all the considered testcases, it was found that F-MBC mechanism was able to coordinate devices having uniform power consumption with good system level and device level performances, with little deviations from the optimal overall generation cost. The least relative error was found to be in situation where the power consumption of the populations were the same, indicating that the optimal demand could be realized with the F-MBC schedule even if it deviates from the optimal allocation, provided the power consumption of the populations are same. Or in other words, the cost minimizing solution is not unique.

The optimality from device' perspective is evaluated by determining the cost of starting and the regret of the device agents. In all the four testcases, the mechanism was able to achieve almost same cost of starting per unit energy for the populations of devices. At some instances, the average cost of

6.4. Summary 59

starting using the F-MBC schedule was found to be lesser than that the corresponding optimal values, indicating that significant fraction of the population got scheduled at instances when the realized demand using F-MBC is lesser than the optimal demand.

In all the four testcases, it was observed that those populations had a higher range of regret, which got scheduled both at the beginning at the end of the scheduling horizon. This indicates the regret of the agent is dependent on the device's availability and deadline, as they influence the payments considered for its determination. While the system coordinates the devices with positive regret values for both the populations, collectively the allocation of the devices is close to the optimal coordination. This implies that on a system level, agents have no benefit from deviating from this schedule. This indicates that the devices benefit from paying close to the optimal costs, thus providing favorable reasons to the users to participate in the F-MBC scheme.

# **Chapter 7**

# Application of F-MBC in realistic setting

This chapter aims to evaluate the performance of F-MBC mechanism in a realistic setting with infinite time horizon where it is used to coordinate two populations of devices with complex power profiles. Section 7.1 explains the method in which the data used in the experiments were generated. Section 7.2 describes parameters considered for performing simulations in MATLAB. Section 7.3 provides a detailed analysis of the results which is summarized in Section 7.5.

# 7.1 Simulation setup

Chapter 6 consisted of experiments which were characterized by devices having the same power consumption throughout their cycle. This chapter investigates the performance of the mechanism when the flexible loads have dynamic load profiles, with different duration and overall energy consumption. The second difference between the experiments conducted in this chapter when compared to chapter 6 is that not all devices are available from the start of the simulation. When simulating a real world setting, devices are started at different times throughout the day depending on the user's preferences. This means that the flexibility that can be offered by the system in such a setting directly depends on the availability of the devices and the deadlines set by the device owner. This section explains how a real world setting is created by means of simulation.

#### 7.1.1 Devices considered for coordination

This section introduces to the devices that will be coordinated in this chapter. Among the residential devices used in the Netherlands, the highest penetration rates belong to Washing Machines (WM) and Dish Washers (DW) with 94 % and 58 % respectively [48]. The load profile of WM and DW is presented in Figure 7.1.



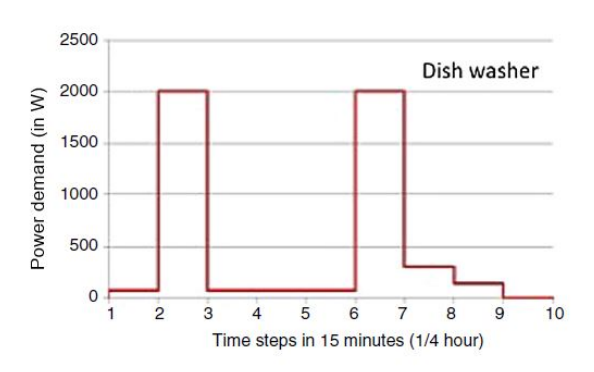


Figure 7.1: Load profiles of Washing Machine and Dish Washer respectively. (Adapted from [48]).

The generic pattern of Washing Machine has a duration of 1 hour and 45 min and consumes about 0.89 kWh per cycle [48]. Cycle of WM operation begins with filling the drum of the machine with water, which consumes only about 0.1 kW. Post that the water in the drum is heated, which is represented by the timesteps 2 and 3 in Figure 7.1a. Most of the power consumed by the device is utilized in this stage of the cycle. Subsequent stages in the cycle involve rotation of the drum, draining out the water, followed by a spin cycle.

Figure 7.1b represents the generic power consumption profile of Dish Washers [48]. At first, water is pumped into the tub located at the base of the DW. This step consumes very little amount of power. Then appropriate voltage is applied across the heating element, which raises the temperature of the water. This water is pumped to several spraying arms located at the top and the bottom of the device, post which the water is sprayed onto the loaded dishes. The washed dishes are dried by again heating the collected water to a high temperature. Post this, the water is drained out from the machine. Similar to the WM, the highest power consumption points in the load profile of DW also occur when water is heated to a certain temperature. This happens at the first and the last rinse cycles. A typical operational cycles consumes about 1.19 kWh of energy and runs for about 2 hours.

Since the load profile used is represented in 15 min intervals, the market is also assumed to clear for every 15 min throughout this chapter.

## 7.1.2 Availability generation

Availability of the devices here refer to the time at which the device is loaded with clothes (for WM) or with dishes(for DW) and is ready to start. This experiment generates the availabilities of the machines based on the average start times observed over the year 2013 in an experimental setup based in Utrecht and Amersfoort [47]. It is assumed that 1000 WM and 1000 DW become available at each day.

From [47], it was evident that the preferable time for the operation of WM is in the morning hours, with 70 % percent of the users starting their devices between 8:00 and 17:00 hrs. To generate similar usage profile, the availability of WM was generated around 10:00 AM, log-normally distributed with mean 15 min and standard deviation of 7.5 min, rounded to nearest 15 min timestep . The availability trend of DW is quite different from WM. From the experimental data presented in [47], it was observed that majority of the devices were operated at the late night and early hours of the day. To simulate this user preference, the availabilities generated were centered around 18:00 hrs log-normally distributed with standard deviation of 7.5 minutes.

From [47], it was evident that the preferable time for the operation of WM is in the morning hours. to generate similar usage profile, the availability of WM was generated around 10:00 AM, lognormally

7.1. Simulation setup 63

distributed with mean 15 min and standard deviation of 7.5 min, rounded to nearest 15 min timestep. The availability trend of DW is quite different from WM. It can be seen from the bottom panel of Figure 7.2, the devices are available to start in large numbers from evening until early hours in the morning. To depict this situation, the availabilities were centered around 18:00 hrs log-normally distributed with standard deviation of 7.5 minutes. Suitable grouping of the data generated led to the availability distribution of devices shown in Figure 7.2.

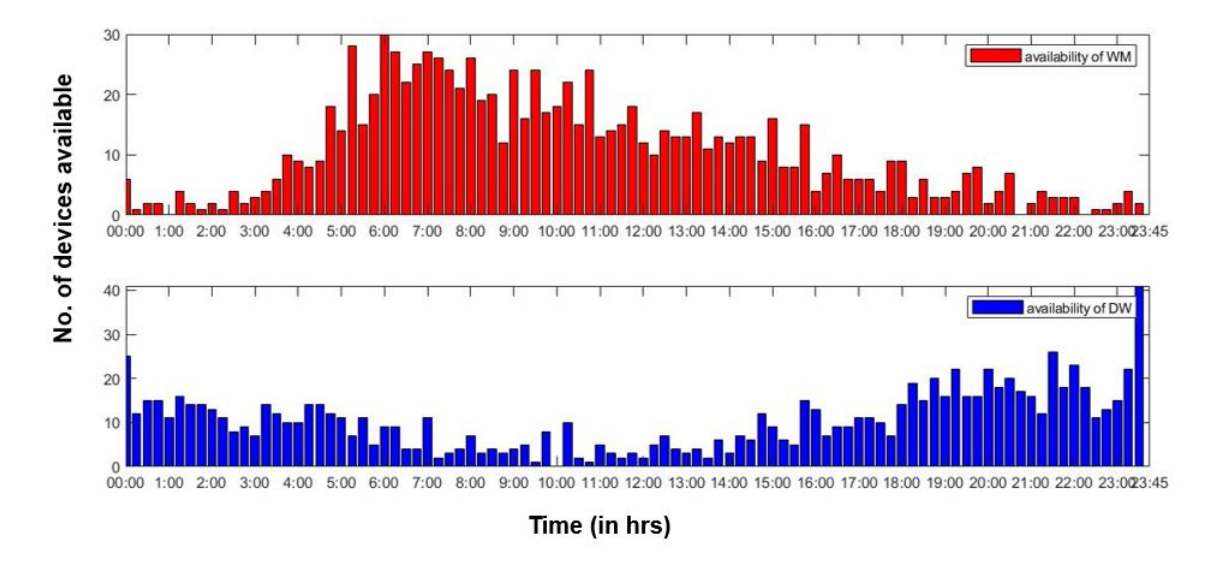


Figure 7.2: Top panel: Average number of WM available in a day Bottom panel: Average number of DW available in a day

## 7.1.3 Deadlines generation

To generate the deadlines, the findings from the SMART-A project is used in conjunction with the availability data generated as explained in Section 7.1.2. It was found in [48] that the majority of the users who own devices with a delay function embedded in their devices prefer to defer their cycles for about 3 hours from the time their devices are available to start. Therefore, deadlines are generated from the time at which the devices become available with a standard deviation of 0.5 hours. The deadline distribution of the devices in a day is given in Figure 7.3. It can be noted from Figure 7.3, devices that become available at the last few hours of the day have their deadlines at the next day.

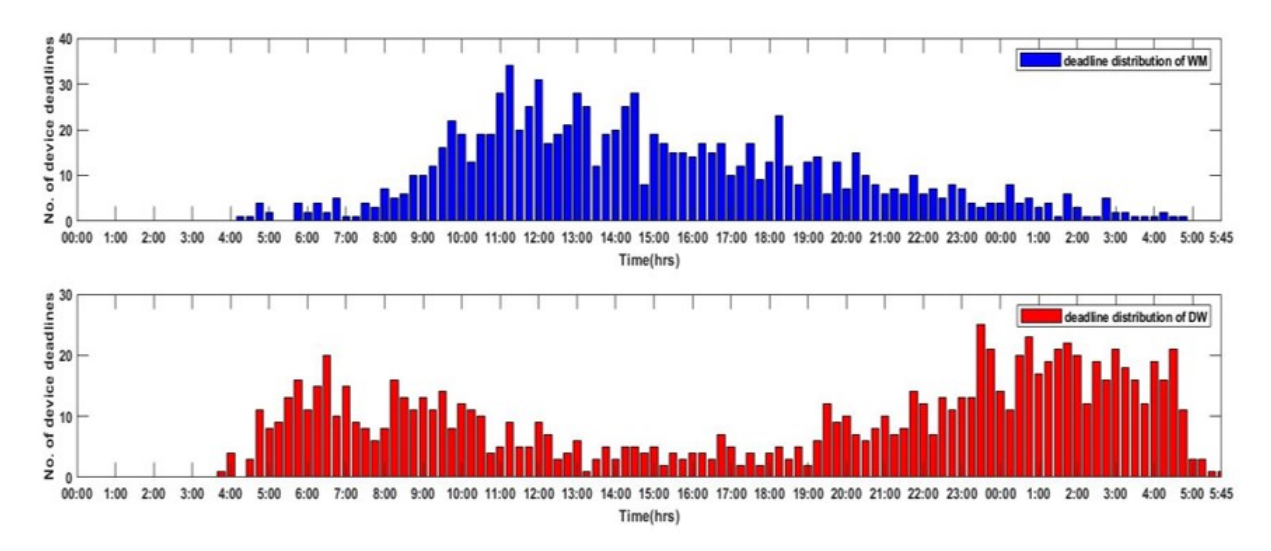


Figure 7.3: Top panel: Deadline distribution of WM Bottom panel: Deadline distribution of DW

# 7.1.4 Inflexible load and generation

Inflexible load refers to the base load that needs to be satisfied by the system. Base load data was generated from [36], which was scaled to a peak of 350 kW and averaged to 15 min intervals.

Inflexible generation here refers to renewable generation. A wind turbine model with a peak generation of 100 kW [1], which utilizes the windspeeds from [20] averaged to 15 min intervals is used in this experiment. The inflexible load and generation data is given in Figure 7.4.

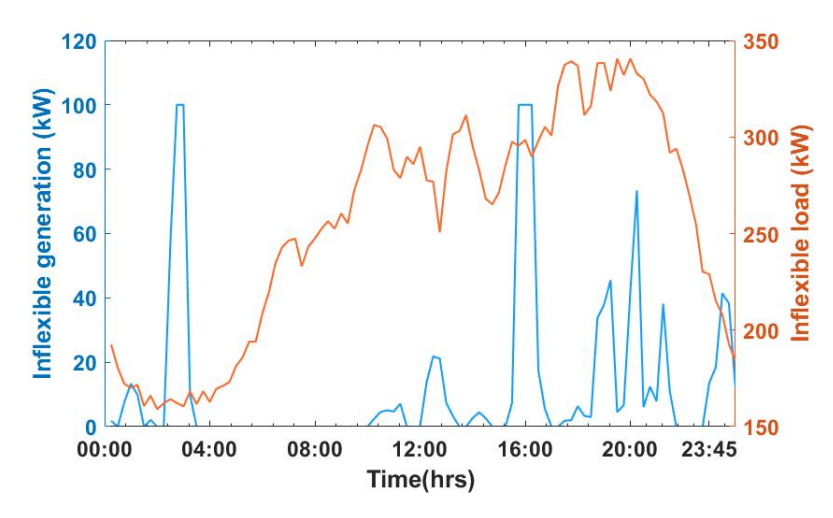


Figure 7.4: Inflexible load and generation data used.

The data discussed in this section namely the availabilities, deadlines of both WM and DW, inflexible load and generation are identical for each day. This is done to avoid end of horizon effects.

7.2. Implementation 65

# 7.2 Implementation

The experiments conducted in this chapter are performed by generating forecast prices on a rolling setting as introduced in 4.3.1 as introduced in Section 5.3. This section introduces the parameters used in simulating such a setting.

The Scheduling Horizon, **Scheduling Horizon** is fixed to be 5 days split into 15 min intervals, leading to **480 iterations**. At each instant, day ahead forecast prices are generated. This means that the **forecast length** is **96 intervals** (24 \*4). It is worthwhile to highlight that in order to generate a forecast of length PH intervals, the data considered is  $PH+D_{max}$ , where  $D_{max}$  represents the longest duration among the flexible devices that needs to be scheduled.

It is assumed that at any time t, only the device that become available at t and the unscheduled devices from the previous market clearings submit their bid.

The experiment was performed by simulating both optimistic and pessimistic scenarios to analyze the robustness of the methodology to variations in the prices.

# 7.3 Results and Analysis

This section presents the analysis of the results for the experiment performed with the methodology explained in Section 7.2.

## 7.3.1 Optimistic forecast scenario

#### **Description of cost minimizing solution**

Before analyzing the performance of the performance of the F-MBC mechanism, the optimal solution predicted by the facilitator at t=0 is discussed. As seen in Figure 7.5, the demand profile is almost flat for most of the instances, except at the beginning and at the end of the day. Those instances are also characterized with low inflexible net load and slightly lesser number of devices available as seen from Figure 7.2. Inflexible net load refers to the difference between the inflexible load and renewable generation. This indicates that the ability of the facilitator to provide almost flat profiles depends upon the availability of the devices for coordination.

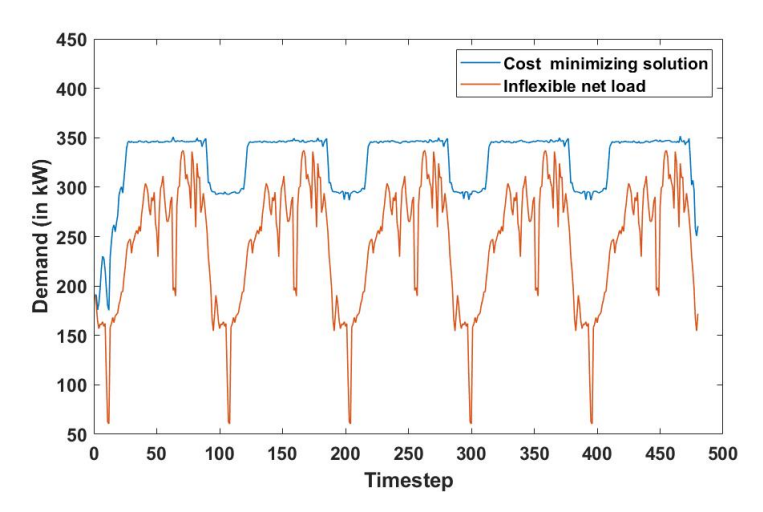


Figure 7.5: Optimal solution compared with inflexible net load.

## **Analysis of F-MBC performance**

Figure 7.6 shows the demand profile achieved using F-MBC is compared with the optimal allocation predicted by the facilitator for the five days and the inflexible net load of the system. For easier reference to a particular time of the day, the horizontal axis is numbered in timesteps.

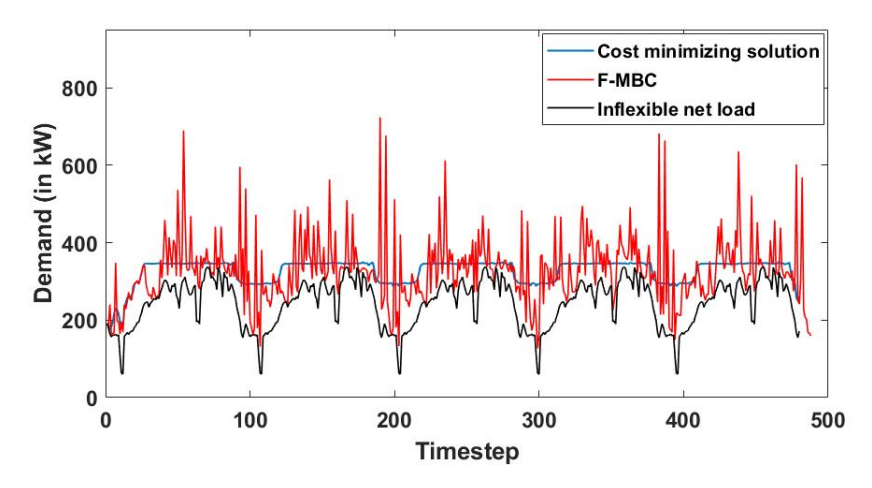


Figure 7.6: Demand profile under optimistic forecasts.

As in Chapter 6, analysis begins with the comparison of the objective function, as provided in Table 7.1.

Objective function value : Optimal	Objective function value : F-MBC
2.58713 e+06	2.75065 e+06

Table 7.1: Objective function comparison: Optimistic forecast scenario

Though the relative error is about 6.32 %, the demand profile is observed to be very fluctuating in nature, with the maximum and minimum power consumption being 723.63 kW and 126.618 kW respectively. The reason for such an allocation is explained in Section 7.3.1

#### **Analysis**

To begin with, the schedule predicted by the facilitator is compared with schedule realized by F-MBC as shown in Figure 7.7.

The F-MBC schedule graphs of both Washing Machines (WM) and Dish Washers (WM) are characterized by occasional big steps, as pointed out in Figure 7.7b. This indicates that a large number of devices are getting allocated at a particular time step.

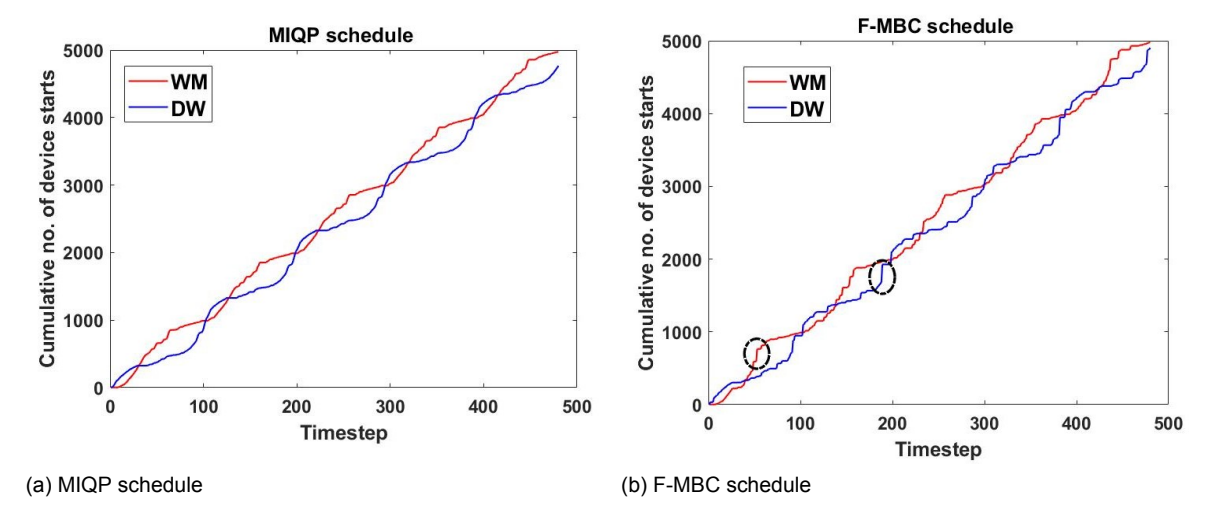


Figure 7.7: Schedule comparison: Optimistic forecast scenario

To understand the reason behind this allocation, the first peak in the graph, which occurs at t=6 is investigated in detail. At this timestep, 57 DWs get scheduled. It can be observed from Figure 7.8b that though the deadlines of the participating agents vary between 21 and 29, the threshold bids submitted by all the agents are the same. This is because the optimal expected costs calculated by the agents based on the price forecasts received via backward induction, leads to the same optimal expected cost at t=7 for all the agents , inspite of commencing their threshold bid determination from different timesteps depending upon their deadlines. This is pictorially represented in Figure 7.9.

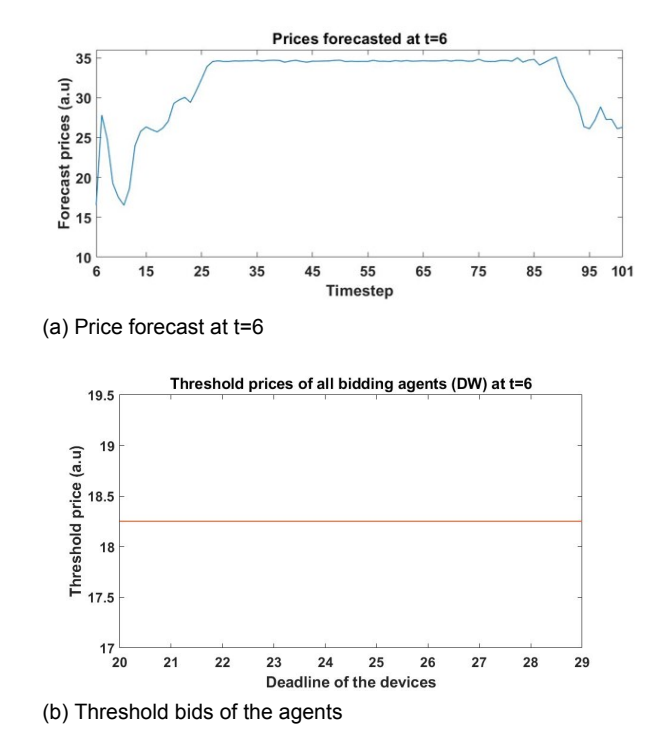


Figure 7.8: Day ahead price forecast and threshold bids calculated by the agents with different deadlines bidding at t=6

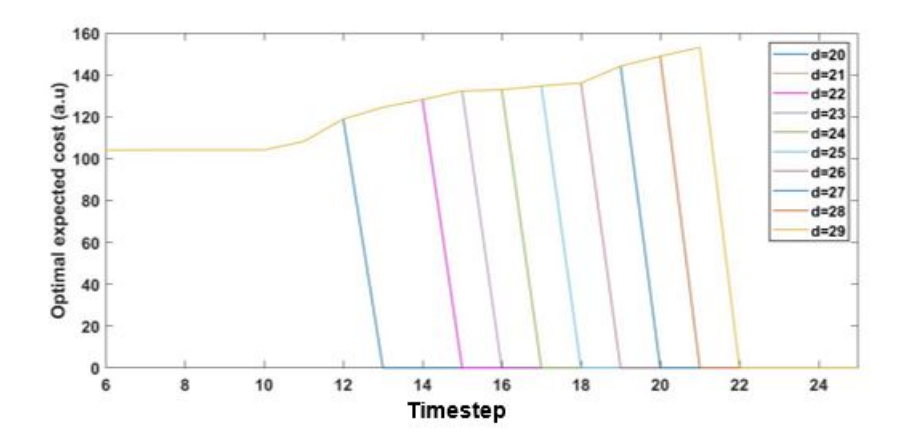


Figure 7.9: Optimal expected costs calculated by the agents bidding at t=6

This indicates that the agents differing in deadlines can also have the same threshold price depending upon the forecast prices it receives from the facilitator. The market was found to be cleared at a price higher than the submitted threshold bids thus leading to all the devices getting allocated as seen in Figure 7.10.

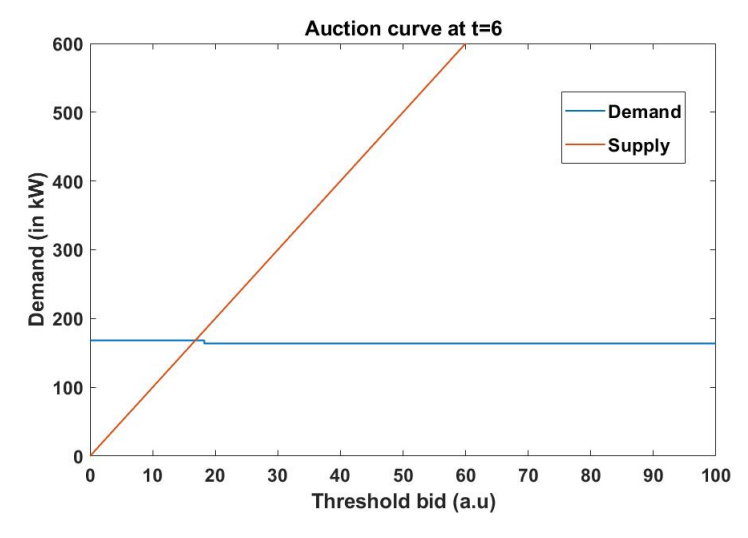


Figure 7.10: Auction curve at t=6

However, upon looking into the aggregated bid curve, it can be identified that the bid function here bids for the power consumption at the first time step, which is 0.08 kW. This means that even in a situation when the market encounters a tie situation, the equilibrium point determined by the tie breaking mechanism is based on the aggregation of the bid functions that have extremely low power consumption values. This presents the possibility of bulk switching due to the amplification of the threshold bid, which can lead to very high bid submissions by the agents leading to their allocation. To understand this statement further, the formula for determining the threshold bid is restated again in Equation 7.1.

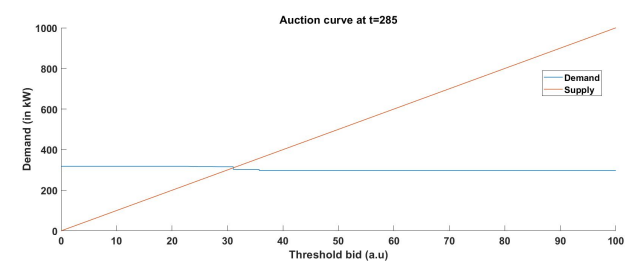
$$z_t^j = \frac{C_{t+1}^{*j} - \sum_{i=1}^{D^{j-1}} \bar{x}_{t+i} \cdot P_i^j \cdot \Delta t}{P_0^j \cdot \Delta t}$$
 (7.1)

where:

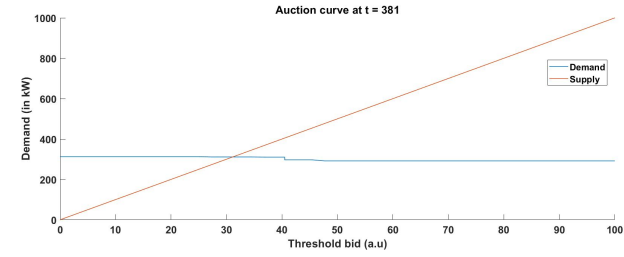
 $C_{t+1}^{*j}$ : Optimal expected cost at t+1

 $\sum_{i=1}^{D^{j}-1} \bar{x}_{t+i} \cdot P_i^j \cdot \Delta t$ : Expected cost for the reminder of the device's cycle, when scheduled at time t.  $P_0^j$ : Power consumption of the devices belonging to population j at the first step of their cycle.

Keeping the load profiles of WM and DW in mind, it can be seen from Equation 7.1 that the difference between the optimal expected cost at t+1 and the expected cost for reminder of the cycle upon starting at t gets scaled by 12.5 and 10 times respectively. Depending upon the numerator, there exists a chance that the aggregation of bids could happen at a very higher price, which can lead to the market clearing at a price lesser than the submitted threshold, again leading to their allocation. Also, once they are allocated, due to their uninterruptible nature, devices stop only after completing their cycle. The auction curves depicting the occurrence of both these possible explanations is presented in Figure 7.11.



(a) Auction curve t=285 (Tie breaking based on bid functions with low power consumption values



(b) Auction curve at t=381 (Devices bidding with high threshold prices)

Figure 7.11: Effects of submitting bid functions with low power consumption

The bulk allocation caused by the low power consumption at the initial stage, followed by the huge power consumption at the subsequent time steps leads to the peaky demand profile as seen in Figure 7.6. The magnitude of the peaks observed is directly proportional to the number of devices that get scheduled due to the reasons explained and the load profiles of the devices. Two close subsequent peaks are due to consumption of 2 kW by the DW at the first and the last spin cycles.

#### 7.3.2 Pessimistic forecast scenario

It is expected that when the SH is long enough, both optimistic and pessimistic scenarios yield the same results. Hence, the demand profile achieved by communicating day ahead forecast which determines the optimal number of starts under pessimistic formulation is also compared with the optimal outcome in the previous section in Figure 7.12.

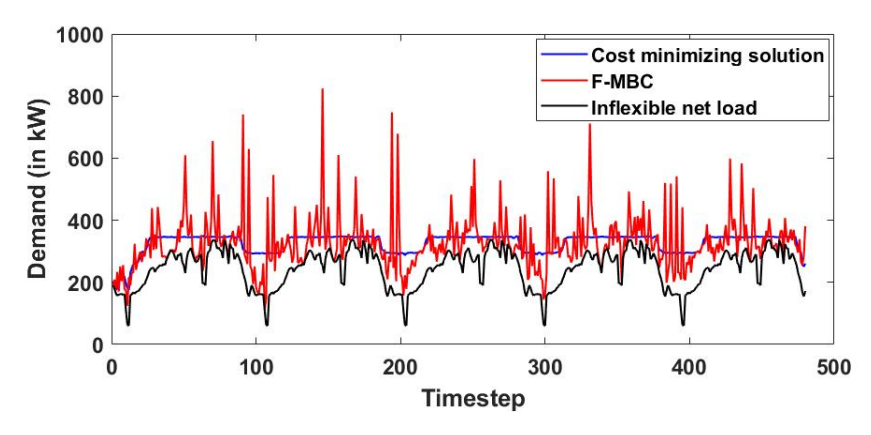


Figure 7.12: Demand profile under pessimistic forecast scenario.

Similar to the optimistic forecast scenario, a peaky profile is obtained. But the range of the demand profile is found to be higher when pessimistic forecasts are used. The maximum and minimum points in the demand profile are 824.397 kW and 115.1547 kW respectively. A higher objective function value was also realized under this case with a relative error of 6.45 % from the optimal solution as seen in Table 7.2.

Objective function value : Optimal	Objective function value : F-MBC
2.58713 e+06	2.75401 e+06

Table 7.2: Objective function comparison: Pessimistic forecast scenario

#### **Analysis**

To identify the reason behind the higher objective function in the pessimistic forecast scenario, the allocation of devices using this forecast is compared with the allocation realized using optimistic forecast.

It can be observed from Figure 7.13a and Figure 7.13b that the schedules of both WM and DW exhibit deviations when coordinated using optimistic and pessimistic forecasts. To investigate the underlying reason behind this, threshold bids submitted by an agent available at t=1 based on both these forecasts is considered. An agent representing a DW which is available at t=1 and having a deadline at t=26 is considered for analysis. The determination of threshold bid by backward induction starts from deadline -duration, i.e; from t=18. The price forecasts from t=1 to 18 at the first time step using both formulations is given in Figure 7.14.

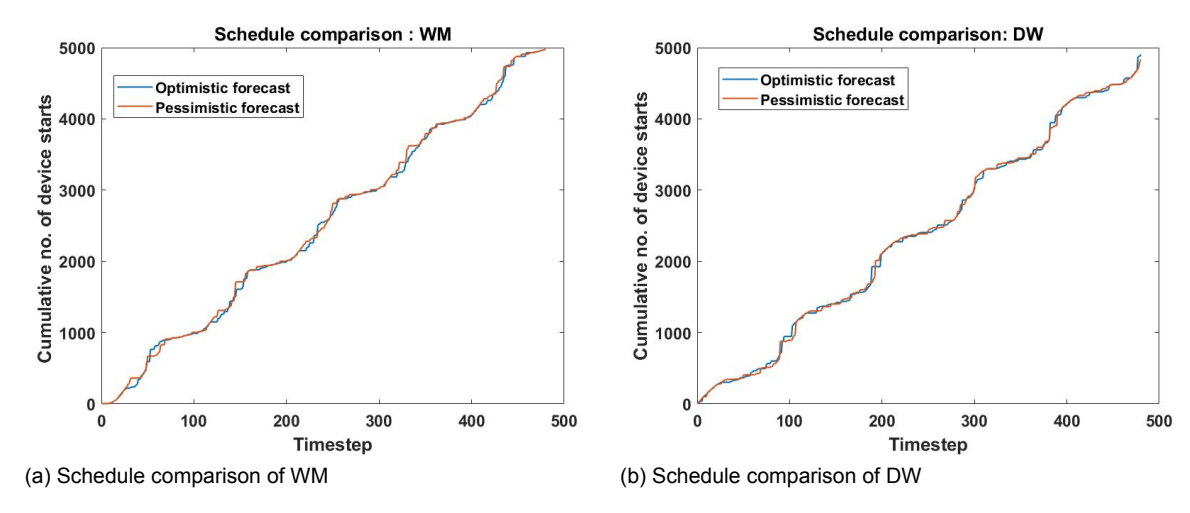


Figure 7.13: Comparison of device schedules under optimistic and pessimistic forecast scenarios

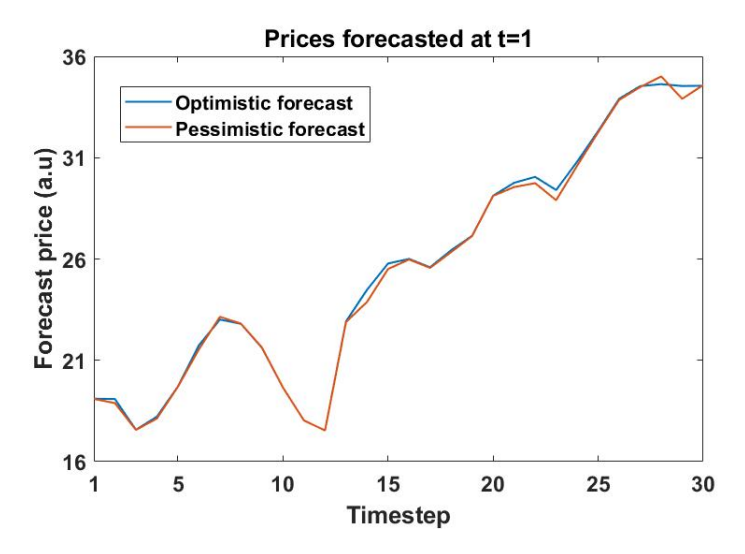


Figure 7.14: Prices forecasted at t=1 under optimistic and pessimistic scenario

While the forecast prices from t=1 to t=18 almost overlap with deviations as little as 0.6 a.u, the threshold bids submitted by the agent based on these forecasts are 13.9761 and 21.8907 respectively. The clearing prices at t=1 were 19.064 and 19.1760 respectively, meaning that the device gets scheduled under pessimistic forecast scenario but does not get scheduled when optimistic forecasts are used by the agents.

This indicates that the threshold bid when divided by low power consumed by the agents at the first stage of their cycle makes it very sensitive to small deviations in the forecast prices. Since the forecasts get updated based on the control actions taken at the previous market clearing, the effect of having different threshold prices results in the realization of different schedules for the system with same characteristics, as seen in Figure 7.13.

Also, it was observed from the simulation data generated that the maximum difference between the deadline and availability of the devices was 27 timesteps. The forecast length of 96 intervals is seen to be able produce almost same prices from t=1 to t=28 at the first iteration for both optimistic and pessimistic formulation, as seen in Figure 7.14. Hence, it can be concluded that the forecast length considered is suitable for testing the robustness of the mechanism.

#### Effect of allocation from device perspective

To understand the effect of this allocation from the point of view of an agent, the total cost paid by the agent for starting at time t when coordinated with F-MBC and the cost minimizing solution is compared as shown in Figure 7.15. It is expressed in terms of unit energy.

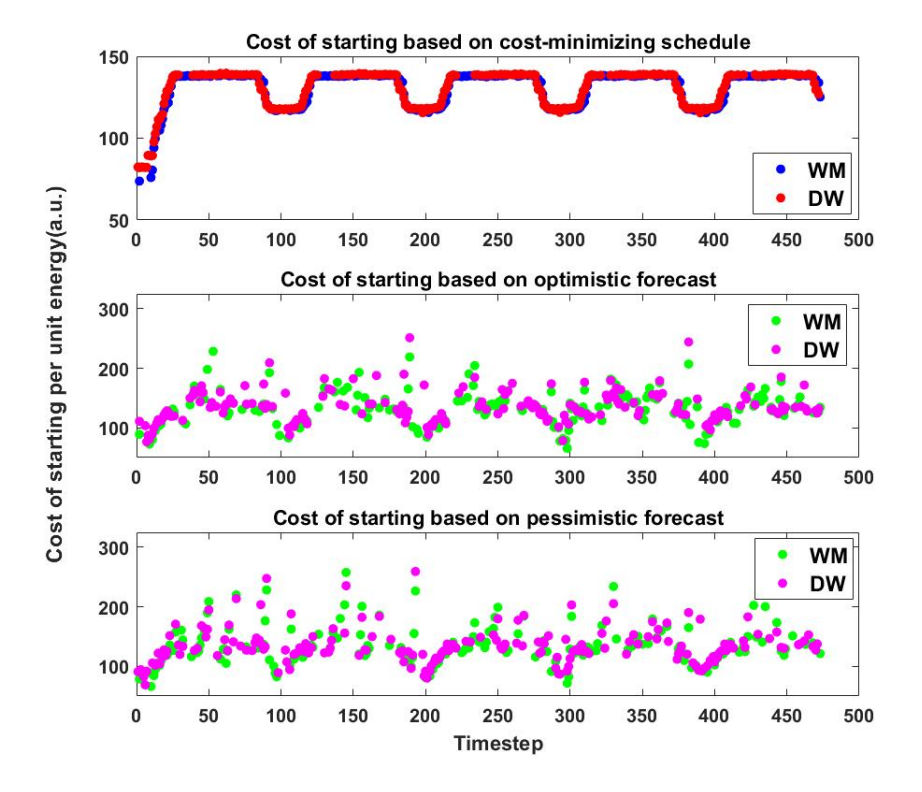


Figure 7.15: Cost of starting comparison

It can be seen from the first panel that the agents pay almost a flat price, except at the start and the end of the day. This can be linked to the lower number of devices that become available and also the inflexible net load at those instances.

The bulk switching leads to high payments incurred for both WMs and DWs. It can be observed from Figure 7.15 that the maximum values of cost of starting under the optimal allocation for both WM and DW are 139.28 a.u and 139.7 a.u respectively. But, costs paid by the agents of WM and DW are observed to go as high as 228.41 a.u and 251.3 a.u respectively in the F-MBC allocation using optimistic forecasts. Similar effects were also found under schedule realized using pessimistic forecasts wherein maximum payments made by WM and DW amount to 257.64 a.u and 259.24 a.u respectively. This is because large number of devices were get allocated by using bid functions corresponding to low power consumption and due to the uninterruptible nature of these loads, the devices do not stop until they finish their cycle. The updated forecasts provide large prices depending upon the number of devices that get scheduled. Since these prices also get associated with the highest power consumption of the device, the overall cost paid by the device ends up being high.

# 7.4 Performance under modified load profiles

It was observed in the previous section that the low power consumption of the devices at the first stage of their cycle led to undesirable outcome, both at the system level and device level. Therefore, the power consumption profiles of both the devices were modified in such a manner that devices have the highest power consumption at the initial stage, to analyze the performance of F-MBC in this setup. The modified load profiles are graphically represented in Figure 7.16.

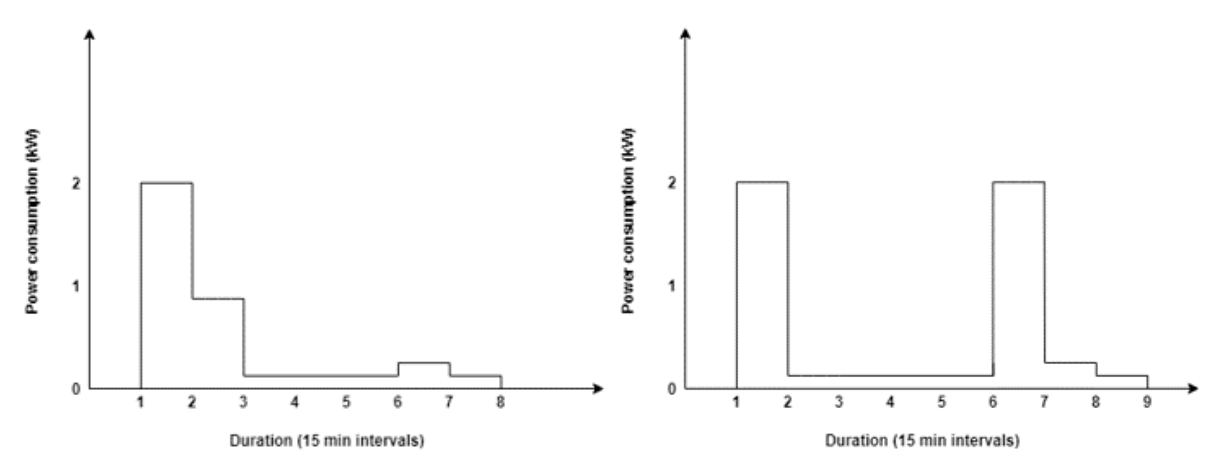


Figure 7.16: Modified load profiles of Washing Machine and Dish Washer respectively

#### Results and analysis

The demand profiles realized by using both optimistic and pessimistic forecasts almost overlapped with the initial optimal demand predicted by the facilitator as seen in Figure 7.17.

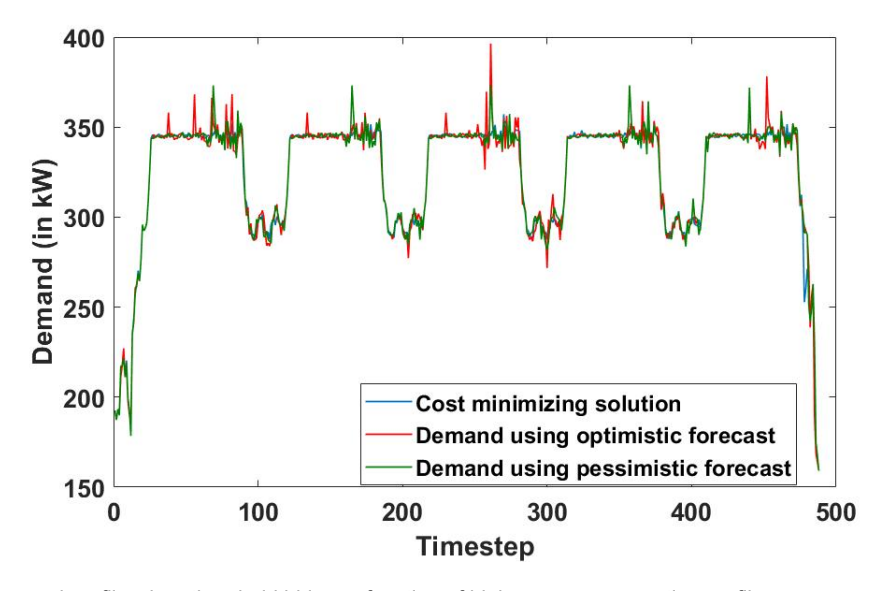


Figure 7.17: Demand profile when threshold bids are function of high power consumption profile

This is because the numerator in the threshold price formula given in Equation 7.1 gets divided by 2 which prevents the possibility of bidding higher than the inflexible loads that needs to be satisfied. Moreover, the bid functions are function of the highest power consumption in their respective load profiles. The equilibrium points determined under this case, even in a tie situation leads to significantly lower number of devices getting allocated. The height of the bids submitted by the agents are also larger. An example of one such auction curve is given in Figure 7.18.

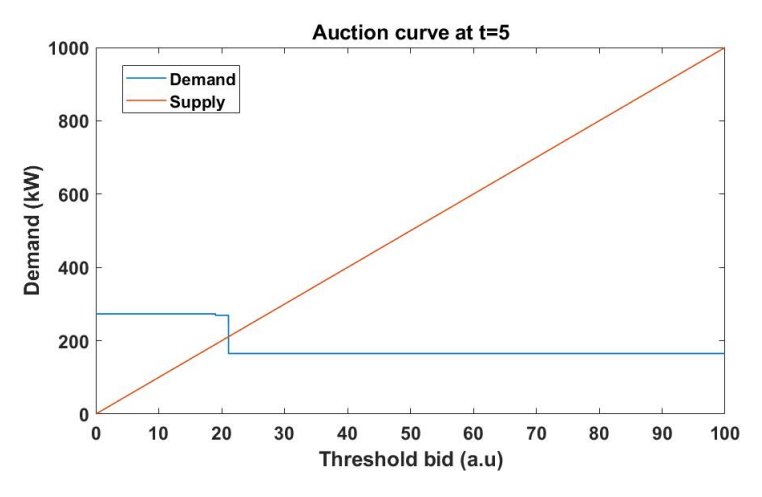


Figure 7.18: Auction curves when the threshold bids are function of the highest power consumption of the device

Apart from good system level performance, the allocation also provided good device level performance. This can be seen by the cost of starting plots as shown in Figure 7.19, where the devices pay almost the same prices as the cost minimizing solution.

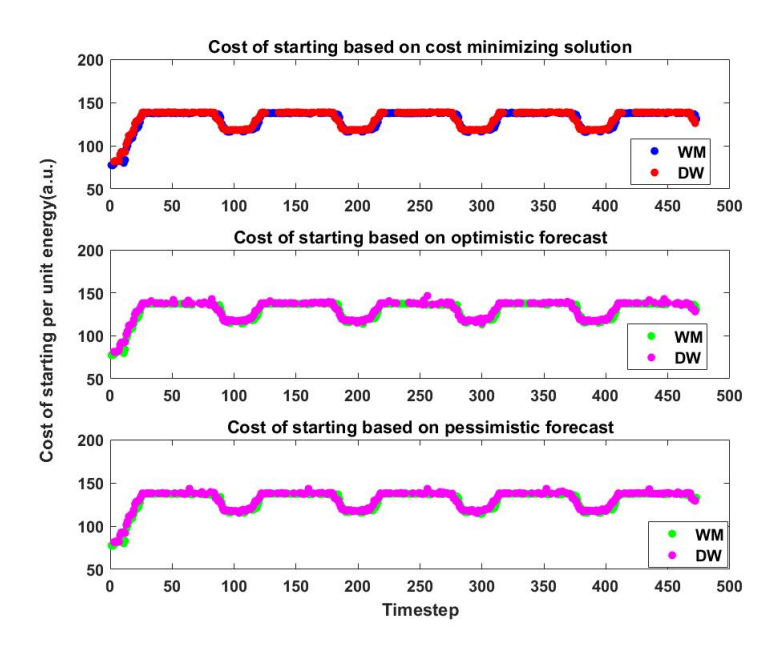


Figure 7.19: Cost of starting comparison when modified load profiles were considered for coordination

7.5. Summary 75

# 7.5 Summary

This chapter investigates the performance of F-MBC mechanism when used for scheduling deferrable loads with dynamic load profiles under a realistic setting. Load profiles of commonly used residential appliances, such as Washing Machines (WM) and Dish Washers(DW) were considered for coordination. Availabilities and deadlines of the devices were generated based on the start times observed in [47] and the preferred delay times of the users as determined in [48]. For the purpose of analyzing the performance of the mechanism, simulation of the infinite coordination problem had to be terminated. But to avoid end of horizon effects that could arise, the setting was tested by having a long scheduling horizon. The robustness of the simulation implementation was tested by including optimistic and pessimistic constraints in the optimal coordination problem. The forecasts were developed on a rolling basis, by which day ahead optimal prices were made available to the agents at each time step. The key observations from the simulation results can be summarized as follows:

The scheduled realized by F-MBC when used to schedule devices with dynamic load profiles was found to be sensitive to the threshold bids submitted by the agents. Threshold bids are inversely proportional to the power consumption of the devices at the first time step  $(P_0)$ .

Depending upon the value of  $P_0$  and its difference from the highest power consumed by the device during its cycle ( $P_{max}$ ), two possible situations were explored:

## • When the difference between $P_0$ and $P_{max}$ is quite large:

In this case, the bid functions submitted by the agents are a function of very small amount of power. This can potentially lead to two possibilities:

- The amplification of the threshold bids by the lower power consumption of the devices may
  make the agents submit very high threshold bids, thereby leading to their allocation.
- In situations when a tie occurs among the agents, the tie breaking mechanism resolves ties based on the equilibrium point determined by the aggregation of bid functions that are a function of very low power consumption. This leads to the problem of bulk switching.

Since deferrable loads are considered for coordination, once allocated, these devices will not turn off until their cycle is complete. Due to these reasons, very high peaks were observed in the demand profiles realized by using both optimistic and pessimistic forecasts. The magnitude of the peaks obtained is relative to the number of devices that get scheduled. Also, it was observed that the threshold bids were very sensitive to minor deviations in the forecasts achieved using the optimistic and pessimistic MIQP formulations.

From the device perspective, higher costs were paid by the agents in the former setting when compared to the latter, under both optimistic and pessimistic forecasts.

## • When $P_0$ is highest power consumed by the device in its cycle:

In this situation, the opposite effect occurs.

- Bid functions submitted are functions of highest power consumption of the participating devices, which leads to well defined steps in the aggregated demand curve.
- Due to this, even when ties are observed in the system, significantly less number of devices get scheduled when compared to the situation when the participating devices consume less power initially.

The demand profiles realized under this setting using both optimistic and pessimistic forecasts were observed to coincide with the initial demand profile predicted by the facilitator. Device agents were also observed to pay almost same prices as that of the cost minimizing solution, under both optimistic and pessimistic scnerios.

Thus, from the results presented in this chapter, it can be concluded that when F-MBC coordinates several populations of devices which do not consume the highest power required by them at the start of their cycle, the resultant allocation can suffer deviations from the optimal allocation ,proportional to the difference  $P_0$  and  $P_{max}$ . However, when the devices consume maximum power once they start, the F-MBC is able to achieve good overall system level and device level performance. This is because the allocation of the devices is based on the threshold bids submitted by the agents, which is inversely dependent on  $P_0$ . While the analysis presented in the chapter compares the performance of the mechanism only belonging to either category, it would be interesting to analyze how the mechanism performs when coordinating populations belonging to both categories and different inflexible net load of the system.

# **Chapter 8**

# Conclusions and recommendations

This chapter summarizes the work carried out in the thesis. First, the main findings of the research work is summarized in Section 8.1, and establishes how it answers the main research question. The chapter then concludes with relevant suggestions for future work in Section 8.2.

## 8.1 Main conclusions

The main aim of the project is to analyze the applicability of the F-MBC in a realistic setting. The first step towards answering that is to evaluate its performance when used to coordinate heterogeneous population of deferrable loads. The main findings from the experimental analyses performed in this project helps in providing a better understanding of the same.

Chapter 6 analyzed the ability of the mechanism in coordinating several combinations of deferrable loads having uniform power consumption over a fixed time horizon. The devices were assumed to have identical deadlines. Results obtained indicate that the mechanism was able to allocate the devices in such a manner that led to good overall system level performance and device level performance.

Chapter 7 deals with a much complicated experimental setup, attempting to demonstrate a real world setting. Devices with complex power profiles were considered for coordination in this chapter. Two populations of devices with dynamic load profiles varying in duration, availabilities and deadlines were considered for coordination. Day ahead forecasts were broadcasted to the agents at each time step and was generated on a rolling basis. While the actual coordination problem is of infinite length, in order to analyze how effectively the mechanism coordinates in such a setup, the simulation was terminated while having a long scheduling horizon. To test the robustness of the mechanism when implemented in different experimental setups, optimistic and pessimistic forecasts were communicated to the participating agents and the performance was investigated.

Results in Chapter 7 indicated the allocation of devices using the mechanism is highly dependent on the threshold bids of the participating agents. It pointed out that when devices with low power consumption at the initial stage, the aggregation of corresponding bid functions happen either at high prices due to amplification of the threshold prices, or leads to bulk switching. This resulted in undesirable outcomes at system and device levels. Such devices were also found to be very sensitive to the price deviations when coordinated using optimistic and pessimistic forecasts. On the other hand, the mechanism was able to provide close to optimal allocation when dynamic load profiles consume high power when it starts.

This opens up several possible avenues to extend the current research work to draw definitive conclusions about the usability of the approach. This will be discussed in the upcoming section.

# 8.2 Recommendations for future work

Based on the analysis presented in this thesis, relevant extensions for future work are listed below.

- Analysis presented in Chapter 7 considered two extreme cases: populations with low initial power consumption and populations with high initial power consumption. To better understand the performance of the mechanism, populations of devices belonging to both categories can be simulated.
- The performance of the mechanism in different deadlines, availabilities and inflexible load and generation profiles can be investigated to better examine the behavior of the mechanism. Devices belonging to each population and the number of populations of flexible devices can also be increased.
- Additional functionality can be added to the auctioneer to identify the number of bids that get aggregated at a particular threshold price to make it aware about the potential issue of bulk switching.
   This also does not demand any private information from the participating agent as it can be acquired from the bid function submitted. This might help in developing better methods to allocate the devices, atleast in a tie situation.

# Appendix A

# Additional results: Realistic setting

# A.1 Demand profiles under different day ahead uncertanties

 $v^{24h} = 0.001$ 

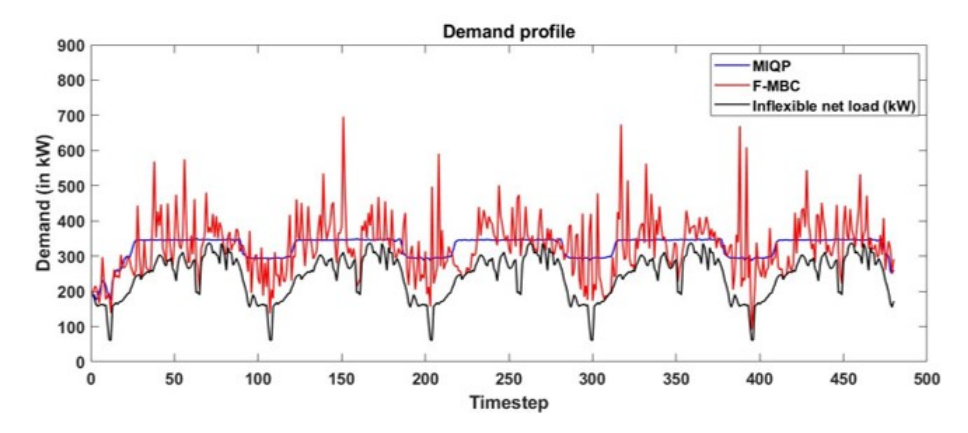


Figure A.1: Demand profile comparison with  $v^{24h} = 0.001$ 

 $v^{24h}=0.01$ 

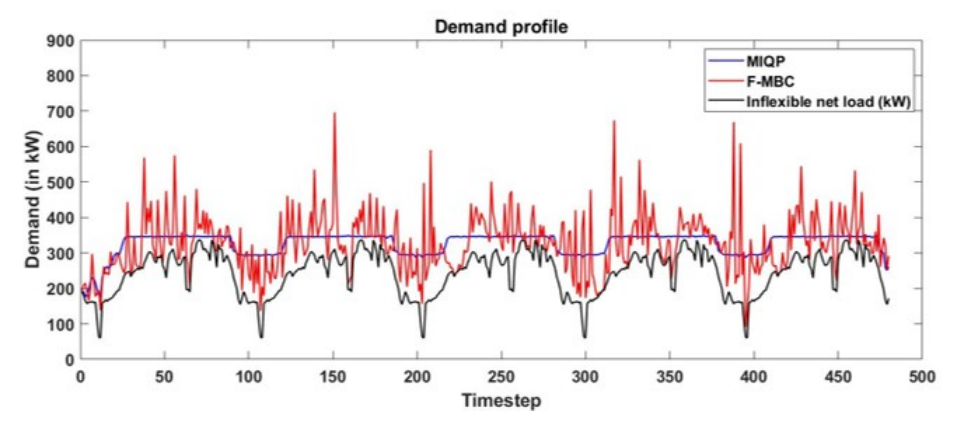


Figure A.2: Demand profile comparison with  $v^{24h} = 0.01$ 

# $v^{24h}=0.1$

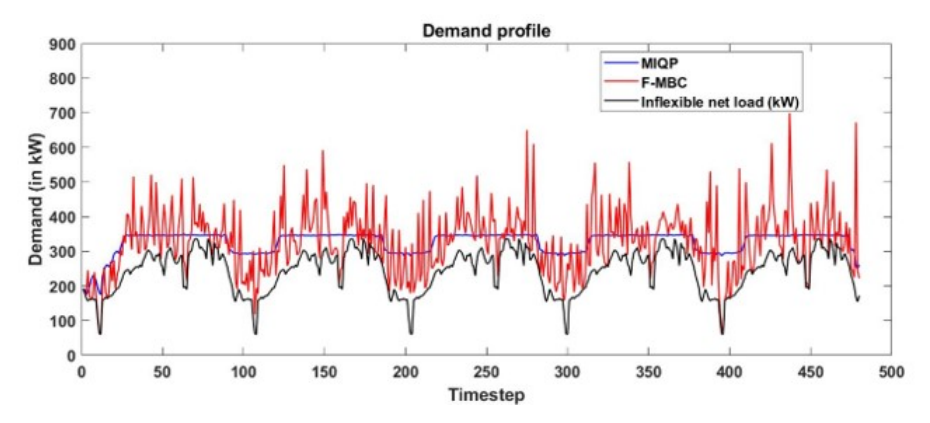


Figure A.3: Demand profile comparison with  $v^{24h}=0.1$ 

- [1] Polaris, 100kw  $\phi$  25m variable pitch wind turbine. [online]. URL http://www.polarisamerica.com/turbines/100kw-wind-turbines/.
- [2] Demand response: An introduction, overview of programs, technologies and lessons learned, 2006. A Southwest Energy Efficiency Project Report.
- [3] Hazem A Abdelghany, Simon H Tindemans, Mathijs M de Weerdt, and Han la Poutré. Distributed coordination of deferrable loads: A real-time market with self-fulfilling forecasts. Sustainable Energy, Grids and Networks, 23:100364, 2020. ISSN 2352-4677. doi: https://doi.org/10.1016/j.segan.2020.100364.
- [4] Jamshid Aghaei and Mohammad Iman Alizadeh. Demand response in smart electricity grids equipped with renewable energy sources: A review, 2013. ISSN 13640321.
- [5] M H Albadi and E F El-Saadany. A summary of demand response in electricity markets. *Electric Power Systems Research*, 78(11):1989–1996, 2008. ISSN 0378-7796. doi: https://doi.org/10.1016/j.epsr.2008.04.002.
- [6] A. G. Azar, H. Nazaripouya, B. Khaki, C. Chu, R. Gadh, and R. H. Jacobsen. A non-cooperative framework for coordinating a neighborhood of distributed prosumers. *IEEE Transactions on In*dustrial Informatics, 15(5):2523–2534, 2019.
- [7] V. S.K.Murthy Balijepalli, Vedanta Pradhan, S. A. Khaparde, and R. M. Shereef. Review of demand response under smart grid paradigm. In 2011 IEEE PES International Conference on Innovative Smart Grid Technologies-India, ISGT India 2011, 2011. ISBN 9781467303163. doi: 10.1109/ ISET-India.2011.6145388.
- [8] Dario Bauso. Game theory: Models, numerical methods and applications. *Foundations and Trends in Systems and Control*, 2014. ISSN 23256826. doi: 10.1561/2600000003.
- [9] Slim Belhaiza, Uthman Baroudi, and Issmail Elhallaoui. A Game Theoretic Model for the Multi-periodic Smart Grid Demand Response Problem. *IEEE Systems Journal*, 2020. ISSN 19379234. doi: 10.1109/JSYST.2019.2918172.
- [10] Bellal Ahmed Bhuiyan. An Overview of Game Theory and Some Applications. *Philosophy and Progress*, 2018. ISSN 1607-2278. doi: 10.3329/pp.v59i1-2.36683.
- [11] Sébastien Bissey, Sebastien Jacques, and Jean-Charles Le Bunetel. The Fuzzy Logic Method to Efficiently Optimize Electricity Consumption in Individual Housing. *Energies*, 10:1701, 2017. doi: 10.3390/en10111701.
- [12] Nilotpal Chakraborty, Arijit Mondal, and Samrat Mondal. Efficient scheduling of nonpreemptive appliances for peak load optimization in smart grid. *IEEE Transactions on Industrial Informatics*, 2018. ISSN 15513203. doi: 10.1109/TII.2017.2781284.
- [13] Yan Chen, Yang Gao, Chunxiao Jiang, and K. J.Ray Liu. Game theoretic Markov decision processes for optimal decision making in social systems. In 2014 IEEE Global Conference on Signal and Information Processing, GlobalSIP 2014, 2014. ISBN 9781479970889. doi: 10.1109/GlobalSIP.2014.7032120.

[14] Lefeng Cheng and Tao Yu. Game-Theoretic Approaches Applied to Transactions in the Open and Ever-Growing Electricity Markets from the Perspective of Power Demand Response: An Overview. *IEEE Access*, 2019. ISSN 21693536. doi: 10.1109/ACCESS.2019.2900356.

- [15] Electric Power Research Institute (EPRI). Automated Demand Response Today, 2012.
- [16] Linas Gelazanskas and Kelum A.A. Gamage. Demand side management in smart grid: A review and proposals for future direction, 2014. ISSN 22106707.
- [17] H.Huang. Introduction to game theory: Extensive games and subgame perfect equilibrium, 2011.
- [18] Ali Ipakchi. Demand side and distributed resource management A transactive solution. In *IEEE Power and Energy Society General Meeting*, 2011. ISBN 9781457710018. doi: 10.1109/PES. 2011.6039272.
- [19] International Renewable Energy Agency (IRENA). Demand-side flexibility for power sector transformation, 2019.
- [20] D. Jager and A. Andreas. NREL national wind technology center (NWTC): M2 tower; boulder, colorado (data),". 1996. doi: 10.5439/1052222.
- [21] Rim Kaddah. Renewable and sustainable energy reviews, 2016. ISSN 13640321.
- [22] Abhilash Kantamneni, Laura E. Brown, Gordon Parker, and Wayne W. Weaver. Survey of multiagent systems for microgrid control, 2015. ISSN 09521976.
- [23] E. Karfopoulos, L. Tena, A. Torres, Pep Salas, Joan Gil Jorda, A. Dimeas, and N. Hatziargyriou. A multi-agent system providing demand response services from residential consumers. *Electric Power Systems Research*, 120, 2015. doi: 10.1016/j.epsr.2014.06.001.
- [24] P. Khajavi, H. Abniki, and A. B. Arani. The role of incentive based demand response programs in smart grid. In *2011 10th International Conference on Environment and Electrical Engineering*, pages 1–4, 2011.
- [25] J. K. Kok, C. J. Warmer, and I. G. Kamphuis. PowerMatcher: Multiagent control in the electricity infrastructure. In *Proceedings of the International Conference on Autonomous Agents*, 2005.
- [26] A. M. Kosek, G. T. Costanzo, H. W. Bindner, and O. Gehrke. An overview of demand side management control schemes for buildings in smart grids. In 2013 IEEE International Conference on Smart Energy Grid Engineering (SEGE), pages 1–9, 2013.
- [27] Harold W. Kuhn, John C. Harsanyi, Reinhard Selten, Jörgen W. Weibull, Eric Van Damme, John F. Nash, and Peter Hammerstein. The Work of John Nash in Game Theory. *Journal of Economic Theory*, 69(1):153–185, apr 1996. ISSN 00220531. doi: 10.1006/jeth.1996.0042.
- [28] I. Lampropoulos, W. L. Kling, P. F. Ribeiro, and J. van den Berg. History of demand side management and classification of demand response control schemes. In *2013 IEEE Power Energy Society General Meeting*, pages 1–5, 2013.
- [29] Jing Li, Yujian Ye, Dimitrios Papadaskalopoulos, and Goran Strbac. In *SEST 2019 2nd International Conference on Smart Energy Systems and Technologies*, 2019. ISBN 9781728111568. doi: 10.1109/SEST.2019.8849136.
- [30] Zhaoxi Liu, Qiuwei Wu, Shaojun Huang, and Haoran Zhao. Transactive energy: A review of state of the art and implementation. In 2017 IEEE Manchester PowerTech, Powertech 2017, 2017. ISBN 9781509042371. doi: 10.1109/PTC.2017.7980892.
- [31] J. Löfberg. Yalmip: A toolbox for modeling and optimization in matlab. In *In Proceedings of the CACSD Conference*, Taipei, Taiwan, 2004.
- [32] Shuai Lu, Nader Samaan, Ruisheng Diao, Marcelo Elizondo, Chunlian Jin, Ebony Mayhorn, Yu Zhang, and Harold Kirkham. Centralized and decentralized control for demand response. In *IEEE PES Innovative Smart Grid Technologies Conference Europe, ISGT Europe*, 2011. ISBN 9781612842189. doi: 10.1109/ISGT.2011.5759191.

- [33] J. C. S. Lui. Introduction to game theory: Finite dynamic games, 2002.
- [34] J. C. S. Lui. Introduction to game theory: Static games, 2002.
- [35] Alberto Maria Metelli, Mirco Mutti, and Marcello Restelli. Configurable Markov decision processes. In 35th International Conference on Machine Learning, ICML 2018, 2018. ISBN 9781510867963.
- [36] Matteo Muratori. Impact of uncoordinated plug-in electric vehicle charging on residential power demand. *Nature Energy*, 2018. ISSN 20587546. doi: 10.1038/s41560-017-0074-z.
- [37] Arun Sukumaran Nair, Tareq Hossen, Mitch Campion, Daisy Flora Selvaraj, Neena Goveas, Naima Kaabouch, and Prakash Ranganathan. Multi-Agent Systems for Resource Allocation and Scheduling in a Smart Grid, 2018. ISSN 21994706.
- [38] N. S.M. Nazar, M. P. Abdullah, M. Y. Hassan, and F. Hussin. Time-based electricity pricing for Demand Response implementation in monopolized electricity market. In SCOReD 2012 - 2012 IEEE Student Conference on Research and Development, 2012. ISBN 9781467351584. doi: 10.1109/SCOReD.2012.6518634.
- [39] John Von Neumann and Oskar Morgenstern. *Theory of games ew: and economic behavior*. 1944. ISBN 0691003629. doi: 10.1090/S0002-9904-1945-08391-8.
- [40] Floris Olsthoorn. The price of anarchy: Measuring the ineffciency of selfsh networking, 2012.
- [41] Peter Palensky and Dietmar Dietrich. Demand side management: Demand response, intelligent energy systems, and smart loads. *IEEE Transactions on Industrial Informatics*, 2011. ISSN 15513203. doi: 10.1109/TII.2011.2158841.
- [42] Simon Parsons and Michael Wooldridge. Game theory and decision theory in multi-agent systems, 2002. ISSN 13872532.
- [43] Thierry PIRONET. Multi-period stochastic optimization problems in transportation management, 2015.
- [44] Ulrich Schwalbe and Paul Walker. Zermelo and the Early History of Game Theory. *Games and Economic Behavior*, 34:123–137, 2001. doi: 10.1006/game.2000.0794.
- [45] Javier Silvente, Georgios M. Kopanos, Vivek Dua, and Lazaros G. Papageorgiou. A rolling horizon approach for optimal management of microgrids under stochastic uncertainty. *Chemical Engineering Research and Design*, 2018. ISSN 02638762. doi: 10.1016/j.cherd.2017.09.013.
- [46] Tiago Sousa, Tiago Soares, Pierre Pinson, Fabio Moret, Thomas Baroche, and Etienne Sorin. Peer-to-peer and community-based markets: A comprehensive review, 2019. ISSN 18790690.
- [47] M. R. Staats, P. D.M. de Boer-Meulman, and W. G.J.H.M. van Sark. Experimental determination of demand side management potential of wet appliances in the Netherlands. *Sustainable Energy, Grids and Networks*, 2017. ISSN 23524677. doi: 10.1016/j.segan.2016.12.004.
- [48] Rainer Stamminger. Synergy Potential of Smart Appliances. D2.3 of WP2 from the Smart-A project. Technical report, 2008.
- [49] Michael Ummels. Stochastic Multiplayer Games: Theory and Algorithms. 2010. doi: 10.5117/9789085550402.
- [50] M. Van Otterlo. Markov decision processes: concepts and algorithms., 2009.
- [51] John S. Vardakas, Nizar Zorba, and Christos V. Verikoukis. A Survey on Demand Response Programs in Smart Grids: Pricing Methods and Optimization Algorithms. *IEEE Communications Surveys and Tutorials*, 2015. ISSN 1553877X. doi: 10.1109/COMST.2014.2341586.
- [52] Zhanle Wang, Raman Paranjape, Asha Sadanand, and Zhikun Chen. Residential demand response: An overview of recent simulation and modeling applications. In *Canadian Conference on Electrical and Computer Engineering*, 2013. ISBN 9781479900329. doi: 10.1109/CCECE. 2013.6567828.

[53] Annette Werth, Alexis André, Daisuke Kawamoto, Tadashi Morita, Shigeru Tajima, Mario Tokoro, Daiki Yanagidaira, and Kenji Tanaka. Peer-to-Peer Control System for DC Microgrids. *IEEE Transactions on Smart Grid*, 2018. ISSN 19493053. doi: 10.1109/TSG.2016.2638462.

- [54] Xing Yan, Yusuf Ozturk, Zechun Hu, and Yonghua Song. A review on price-driven residential demand response. *Renewable and Sustainable Energy Reviews*, 96:411–419, 2018. ISSN 1364-0321. doi: https://doi.org/10.1016/j.rser.2018.08.003.
- [55] M. F. Zia, M. Benbouzid, E. Elbouchikhi, S. M. Muyeen, K. Techato, and J. M. Guerrero. Microgrid transactive energy: Review, architectures, distributed ledger technologies, and market analysis. *IEEE Access*, 8:19410–19432, 2020.